

NAVAL POSTGRADUATE SCHOOL MONTEREY, CALIFORNIA



THESIS

**EVALUATION OF POTENTIAL CHANGES TO THE
SPACE SHUTTLE ORBITER'S FLIGHT CONTROL
SYSTEM TO INCREASE DIRECTIONAL CONTROL
DURING POST LANDING ROLLOUT**

by

Linda J. Ham

September 1997

Thesis Advisor:

Terrence W. Wilcut

Co-Advisor:

Richard M. Howard

Approved for public release; distribution is unlimited

DTIC QUALITY INSPECTED 3

19980406 000

REPORT DOCUMENTATION PAGE

Form Approved
OMB No. 0704-0188

Public reporting burden for this collection of information is estimated to average 1 hour per response, including the time for reviewing instruction, searching existing data sources, gathering and maintaining the data needed, and completing and reviewing the collection of information. Send comments regarding this burden estimate or any other aspect of this collection of information, including suggestions for reducing this burden, to Washington headquarters Services, Directorate for Information Operations and Reports, 1215 Jefferson Davis Highway, Suite 1204, Arlington, VA 22202-4302, and to the Office of Management and Budget, Paperwork Reduction Project (0704-0188) Washington DC 20503.

1. AGENCY USE ONLY (Leave blank)

2. REPORT DATE

September 1997

3. REPORT TYPE AND DATES COVERED

Master's Thesis

4. TITLE AND SUBTITLE EVALUATION OF POTENTIAL CHANGES TO THE SPACE SHUTTLE ORBITER'S FLIGHT CONTROL SYSTEM TO INCREASE DIRECTIONAL CONTROL DURING POST LANDING ROLLOUT

5. FUNDING NUMBERS

6. AUTHOR(S)

Ham, Linda J.

7. PERFORMING ORGANIZATION NAME(S) AND ADDRESS(ES)

Naval Postgraduate School
Monterey, CA 93943-5000

8. PERFORMING ORGANIZATION REPORT NUMBER

9. SPONSORING / MONITORING AGENCY NAME(S) AND ADDRESS(ES)

None

10. SPONSORING / MONITORING AGENCY REPORT NUMBER

11. SUPPLEMENTARY NOTES

The views expressed in this thesis are those of the author and do not reflect the official policy or position of the Department of Defense or the U.S. Government.

12a. DISTRIBUTION / AVAILABILITY STATEMENT

Approved for public release; distribution unlimited.

12b. DISTRIBUTION CODE

13. ABSTRACT (maximum 200 words)

Space Shuttle Orbiter landings indicate both long term directional instability and the potential for pilot induced oscillations during landing and rollout before nosewheel touchdown. The Orbiter's Flight Control System requires improvements to increase directional control in the two point stance (after main gear touchdown with the nose in the air). A number of modifications are proposed to improve directional control. This thesis describes the control deficiency, potential improvements to the Flight Control System (FCS), and evaluates a number of these improvements. The evaluation was performed by modeling the Orbiter's postlanding lateral/directional control laws using a commercially available engineering software package known as MATLAB 5.0. Directional control of the Orbiter was evaluated with and without the proposed modification to obtain a comparison of control response.

Initial evaluation of future Orbiter FCS modifications could be performed using commercially available engineering software packages such as MATLAB; rather than costly full-up Orbiter simulators. A low cost initial evaluation of changes may save NASA resources.

14. SUBJECT TERMS

Space Shuttle, Orbiter, National Aeronautics and Space Administration (NASA), MATLAB, Flight Control Systems, Pilot Induced Oscillation (PIO), Landing and Rollout, Directional Control

15. NUMBER OF PAGES 130

16. PRICE CODE

17. SECURITY CLASSIFICATION OF REPORT

Unclassified

18. SECURITY CLASSIFICATION OF THIS PAGE

Unclassified

19. SECURITY CLASSIFICATION OF ABSTRACT

Unclassified

20. LIMITATION OF ABSTRACT

UL

NSN 7540-01-280-5500

Standard Form 298 (Rev. 2-89)
Prescribed by ANSI Std. Z39-18

Approved for public release; distribution is unlimited

**EVALUATION OF POTENTIAL CHANGES TO THE SPACE SHUTTLE
ORBITER'S FLIGHT CONTROL SYSTEM TO INCREASE
DIRECTIONAL CONTROL DURING POST LANDING ROLLOUT**

Linda J. Ham
Flight Director, NASA
B.S., University of Wisconsin, 1982

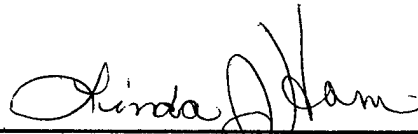
Submitted in partial fulfillment of the
requirements for the degree of

MASTER OF SCIENCE IN ASTRONAUTICAL ENGINEERING

from the

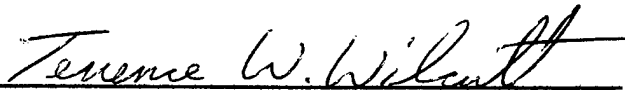
**NAVAL POSTGRADUATE SCHOOL
September 1997**

Author:

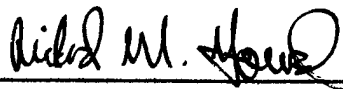


Linda J. Ham

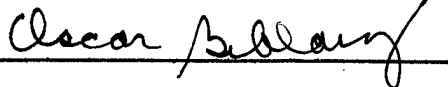
Approved by:



Terrence W. Wilcutt, Thesis Advisor



Richard M. Howard, Co-Advisor



for Gerald Lindsey, Chairman
Department of Aeronautics and Astronautics

ABSTRACT

Space Shuttle Orbiter landings indicate both long term directional instability and the potential for pilot induced oscillations during landing and rollout before nosewheel touchdown. The Orbiter's Flight Control System requires improvements to increase directional control in the two point stance (after main gear touchdown with the nose in the air). A number of modifications are proposed to improve directional control. This thesis describes the control deficiency, potential improvements to the Flight Control System (FCS), and evaluates a number of these improvements. The evaluation was performed by modeling the Orbiter's postlanding lateral/directional control laws using a commercially available engineering software package known as MATLAB 5.0. Directional control of the Orbiter was evaluated with and without the proposed modification to obtain a comparison of control response.

Initial evaluation of future Orbiter FCS modifications could be performed using commercially available engineering software packages such as MATLAB; rather than costly full-up Orbiter simulators. A low cost initial evaluation of changes may save NASA resources.

TABLE OF CONTENTS

I. INTRODUCTION	1
A. BACKGROUND	1
1. Operational Impacts	3
2. Hardware Modifications	4
3. Software Modifications	4
B. PURPOSE	5
II. ORBITER DIRECTIONAL STABILITY AND CONTROL	7
A. NOMINAL ROLLOUT PROFILE	7
B. DIRECTIONAL STABILITY IN THE TWO POINT ATTITUDE	8
1. Center of Gravity (COG) Effects	8
2. Dihedral Effect	9
3. Weathercock Effect	11
4. Drag Chute Effect	12
5. Frequency and Damping	13
C. DIRECTIONAL CONTROL IN THE TWO POINT ATTITUDE	14
1. Rudder	14
2. Directional FCS Susceptibility to PIO	15
III. RUDDER CONTROL	17
A. RUDDER COMMAND PATH	17
1. Rudder Command Feedback	17
a. Rudder Pedals	18
b. Rudder Command Shaper	18
c. Rudder Pedal Gain Scheduler	18
d. Rudder Trim Command	19
e. Lateral Accelerometers	20
f. Lateral Acceleration Feedback Compensator	20
2. Rudder Deflection Command	20
a. Lateral Acceleration Gain	21
b. Cosine of the Angle of Attack (α)	21
c. Rate Gyro Assemblies	22
d. Yaw Rate Structural Filter	22
e. Yaw Rate Error Determination	22
f. Structural Bending Filter	23
g. Yaw Rate Gain	23
h. Rudder Deflection Limiter	23
i. Priority Rate Limiting (PRL)	24
B. RUDDER ACTUATOR	24
IV. EQUATIONS OF MOTION AND STABILITY AND CONTROL DERIVATIVES	27

A. ASSUMPTIONS	27
B. EQUATIONS OF MOTION	28
1. Longitudinal Equations of Motion	29
2. Lateral-Directional Equations of Motion	31
3. Longitudinal and Lateral-Directional EOM in State Space Form	33
4. Determination of the Non-Dimensional Stability Derivatives.....	34
a. Longitudinal Stability Derivatives	34
b. Lateral-Directional Stability Derivatives.....	35
V. PROPOSED FCS MODIFICATIONS TO IMPROVE DIRECTIONAL CONTROL IN THE TWO POINT STANCE	39
A. LINEARIZE THE RUDDER PEDAL COMMAND SHAPER	40
B. REDUCE THE RUDDER PEDAL GAIN	40
C. DECREASE TIME LAGS	40
D. DISABLE LATERAL ACCELERATION FEEDBACK	40
VI. YAW FCS SIMULATION	41
A. SIMULATION INITIAL CONDITIONS	41
B. FCS CONFIGURATIONS EVALUATED	42
C. SIMULATION	42
VII. RESULTS.....	45
A. MODEL VALIDATION	45
B. RUDDER DEFLECTION	46
C. LATERAL ACCELERATION AT THE COMMANDER'S STATION	47
D. SIDESLIP.....	49
E. YAW RATE AND HEADING.....	50
F. ROLL RATE AND ANGLE OF BANK	52
G. NATURAL FREQUENCY AND DAMPING RATIO	54
VIII. CONCLUSIONS.....	57
A. RECOMMENDATIONS	57
B. USE OF COTS SOFTWARE FOR ENGINEERING EVALUATION	58
APPENDIX A. MATLAB CODE FOR SCRIPT PROGRAM	59
APPENDIX B. MATLAB CODE FOR SIMULATION.....	63
APPENDIX C. MATLAB CODE FOR PLOT PROGRAM.....	97
APPENDIX D. STS-62 FLIGHT DATA AND SES SIMULATION RESULTS.....	99
LIST OF REFERENCES	111
INITIAL DISTRIBUTION LIST.....	113

LIST OF FIGURES

Figure 1. Orbiter Flight Control Surfaces.....	2
Figure 2. Orbiter Center of Gravity Location.....	9
Figure 3. Orbiter Dihedral.....	10
Figure 4. Orbiter Yaw Due to Dihedral.....	11
Figure 5. Orbiter Yaw Due to Weathercock.....	12
Figure 6. Orbiter Yaw Due to Drag Chute.....	13
Figure 7. Orbiter Rudder/Speedbrake.....	15
Figure 8. Rudder Command Feedback.....	17
Figure 9. Rudder Command Shaper.....	18
Figure 10. Rudder Pedal Gain Scheduler.....	19
Figure 11. Rudder Trim Commands.....	19
Figure 12. Lateral Acceleration Feedback Compensator.....	20
Figure 13. Rudder Deflection Command.....	21
Figure 14. Lateral Acceleration Gain Schedule.....	21
Figure 15. Yaw Rate Error Determination.....	22
Figure 16. Yaw Rate Gain Scheduler.....	23
Figure 17. Rudder Deflection Limiter.....	24
Figure 18. Rudder/Speedbrake Actuator Location [Ref. 6].....	25
Figure 19. Rudder Pedal Deflection.....	42
Figure 20. Simulink Block Diagram of Rudder Doublet Effect on Directional Control.....	43
Figure 21. YAW FCS Block Diagram.....	44
Figure 22. Rudder Surface Deflection.....	47
Figure 23. Lateral Acceleration at the Commander's Station.....	48
Figure 24. Sideslip Angle.....	50
Figure 25. Yaw Rate.....	51
Figure 26. Heading Angle.....	52
Figure 27. Roll Rate.....	53
Figure 28. Angle of Bank.....	54

LIST OF TABLES

Table 1. Nominal Touchdown/Rollout Profile.....	7
Table 2. Summary of Directional Stability Parameters.....	13
Table 3. Lift and Drag Coefficients.....	35
Table 4. Side Force, Rolling Moment, and Yawing Moment Coefficients.....	37
Table 5. Potential Changes to the FCS.....	39
Table 6. Initial Conditions.....	41
Table 7. FCS Configurations Evaluated.....	42

LIST OF SYMBOLS, ACRONYMS AND/OR ABBREVIATIONS

<u>Symbol</u>	<u>Definition (units)</u>
α	Angle of Attack
β	Sideslip
δ_a	Aileron deflection angle (deg)
δ_d	Elevator deflection angle (deg)
δ_r	Rudder deflection angle (deg)
δ_{pedal}	Rudder pedal deflection (deg)
Φ, ϕ	(Total, perturbed) bank (roll) angle (rad)
μ	Runway coefficient of friction
Θ, θ	(Total, perturbed) pitch attitude angle (rad)
Ψ, ψ	(Total, perturbed) heading angle (rad)
τ	time constant (seconds)
ω_D	Directional natural frequency in the two point stance
ζ_D	Directional damping ratio in the two point stance
b	Wing span (ft.)
c	Chord Length (ft.)
C_D	Drag coefficient
C_L	Lift coefficient
C_l	Rolling moment coefficient
C_m	Pitching moment coefficient
C_n	Yawing moment coefficient
C_y	Side force coefficient
D	Drag (lbs)
F_x, F_y, F_z	Applied forces in the X, Y, and Z direction respectively
f_x, f_y, f_z	Perturbed forces in the X, Y, and Z direction respectively
g	Acceleration of gravity (ft/sec ²)
I_{xx}, I_{yy}, I_{zz}	Moments of inertia about X, Y, Z axes respectively (slug ft ²)
$I_{xy}, I_{yx}, I_{yz},$	Products of inertia in XYZ system (slug ft ²)
I_{zy}, I_{xz}, I_{zx}	Products of inertia in XYZ system (slug ft ²)

I_{ymg} I_{zmg}	Shifted I_{yy} and I_{zz} to COR
L, l	(Total, perturbed) rolling moment about X (ft-lbs)
L_{β}	Dihedral - Roll due to sideslip
L	Lift (lbs)
m	mass of the Orbiter (slugs)
M	Mach
M, m	(Total, perturbed) pitching moment about Y (ft-lbs)
N, n	(Total, perturbed) yawing moment about Z (ft-lbs)
N_{β}	Weathercock - Yaw due to sideslip
N_r	Yaw damping - Yaw due to yaw rate
N_{TD}	Total directional damping in the two point stance
N_{TS}	Total directional stability in the two point stance
N_y	Lateral Acceleration
P	Roll rate about X (rad/sec)
p	Perturbed roll rate about X (rad/sec)
Q	Pitch rate about Y (rad/sec)
q	Perturbed pitch rate about Y (rad/sec)
q_{dym}	Dynamic pressure (lbs/ft ²)
R	Yaw rate about Z (rad/sec)
r	Perturbed yaw rate about Z (rad/sec)
S	Surface are of the wing (ft ²)
U	Forward velocity along X (ft/sec)
u	Perturbed forward velocity along X (ft/sec)
V	Side velocity along Y (ft/sec)
v	Perturbed forward velocity along Y (ft/sec)
W	Downward velocity along Z (ft/sec)
w	Perturbed forward velocity along Z (ft/sec)

<u>Acronym</u>	<u>Definition</u>
AA	Accelerometer Assembly
APU	Auxiliary Power Unit

ARC	Ames Research Center
BCOSALF	$\beta * \text{Cos}(\alpha)$
BIT	Built In Test
COG	Center Of Gravity
COR	Center Of Rotation
COTS	Commercial Off -The-Shelf
DAXFDC	Yaw rate command
DAY	Commanded yaw rate (Lateral Acceleration error command*GRAY)
DRC	Rudder command
DRC_LIM	Rudder command limit
DRCPF	Preliminary rudder command
DRERR	Yaw rate error
DRMAN	Rudder pedal command
DRMS	Shaped and scaled rudder pedal command
DRPRM	Filtered body yaw rate
DRRC	Yaw command
DRRCUF	Unfiltered yaw rate command
DRTMS	DRMS converted to a lateral accelerations command
DRT	Rudder trim command signal
DRTI	Lateral acceleration trim command
EAFB	Edwards Air Force Base
EOM	Equations Of Motion
ET	External Tank
FCS	Flight Control System
GDRC	Yaw rate gain
GERYYFWDS	Constant from the roll channel
GNYDRM	Rudder pedal command to lateral acceleration command gain
GRAY	Lateral acceleration command gain
JSC	Johnson Space Center
KEAS	Knots Equivalent Air Speed
KGS	Knots Ground Speed

KSC	Kennedy Space Center
NASA	National Aeronautics and Space Administration
NSTS	National Space Transportation System
NWS	Nose Wheel Steering
NYP	Actual Lateral Acceleration
PC	Personal Computer
PIO	Pilot Induced Oscillation
PRL	Priority Rate Limiting
RGA	Rate Gyro Assembly
RPTA	Rudder Pedal Transducer Assembly
RTLS	Return To Launch Site
TAS	True Air Speed
SES	Shuttle Entry Simulator
SLF	Shuttle Landing Facility
SSP	Space Shuttle Program
SRB	Solid Rocket Booster
TAL	Trans-Atlantic Landing
TAS	True Airspeed
V&V	Verification and Validation
VMS	Vertical Motion Simulator
WOWLON	Weight on wheels lock-on

I. INTRODUCTION

The Space Shuttle, operated by the National Aeronautics and Space Administration (NASA), is the only manned space flight vehicle currently operated by the United States. The Space Shuttle consists of the Orbiter, External Tank (ET), and two Solid Rocket Boosters (SRB's). The Orbiter contains the astronauts and payloads. It is the only piece of the Space Shuttle that completes the entire mission. The Orbiter returns from space to land similar to a conventional gliding airplane. The continued safe operation of the Space Shuttle is the number one concern of the Space Shuttle Program (SSP). A recent safety concern is the directional control of the Orbiter during one segment of the landing/rollout phase [Ref. 1]. This perceived directional control deficiency is described below.

A. BACKGROUND

During the landing and rollout phase of flight, the gains associated with the piloting task are greatly increased. The margin for error is vastly decreased as pitch, roll, and yaw requirements become more stringent through the flare-to-touchdown and subsequent rollout. During this critical phase, pilot control commands will be more frequent and often of greater magnitude to make timely corrections to flight path and counter external perturbations such as crosswinds, wind shear, or gusty conditions. These increased demands on the control system can occasionally result in a condition known as Pilot Induced Oscillation (PIO).

PIO occurs when a pilot attempts a particular control task which is beyond the capabilities of the aircraft control system. PIO can only occur with the pilot actively in the vehicle control loop and is therefore not a stability concern. A PIO is typically manifested by an uncommanded oscillatory motion that can only be stopped when the pilot reduces control inputs or 'backs out of the loop.' The severity of PIO can range from an annoyance to complete loss of control. The result of a PIO situation can often be unpredictable. What might be an annoyance during landing one day, might be disastrous on the next. PIO can result from many different root causes including an excess amount of friction in a mechanical control system, actuator rate limiting, or transport delays in today's most advanced flight control systems. In all cases, a large phase lag from the control input to aircraft response, lies at the heart of the problem.

The Orbiter incorporates a 'fly-by-wire' control system to command the flight control surfaces, depicted in Figure 1.

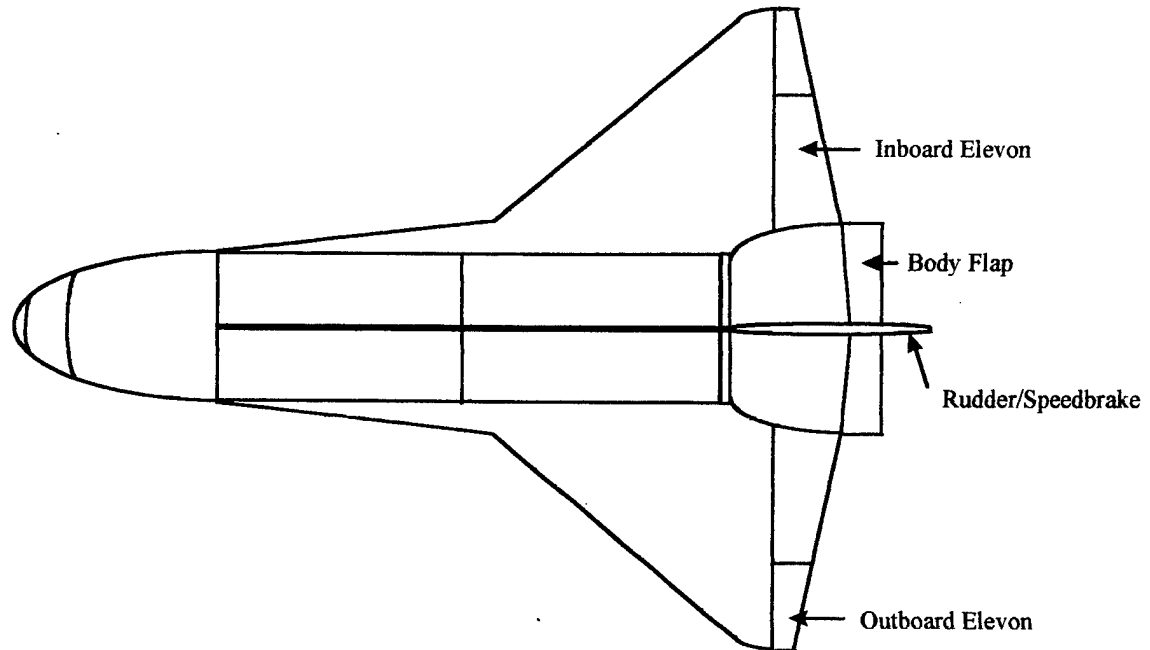


Figure 1. Orbiter Flight Control Surfaces

The flight controls, control stick, rudder pedals, and speed brake switch are not mechanically connected to their respective control surfaces. Orbiter control is afforded through a myriad of feedback control loops, filters, gain multipliers, integrators, differentiators, etc. The goal of these components, in conjunction with a feel system, is to supply the pilot with an Orbiter which responds acceptably to all control inputs. Fly-by-wire control systems, if not carefully designed, can be susceptible to PIO.

The directional control problem of interest is most evident after touchdown while the Orbiter is in the two point stance with the mainwheels on the ground and the nosewheel in the air. This flight segment, from initial touchdown until derotation is complete, is approximately 20 seconds in duration. With dispersed touchdown speeds between 185 and 225 knots, a small deviation in track can result in a runway departure very quickly. Recent Orbiter landings have shown that there is a directional PIO problem in the two point stance[Ref. 1]. The problem seems to abate after nose gear touchdown due to the additional directional control afforded by the Nose Wheel Steering (NWS) system. The PIO is associated with the task of capturing and tracking the runway centerline and may be exaggerated in conditions of greater crosswind. The possibility of the Orbiter becoming directionally uncontrollable and departing the runway is unacceptable. This problem raises some critical questions including:

1. Are there operational impacts? Must the crosswind limit be reduced to protect against PIO? Should Shuttle landings require wider runways and/or lakebed landings?
2. Are there hardware modifications such as changes to the rudder actuators that would improve directional control?
3. Are there potential software modifications to the control laws which will reduce or eliminate this PIO condition?
4. If PIO is evident in a nominal landing, what would happen in the case of a blown main gear tire?

1. Operational Impacts

Reducing the crosswind limit may reduce the potential for direction PIO; however, it will not eliminate the problem. In fact, the landing which experienced the most significant directional PIO had a 2 knot crosswind [Ref. 2]. Other flight data also shows that even with minimal crosswind, directional PIO can occur.

In addition, there is appreciable pressure to increase the crosswind limits for the following reason. The commitment of the United States to building the International Space Station has extended the mission of the SSP from pure science to upholding national political obligation. The proposed International Space Station will be in a high inclination orbit which will reduce launch opportunities and decrease the length of launch windows. Landing weather conditions are a concern on launch day since the potential for an emergency landing such as a Return To Launch Site (RTL) or Trans-Atlantic Landing (TAL) can occur on launch day. Meeting the Space Station construction schedule would be much easier if launches and landings could be performed in a greater variety of wind conditions.

Requiring lakebed landings for all Shuttle flights is unacceptable. Orbiter landing mass properties are greatly restricted for lakebed landings to maintain nose gear loads within limits [Ref. 3]. Most Orbiter landing mass properties require concrete runways. Further, landing on a lakebed requires landing at either Edwards Air Force Base (EAFB) in California or Northrup, New Mexico which is impossible for most ascent aborts modes.

The Shuttle Landing Facility (SLF) at Kennedy Space Center (KSC) and the concrete runway used for Shuttle landings at EAFB are 300 ft. wide. The SLF has 50 ft. of usable shoulder on each side. In comparison, some contingency and abort runways are less than 150 ft. wide. Obviously, it is impossible for the SSP to widen all runways available for landing. Restricting the

Orbiter from landing on runways considered too narrow, greatly reduces abort coverage (no where to landing with an SSME failed) to an unacceptable level.

2. Hardware Modifications

Hardware modifications, such as redesign of the rudder actuator to increase deflection rate, may reduce susceptibility to PIO. However, hardware modifications are expensive, require recertification, and demand vehicle down time to implement the changes.

3. Software Modifications

The obvious long term solution to the PIO problem lies in redesigning the existing flight control laws to afford better directional control in a wider variety of wind conditions.

A redesign of this magnitude would traditionally require the control engineer to estimate the new control laws followed by experimental Verification and Validation (V&V) of the new control laws in the Vertical Motion Simulator (VMS) located at the NASA Ames Research Center (ARC) located in Sunnyvale, California. This procedure typically entails qualified astronauts traveling from the Johnson Space Center (JSC) in Houston, Texas to the ARC VMS to fly numerous simulated approaches in varying wind conditions. This evolution can be time consuming and costly.

With the advent of faster more powerful personal computers and workstations, and the availability of very capable software packages which can operate in both the frequency and time domains, the possibility of writing and evaluating new control laws immediately has become a reality. This breakthrough can eliminate the costly iterative process of tweaking and reevaluating control laws in an expensive motion base simulator. The final V&V is still necessary, but the total time and cost are drastically reduced.

The use of simulation to evaluate control laws rely heavily on the numerous models used to develop the simulation. A normal flight test program would not rely solely on simulation results for solutions to PIO problems. The Shuttle Program must rely on these simulations results due to the nature, cost, and risk of flying Shuttle flights only to evaluate control law changes. Flight data is gathered from each flight; however, flight conditions do not test the extreme ends of the envelope. There is no possibility of performing a complete flight test program.

B. PURPOSE

This thesis has two objectives:

- (1) Develop changes to the control laws to reduce the directional PIO tendency present between mainwheel touchdown and completion of derotation while the Orbiter is in the two point attitude.
- (2) Evaluate these changes using a Commercial Off-The-Shelf (COTS) PC-based software package.

II. ORBITER DIRECTIONAL STABILITY AND CONTROL

The nominal Orbiter rollout profile, directional stability, and directional control in the two point stance are described in this chapter.

A. NOMINAL ROLLOUT PROFILE

The nominal touchdown and rollout profile, with approximate speeds and time from touchdown, is described in Table 1 [Ref. 2, 3 and 4].

Table 1. Nominal Touchdown/Rollout Profile

Event	Airspeed (KEAS)	Time (sec.)
Touchdown ⁽¹⁾	205 (195)	0
Brakes functional ⁽²⁾	200	1.9
Drag chute deploy ⁽³⁾	195	3.0
Commence auto derotation ⁽⁴⁾	185	11.0
Commence manual derotation ⁽⁵⁾	175	16.0
Drag chute fully disreefed	175	16.0
Nosewheel touchdown	145 to 155	19.0
First brake application ⁽⁶⁾	140 (KGS)	23.0
Drag chute Jettison ⁽⁷⁾	60 ± 20 (KGS)	34.0
Wheels stop	0	50.0

- Notes:
1. Targeted touchdown speed of 205 KEAS for Orbiter gross weights \geq 220K lbs. (195 KEAS for Orbiter weights < 220K lbs.).
 2. Built In Test (BIT) requires 1.9 sec. after Weight On Wheels Lock-On (WOWLON).
 3. Chute deploy after main gear touchdown.
 4. Nominal derotation is automatic with beep trim activation targeting 1.5 deg/sec.
 5. Only performed if beep trim fails.
 6. Brake initiation at 140 KGS or 5,000 ft. runway remaining, whichever occurs first.

7. If drag chute is not jettisoned by 40 KGS, the chute will remain on to minimize damage to main engine bells.

B. DIRECTIONAL STABILITY IN THE TWO POINT ATTITUDE

Directional stability in the two point stance is different than the directional stability of the Orbiter in flight. In flight, the Orbiter would typically rotate about the Center Of Gravity (COG). In the two point stance, assuming no lateral skidding of the mainwheel tires, the Orbiter is constrained to rotate directionally about a point on a line that runs laterally through the areas of contact between the mainwheels and the runway. This point is referred to as the Center Of Rotation (COR). Directional stability is governed by four main factors in the two point attitude:

- (1) The relative position of the COG to the COR.
- (2) The increased friction on the downwind mainwheel caused by the rolling moment generated as a result of the dihedral effect or roll due to sideslip, L_{β} , generated primarily by the highly swept wing.
- (3) The aerodynamic 'weathercock' effect or yaw due to sideslip, N_{β} , generated primarily by the large vertical tail.
- (4) The relative position of the drag chute to the COR.

The first factor will attempt to keep the Orbiter traveling in a straight line with respect to the runway in a zero crosswind condition but can act to direct the Orbiter away from a crosswind as a result of the second factor. The third factor will tend to fair the Orbiter into a crosswind in flight. After touchdown, with the COR shifting aft, this 'weathercock' effect becomes a much weaker contributor. The fourth factor will attempt to fair the Orbiter into a crosswind.

1. Center of Gravity (COG) Effects

The nominal COG envelope is 32 in. long and 3 in. wide, centered laterally and positioned approximately 8 ½ ft. forward of the mainwheels [Ref. 5]. The COG will always be well ahead of the mainwheels in the two point stance. The COG geometry with respect to the mainwheels is depicted in Figure 2.

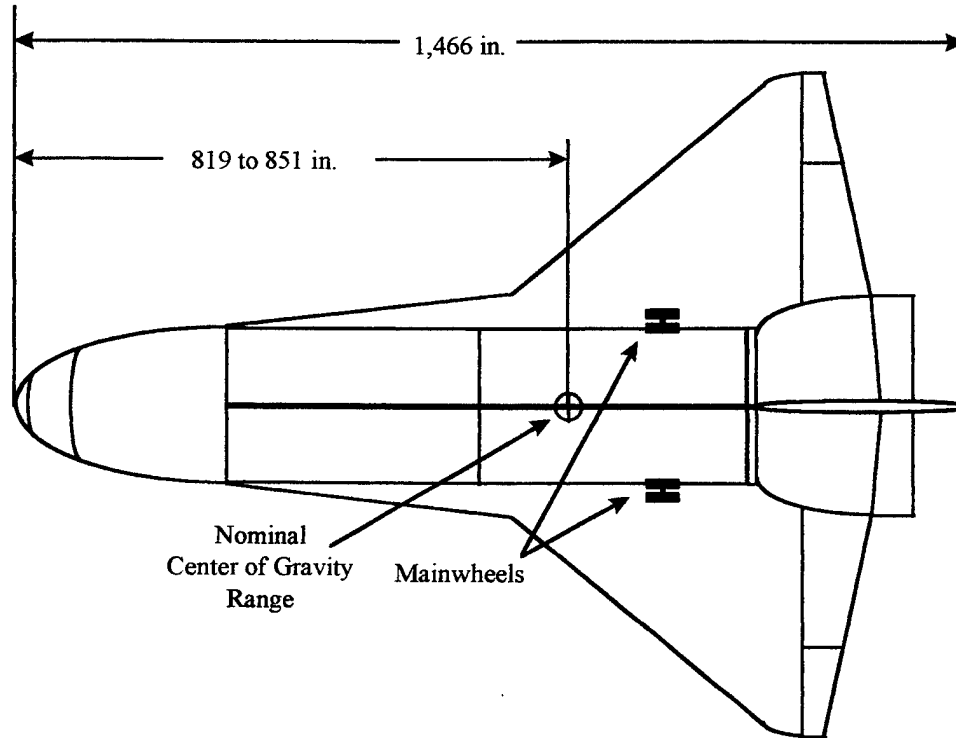


Figure 2. Orbiter Center of Gravity Location

With this geometry, the COG acts as a pendulum in the horizontal plane. The deceleration of the Orbiter caused by the friction in the mainwheels and the mainwheel brakes acts on the COG to produce a force in the Orbiter's direction of motion. This force is analogous to the gravitational force on a normal, vertically oriented, pendulum. The result is a restoring yaw moment which is always attempting to maintain the Orbiter on a straight track in the direction from the COR through the COG. In a zero crosswind condition with no mainwheel braking, the COR will most likely be positioned directly between the mainwheels. In this event, the Orbiter will have positive directional stability in the direction of motion. In a crosswind case, the high dihedral of the Orbiter can become a directionally destabilizing factor.

2. Dihedral Effect

The Orbiter has a large dihedral effect due primarily to the highly swept wing. Dihedral is the tendency for an aircraft to roll away from sideslip. In a landing scenario, the sideslip angle can be calculated as follows:

$$\beta = \tan^{-1} \frac{\text{crosswind component}}{\text{Orbiter Indicated Airspeed}}$$

The rolling moment generated in a highly swept wing aircraft in response to sideslip can be explained by two factors. First, the upwind wing senses flow closer to perpendicular to the leading edge which decreases flow in the spanwise direction; thereby increasing lift. The downwind wing has the opposite effect of increased spanwise flow; therefore decreased lift. The second, compounding effect, is a blanking effect on the downwind wing caused by the large fuselage structure of the Orbiter. This reduction in airflow also decreases lift.

Another contributor to positive dihedral is the high vertical tail. The center of pressure associated with the airflow across the vertical tail is well above the COR which would cause a further roll away from crosswind. The net result is a rolling moment away from crosswind as depicted in Figure 3.

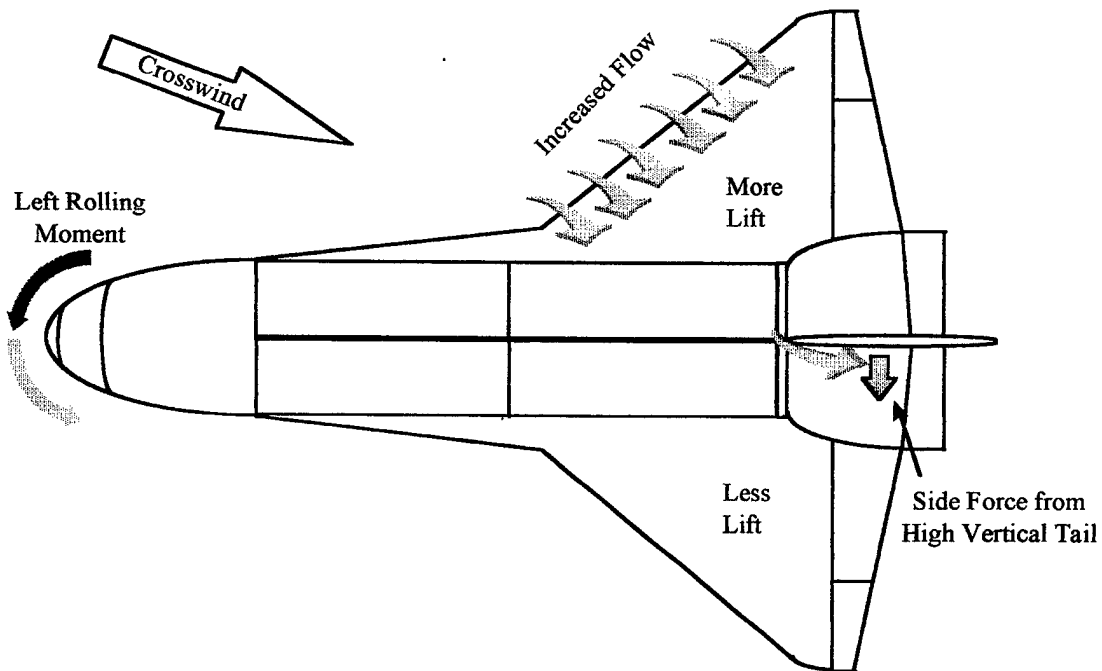


Figure 3. Orbiter Dihedral

This rolling moment will cause an increased down force on the downwind strut and a lighter force on the upwind strut. This differential load will cause increased friction on the downwind wheel and a subsequent shift in the directional COR to the downwind side of Orbiter

centerline. This shift in the COR, in conjunction with the COG effect discussed in subsection 1, will act to cause the Orbiter to deviate away from crosswind as depicted in Figure 4.

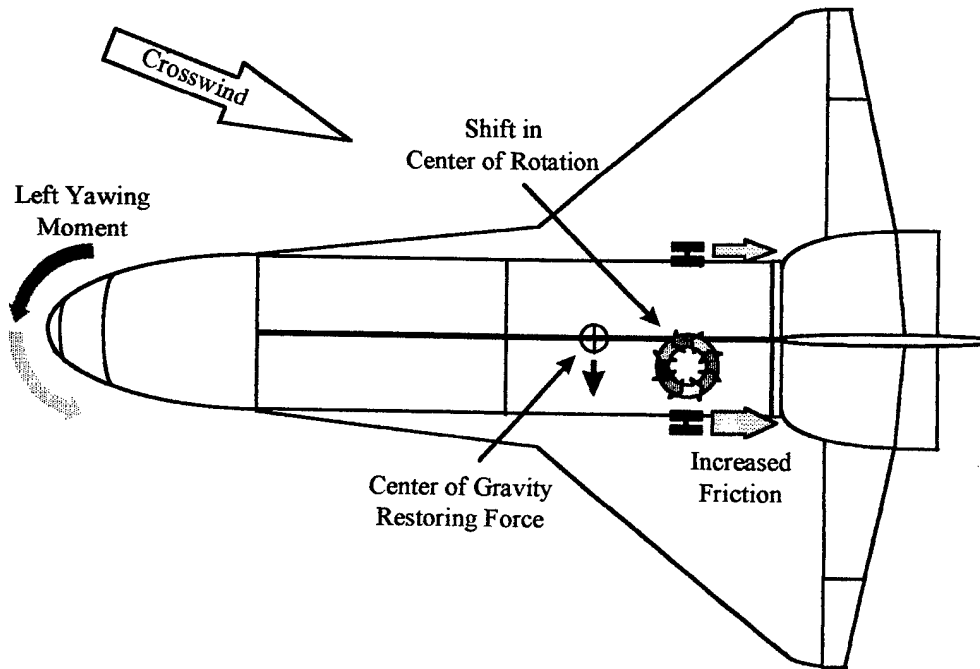


Figure 4. Orbiter Yaw Due to Dihedral

3. Weathercock Effect

The weathercock effect is typically a tradeoff between the destabilizing effect of the fuselage and the stabilizing effect of the vertical tail. The aft location of the COG of the Orbiter in flight is somewhat destabilizing since the stabilizing moment arm associated with the fin is shorter and the destabilizing moment arm of the fuselage is longer. When the Orbiter attains the two point stance, the COR shifts even further aft. This change creates a condition of weak instability. The Orbiter will tend to point away from a crosswind as depicted in Figure 5.

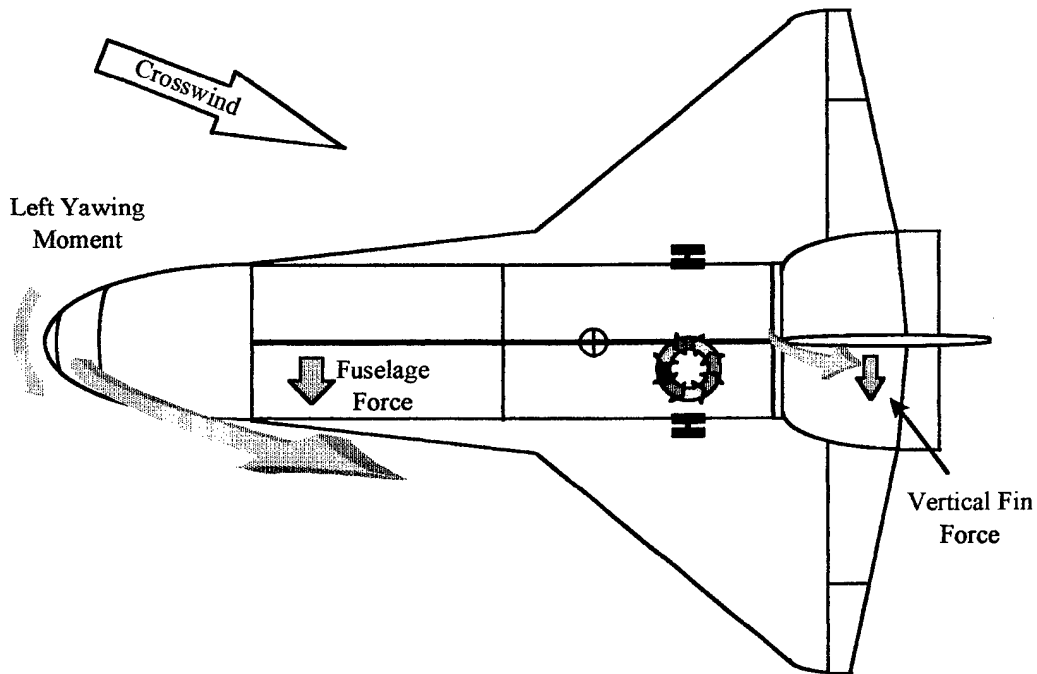


Figure 5. Orbiter Yaw Due to Weathercock

4. Drag Chute Effect

The drag chute was incorporated on to the Orbiter to decrease landing rollout distances for certain contingency runways. Along with the decreased rollout, there is a small amount of positive weathercock effect. It is important to note that the drag chute is nominally fully disreefed three seconds prior to nosewheel touchdown as described in section II.A [Ref. 2 and 3]. Therefore, the drag chute will only be a brief factor to steady-state directional stability in the two point stance. Yet the three second impulse may be enough to perturb the steady case. The drag chute will blow downwind from a crosswind. Since the drag chute is attached aft of the center of rotation, the resulting yaw moment on the Orbiter is into the crosswind as depicted in Figure 6.

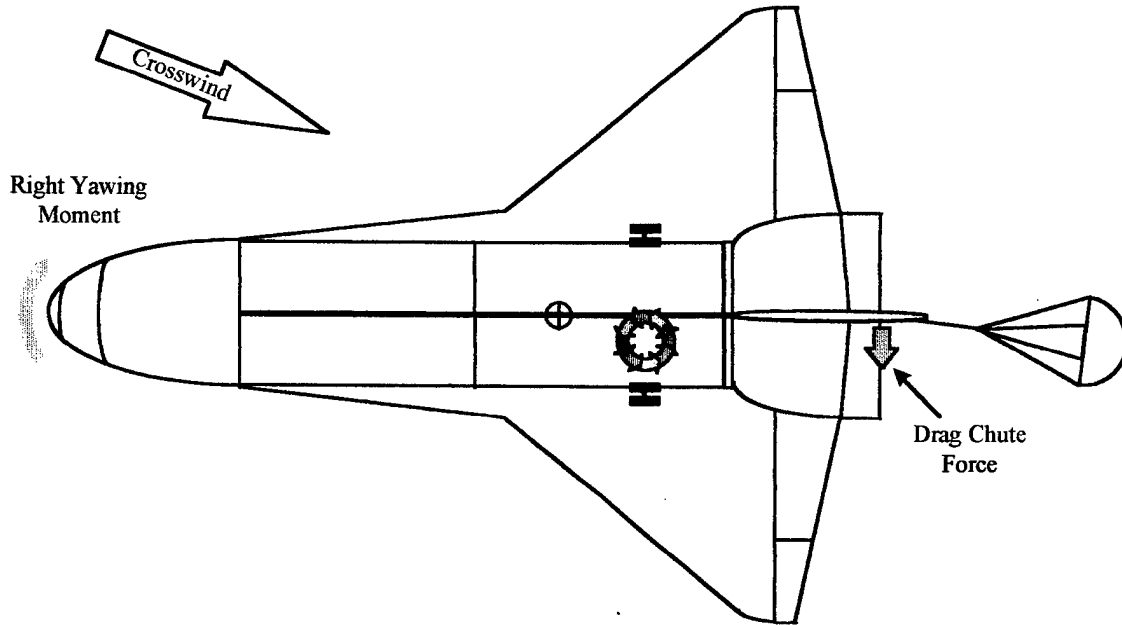


Figure 6. Orbiter Yaw Due to Drag Chute

5. Frequency and Damping

A summary of the directional stability parameters is shown in Table 2 along with their relative strengths.

Table 2. Summary of Directional Stability Parameters

Parameter	Type	Relative Strength	Direction
COG	Inertial	Strong	In direction of motion
Dihedral	Aerodynamic	Weak	Away from crosswind
Weathercock	Aerodynamic	Weak	Away from crosswind
Drag Chute	Aerodynamic	Weak	Into crosswind

All of these factors combine to yield fairly weak directional stability in the two point stance. This weak stability, when modeled with a simple second order system, would yield a low open loop frequency response to a disturbance. While this data point has never been collected in flight, a rough estimate of what one might call 'the directional natural frequency', ω_D , can be made by observing video of actual closed loop cases of PIO. The videoThe open loop natural frequency, ω_D , is estimated to be on the order of 1 rad/sec. The only yaw damping, N_r , is most

likely due to the large vertical tail and possibly any differential friction in the mainwheels. Both of these factors would be small which yields very low directional damping. The complete dynamic stability of the Orbiter in the two point stance can be modeled by the following second order equation where N_{TD} is total damping and N_{TS} is total stability.

$$s^2 + N_{TD}s + N_{TS}$$

where $\omega_D = \sqrt{N_{TS}}$

and the damping ratio, $\zeta_D = \frac{N_{TD}}{2\omega_D}$

The natural frequency and damping ratio will be estimated from the simulation results. A low frequency and low damping ratio will indicate the tendency of the FCS to be susceptible to PIO.

C. DIRECTIONAL CONTROL IN THE TWO POINT ATTITUDE

Directional control in the two point stance can be affected with two controllers; aerodynamically with the rudder, and mechanically with differential braking. Brakes are not employed until derotation is complete to avoid excessive nosewheel slapdown rates and to reduce the risk of a blown main tire. Braking nominally begins at 140 knots [Ref. 3]. Differential braking would only be employed in extreme situations, such as a flat main gear tire. Therefore, directional control in the two point stance would be afforded only by the rudder.

1. Rudder

The rudder is actually a dual purpose control surface acting as both a directional controller and a speedbrake as depicted in Figure 7.

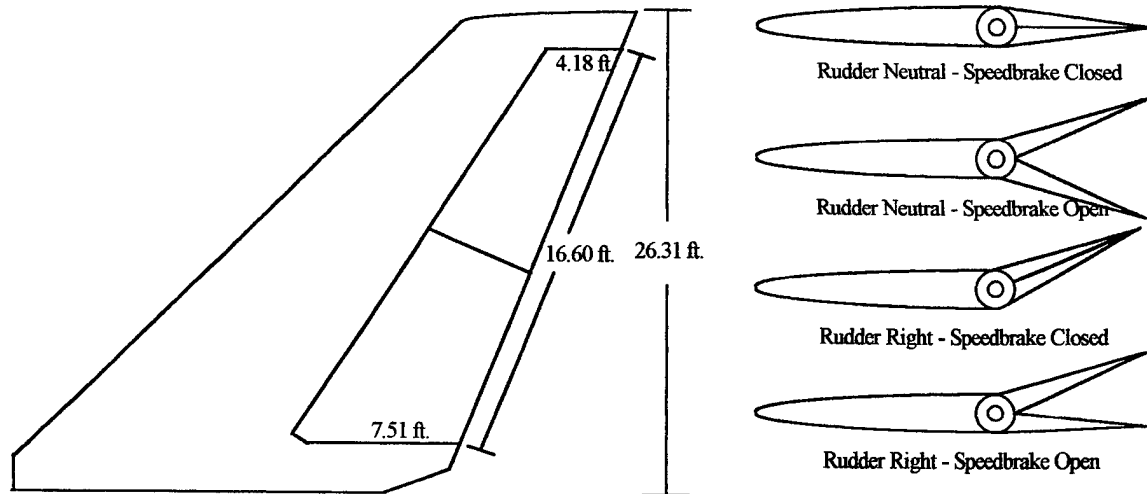


Figure 7. Orbiter Rudder/Speedbrake

The surface is mechanically limited to a maximum deflection rate of 16 deg/sec normally [Ref. 6]. Postlanding the deflection rate is further limited to 13 deg/sec since the speedbrake is full open. The software limits the deflection rate to 14 deg/sec so that sufficient hydraulic fluid is available to other control surfaces. In the event of the loss of one or two hydraulic systems, the rate is limited to 12 deg/sec and 7 deg/sec, respectively [Ref. 4]. The surface area is approximately 97 ft.² and can generate up to 2.25 lateral g's.

2. Directional FCS Susceptibility to PIO

The FCS has many limitations which result in the high potential for directional PIO in the two point stance. The slow surface rate of the rudder, slow response time, high control power of the rudder due to the large surface area, and rudder placement with respect to the gear are conducive to PIO. If a large pedal input is sustained until the yaw rate is well underway, loss of control is probable. The slow surface rate does not allow an opposite input to be effected quickly enough to counteract the yaw rate.

In addition, ARC VMS studies have indicated rudder rate saturation is encountered in high crosswind landings or in performing postlanding lateral maneuvers stress tasks [Ref. 7].

III. RUDDER CONTROL

This chapter describes the rudder control path including the software command path and rudder actuator. Detailed drawings and description of the Orbiter FCS control laws are found in the Software Requirements Document [Ref. 8] and Lockheed drawings [Ref. 9].

A. RUDDER COMMAND PATH

The control logic for the rudder surface may be broken down into two basic steps. The first converts rudder pedal deflection angle into lateral acceleration error command. The Orbiter's flight control system uses lateral acceleration feedback to null errors to the commanded lateral acceleration and provide directional stability augmentation. The second step converts the lateral acceleration error command into a yaw rate which is filtered of Orbiter structural bending modes and finally converted into a command to the control surface for degrees of deflection. This command is sent to Priority Rate Limiting (PRL), which limits the rudder deflection rate depending on the number of hydraulic systems available. These two steps will be henceforth referred to as the rudder command feedback and rudder deflection command portions.

1. Rudder Command Feedback

A simplified block diagram of rudder pedal position conversion to lateral acceleration error command is shown in Figure 8.

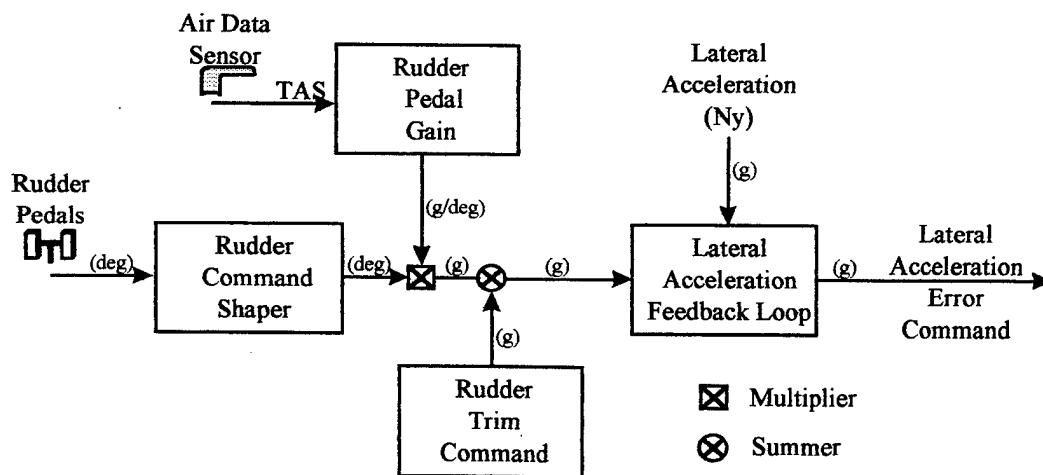


Figure 8. Rudder Command Feedback

The various components of the rudder command feedback path are discussed in the subsections below.

a. Rudder Pedals

There is a Rudder Pedal Transducer Assembly (RPTA) located at both the Commander and Pilot stations. Each RPTA consists of two pedals and a transducer which converts degrees of rudder pedal deflection into electronic signal. The RPTA uses a time constant of 100 ms in the mechanical to electronic transfer. This signal is processed at 6.25 Hz and passed to the rudder command shaper with the name tag DRMAN.

b. Rudder Command Shaper

The rudder command shaper converts DRMAN into a shaped and scaled rudder pedal command named DRMS as shown in Figure 9.

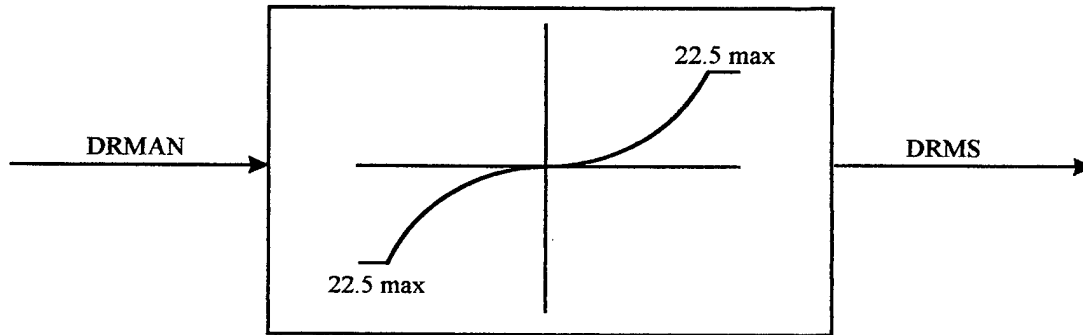


Figure 9. Rudder Command Shaper

The shaping schedule is parabolic and conforms to the following function: $DRMS = (0.042)DRMAN^2 + (0.131)DRMAN$. A maximum deflection limit of 22.5 degrees is imposed on the output signal.

c. Rudder Pedal Gain Scheduler

The rudder pedal gain scheduler produces a gain signal, which when multiplied with the shaped and scaled rudder pedal command, DRMS, produces a lateral acceleration command. This gain is scheduled as a function of True Airspeed (TAS) and is given the name GNYDRM as depicted in Figure 10. This gain also converts the units of the signal from degrees of pedal deflection to lateral g's. The rudder pedal gain scheduler samples at 1.04 Hz.

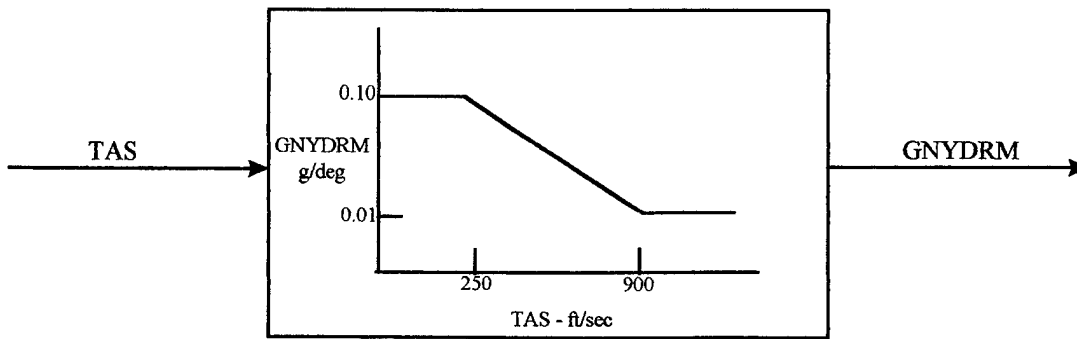


Figure 10. Rudder Pedal Gain Scheduler

d. Rudder Trim Command

The rudder trim command signal is generated by converting the command signal from the rudder trim panel into a commanded lateral acceleration bias. This is performed with a rectangular integrator which ramps the output signal and also limits the maximum bias to 0.1 g's. This signal is sampled at 6.25 Hz. The output signal is the lateral acceleration trim signal, DRTI, which is summed with GNYDRM from the rudder pedals to produce a total lateral acceleration command, DRTMS, as depicted in Figure 11.

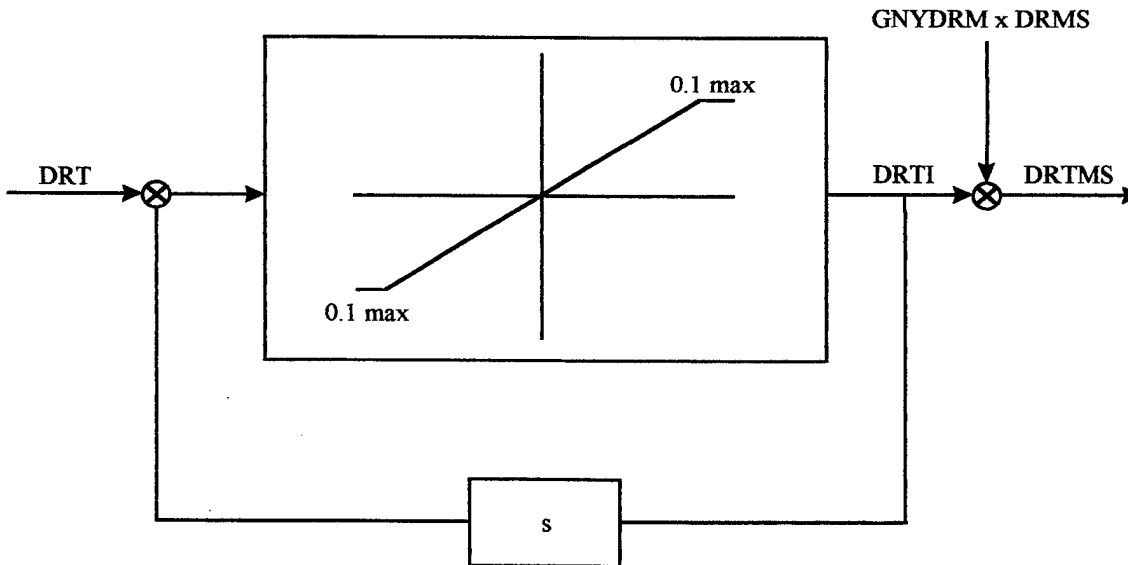


Figure 11. Rudder Trim Commands

e. Lateral Accelerometers

There are four Accelerometer Assemblies (AA) located forward of the crew compartment. These AA's directly measure lateral acceleration and simultaneously filter the signal as shown below:

$$\frac{\text{Measured Acceleration}}{\left(\frac{15^2}{s^2 + 2(.5)(15)s + 15^2} \right) \left(\frac{146^2}{s^2 + 2(.8)(146)s + 146^2} \right)} \rightarrow \text{Lateral Acceleration Signal(NYP)}$$

This signal is sampled at 25 Hz and passed to the lateral acceleration feedback compensator.

f. Lateral Acceleration Feedback Compensator

The lateral acceleration feedback compensator compares the actual lateral acceleration, NYP, as passed from the AA's, to the commanded lateral acceleration, DRTMS, to generate an error signal, or additional lateral acceleration command. A low pass filter is incorporated in this procedure to smooth the output. The resulting signal is sampled at 25 Hz. The process is depicted in Figure 12.

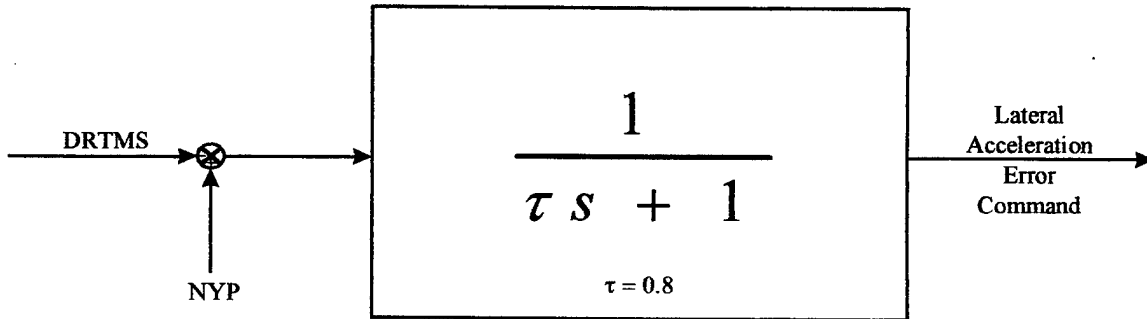


Figure 12. Lateral Acceleration Feedback Compensator

2. Rudder Deflection Command

A simplified block diagram of lateral acceleration conversion to rudder deflection command is shown in Figure 13.

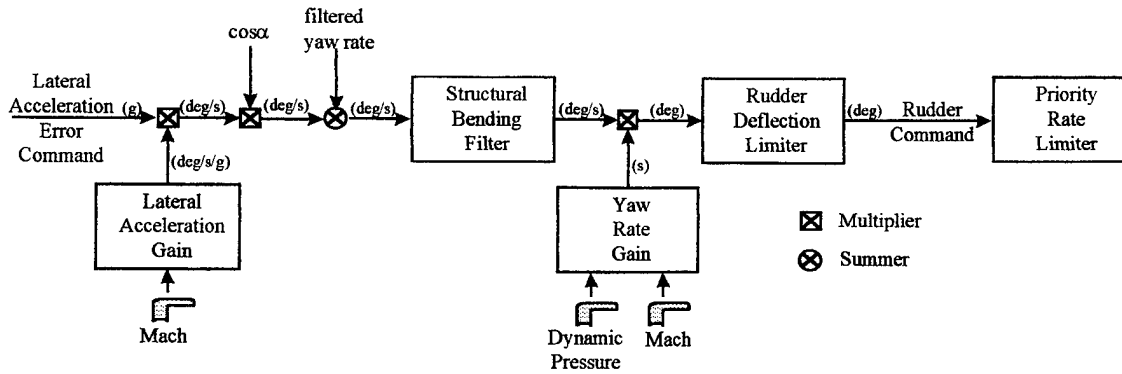


Figure 13. Rudder Deflection Command

The various components of the rudder deflection command path are discussed in the subsections below.

a. Lateral Acceleration Gain

The lateral acceleration gain scheduler produces a gain signal, GRAY, which when multiplied with the lateral acceleration error command, DRTMS, produces a yaw rate command, DAY. This gain is scheduled as a function of Mach as depicted in Figure 14. This gain also converts the units of the signal from g's to deg/sec. The sample rate for this scheduler is 1.04 Hz.

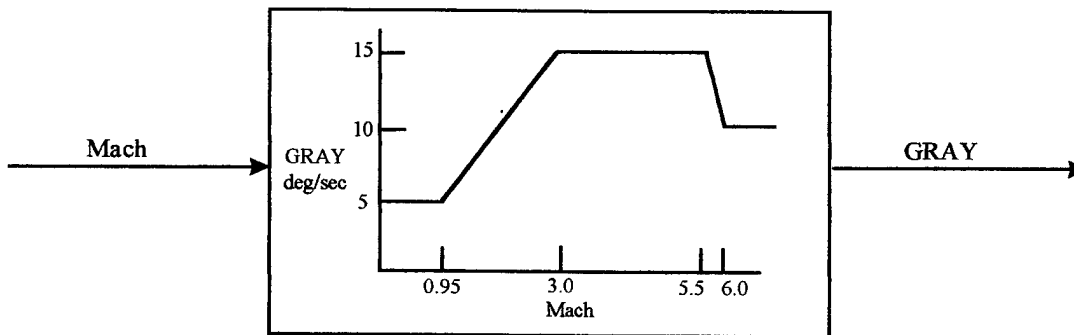


Figure 14. Lateral Acceleration Gain Schedule

b. Cosine of the Angle of Attack (α)

A dimensionless signal, $\cos(\alpha)$, is mixed with the yaw rate command signal and summed with the yaw rate error to produce a yaw rate command about an inertial axis. This signal will always reduce the yaw rate command signal in producing a yaw rate with respect to the

runway. The $\cos(\alpha)$ is sampled at 1.04 Hz. The output signal from this mix is referred to as the unfiltered yaw rate command, DRRCUF.

c. Rate Gyro Assemblies

There are four Rate Gyro Assemblies (RGA's) located on the aft bulkhead below the floor of the payload bay. Each of the RGA's sense rotation about the three vehicle axes and simultaneously filter the signal as shown below:

$$\frac{\text{Measured Acceleration}}{\left(\frac{50}{s + 50} \right) \left(\frac{420^2}{s^2 + 2(.7)(420)s + 420^2} \right)} \rightarrow \text{Body Rates } (P, R, Q)$$

These rates are the primary feedback to the flight control system to maintain control.

d. Yaw Rate Structural Filter

A second-order structural bending filter is applied to the yaw rate feedback.

e. Yaw Rate Error Determination

The filtered body yaw rate, DRPRM, is summed with the product of the sideslip angle times the cosine of the angle of attack, BCOSALF, and yaw rate command, DAXFDC, to determine the yaw rate error, DRERR, as shown in Figure 15. The sideslip angle is not used in the approach and landing flight phase. Therefore, BCOSALF is zero in this analysis. The resulting signal is sampled at 25 Hz.

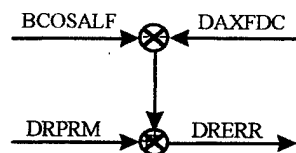


Figure 15. Yaw Rate Error Determination

f. Structural Bending Filter

A structural bending filter is included in series to remove any known Orbiter body bending modes. The resulting signal is the yaw command, DRRC, which is processed at 25 Hz. The filter is made of two consecutive second order notch filters. This fourth order system will inherently result in transport delays which would only contribute to the time lag problem.

g. Yaw Rate Gain

The yaw rate gain scheduler produces a gain signal, GDRC. This gain and a constant, GERYFWDS, is multiplied with the yaw command signal, DRRC, to produce an initial rudder deflection command, DRCPF. This gain is scheduled as a function of Mach and dynamic pressure as depicted in Figure 16. This gain also converts the units of the signal from deg/sec to deg. The sample rate for this scheduler is 1.04 Hz.

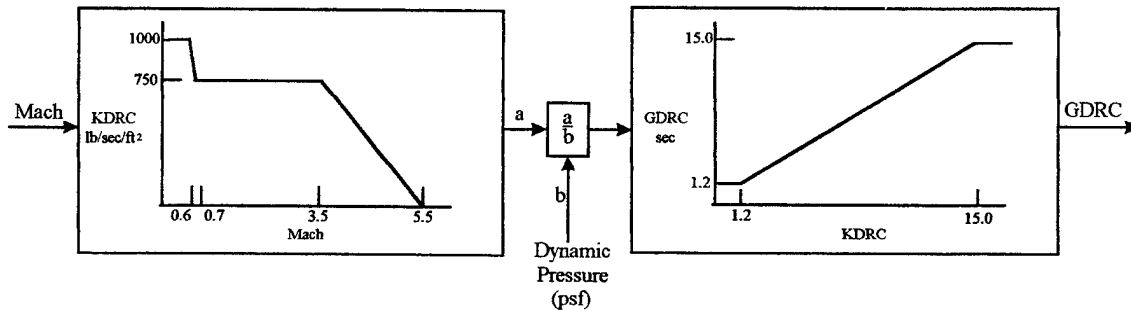


Figure 16. Yaw Rate Gain Scheduler

h. Rudder Deflection Limiter

The rudder deflection limiter provides a maximum rudder deflection limit in the positive and negative directions. The deflection limit, DRC_LIM, is 24.1° and 27.1° in flight and post Weight On Wheels Lock-On (WOWLON), respectively. Within these limits, the limiter passes a one-to-one correlation from the filtered rudder deflection command, DRCPF, to the actual rudder deflection command, DRC. The WOWLON signal is sampled at 6.25 Hz, but the rudder deflection limiter processes at 25 Hz. The system is configured as shown in Figure 17.

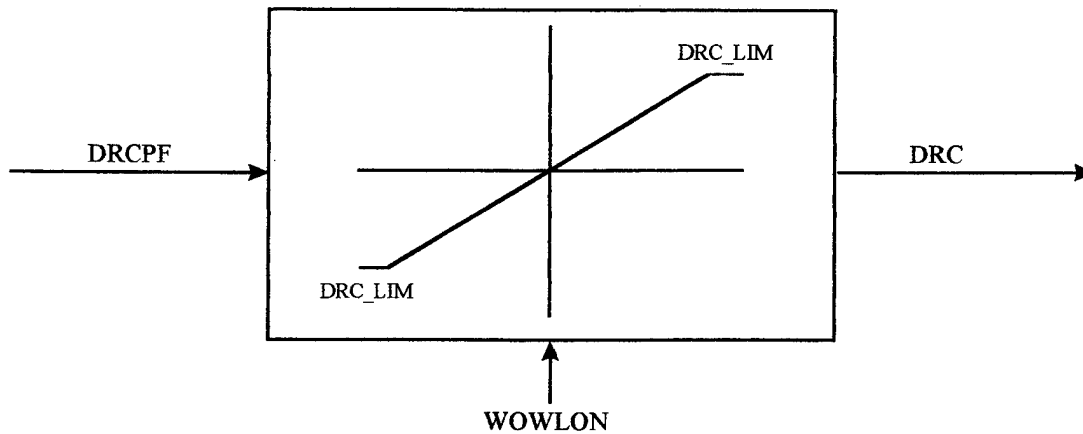


Figure 17. Rudder Deflection Limiter

i. Priority Rate Limiting (PRL)

The rudder deflection command is sent to PRL. PRL limits control surface deflection rates to manage the amount of hydraulic fluid sent to each of the actuators. There are three Auxiliary Power Unit (APU)/hydraulic systems available to provide hydraulic fluid to the control surface actuators. Normally, with three hydraulic systems available, PRL limits the rudder deflection rate to 14 deg/sec [Ref. 4]. This slow deflection rate is conducive to the pilot's rudder inputs being out of phase with Orbiter response. The deflection rate is further reduced depending upon the number of hydraulic systems failed. With one and two systems failed, the rudder deflection rate is limited to 12 and 7 deg/sec, respectively.

B. RUDDER ACTUATOR

The rudder/speedbrake actuators receive hydraulic fluid from all three hydraulic systems through a switching valve. The switching valve produces one hydraulic output pressure source for the rudder/speedbrake servovalves. The power drive unit, mechanical actuator, and actuator drive shaft are shown in Figure 18.

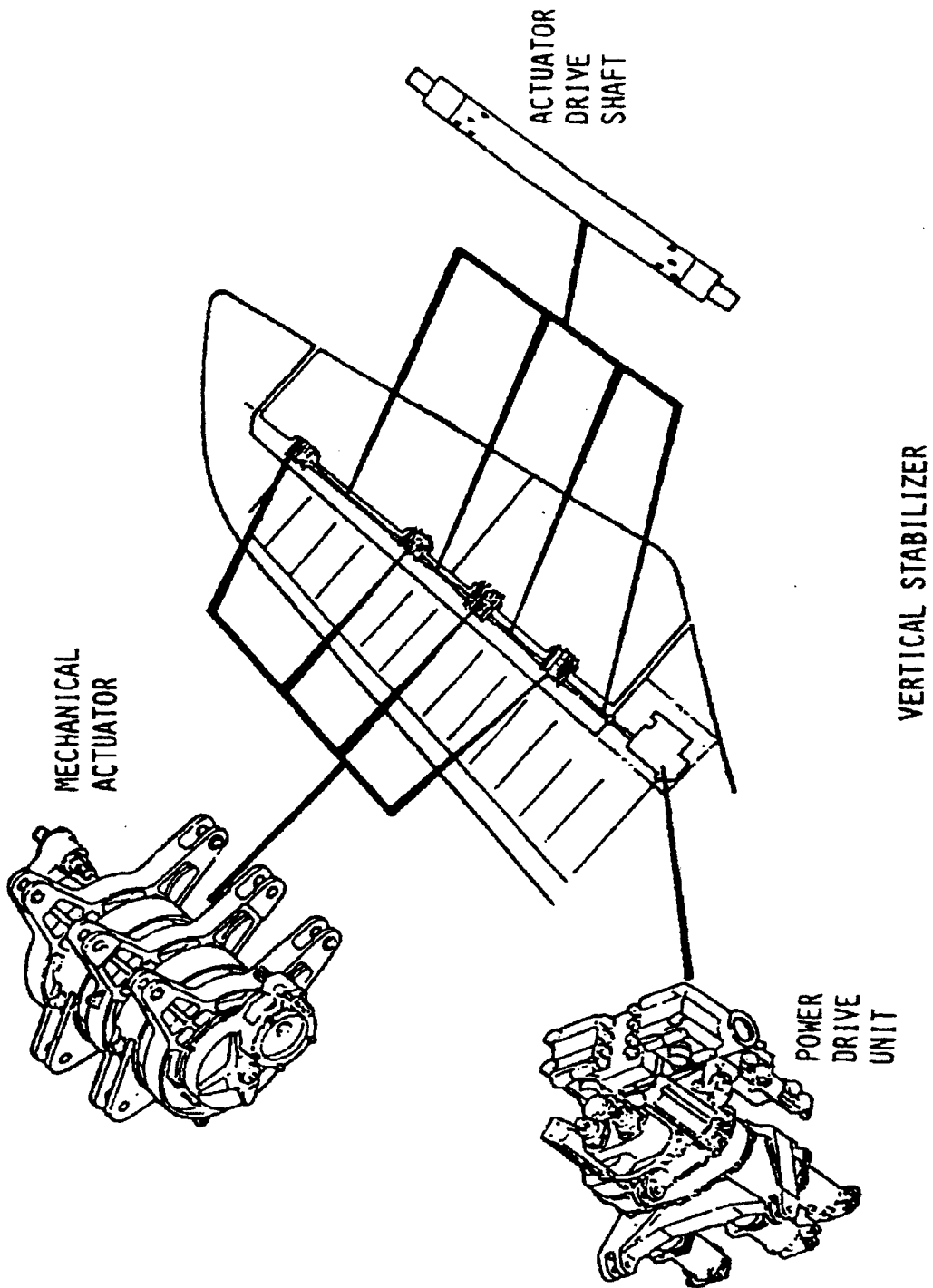


Figure 18. Rudder/Speedbrake Actuator Location [Ref. 6]

IV. EQUATIONS OF MOTION AND STABILITY AND CONTROL

DERIVATIVES

A. ASSUMPTIONS

The following assumptions were used in developing the Equations of Motion (EOM) for the Orbiter in the two point stance:

1. Inertial frame fixed to the flat Earth since the Orbiter is on the ground.
2. Constant vehicle mass properties since there is no propellant consumption and nothing ejected until drag chute deploy.
3. Vehicle is symmetric about the XZ plane. Therefore, $I_{xy} = I_{yz} = C_{y0} = C_{l0} = C_{no} = 0$.
4. Equations of motion are linear about a steady state flight condition. Small perturbation theory implies that the squares and products of perturbations may be neglected. For every perturbation angle α , $\sin(\alpha) = \alpha$ and $\cos(\alpha) = 1$.
5. Atmospheric property variations are negligible. Air density, temperature, pressure changes are negligible over a twenty second period and less than 10,000 feet rolling distance on the ground.
6. Steady state rotation rates, side velocity, and bank angle are all zero. The Orbiter in the two point stance will not perform rapid maneuvers or fly with significant steady state sideslip.
7. The air flow is quasi-steady. In other words, the pressure distributions adjust instantly to rate changes. This assumption is generally valid for angle of attack rate α' if the following condition is satisfied [Ref. 10]: $\alpha'c/2U_1 < 0.04$. For the Orbiter, the chord length $c = 39.56$ ft. and the initial velocity $U_1 = 353$ ft./sec. The inequality is satisfied if $\alpha' < 0.714$ rad/s = 40.9 deg/s. In the two point stance prior to the initiation of derotation, α is essential constant. After initiation of derotation, α' is 1.5 deg/sec. The stability derivatives with respect to α' may be neglected.
8. Motion in the Z direction is constrained due to the runway. Therefore, the downward velocity $W=0$ and the associate forces and moments are zero.
9. Vehicle is at constant α . Therefore, all pitching moment derivatives are zero, the pitch rate, q , is zero, and all control derivatives with respect to q are zero.

10. The elevons are at trail (0°) at touchdown and remain there until the initiation of derotation [Ref. 2]. Therefore, all variations of the coefficients due to elevator and aileron are zero.

11. Forward velocity, U is constant.

B. EQUATIONS OF MOTION

The general EOM in the body-fixed coordinate system obtained from Roskam [Ref. 10] are defined below. The subscript denotes the axis and the apostrophe denotes time derivative. All symbols are defined in the List of Symbols, Acronyms, and/or Abbreviations on page xii. Although the control problem under investigation is a directional control problem, both the longitudinal and lateral/directional equations are included in the derivation and simulation for completeness. The general force, moment, and kinematic equations are:

$$F_x = m(U' - VR + WQ) + mg \sin(\Theta)$$

$$F_y = m(V' + UR - WP) - mg \cos(\Theta) \sin(\Phi)$$

$$F_z = m(W' - UQ + VP) - mg \cos(\Phi) \cos(\Theta)$$

$$L = I_{xx}P' - I_{xz}R' - I_{xz}PQ + (I_{zz} - I_{yy})RQ$$

$$M = I_{yy}Q' + (I_{xx} - I_{zz})PR + I_{xz}(P^2 - R^2)$$

$$N = I_{zz}R' - I_{xz}P' + (I_{yy} - I_{xx})PQ + I_{xz}QR$$

$$P = \Phi' - \psi' \sin(\Theta)$$

$$Q = \Theta' \cos(\Phi) + \psi' \cos(\Theta) \sin(\Phi)$$

$$R = \psi' \cos(\Theta) \cos(\Phi) - \Theta' \sin(\Phi)$$

Each variable is the sum of a steady state components, denoted with a subscript "1", and perturbation components, denoted with lower case:

$$U = U_1 + u \quad V = V_1 + v \quad W = W_1 + w$$

$$P = P_1 + p \quad Q = Q_1 + q \quad R = R_1 + r$$

$$\Psi = \Psi_1 + \psi \quad \Theta = \Theta_1 + \theta \quad \Phi = \Phi_1 + \phi$$

$$\Psi' = \Psi_1' + \psi' \quad \Theta' = \Theta_1' + \theta' \quad \Phi' = \Phi_1' + \phi'$$

$$F_x + F_{x1} + f_x \quad F_y + F_{y1} + f_y \quad F_z + F_{z1} + f_z$$

$$L = L_1 + l \quad M = M_1 + m_a \quad N = N_1 + n$$

The steady state forces, moment, and kinematic equations are as follows:

$$F_{x1} = m(U_1 - V_1 R_1 + W_1 Q_1) + mg \sin(\Theta_1)$$

$$F_{y1} = m(\dot{V}_1 + U_1 R_1 - W_1 P_1) - mg \cos(\Theta_1) \sin(\Phi_1)$$

$$F_{z1} = m(\dot{W}_1 - U_1 Q_1 + V_1 P_1) - mg \cos(\Phi_1) \cos(\Theta_1)$$

$$L_1 = I_{xx} \dot{P}_1 - I_{xz} \dot{R}_1 - I_{xz} P_1 Q_1 + (I_{zz} - I_{yy}) R_1 Q_1$$

$$M_1 = I_{yy} \dot{Q}_1 + (I_{xx} - I_{zz}) P_1 R_1 + I_{xz} (P_1^2 - R_1^2)$$

$$N_1 = I_{zz} \dot{R}_1 - I_{xz} \dot{P}_1 + (I_{yy} - I_{xx}) P_1 Q_1 + I_{xz} Q_1 R_1$$

$$P_1 = \dot{\Phi}_1 - \dot{\psi}_1 \sin(\Theta)$$

$$Q_1 = \dot{\Theta}_1 \cos(\Phi_1) + \dot{\psi}_1 \cos(\Theta_1) \sin(\Phi_1)$$

$$R_1 = \dot{\psi}_1 \cos(\Theta_1) \cos(\Phi_1) - \dot{\Theta}_1 \sin(\Phi_1)$$

The pitch and bank angles are defined such that:

$$\sin(\theta) \cong \theta \quad \sin(\phi) \cong \phi \quad \cos(\theta) \cong \cos(\phi) \cong 1.0$$

This small angle assumption restricts the pitch and bank angle perturbations to less than 15 degrees. This limit is reasonable for landing and rollout and does not constitute any serious restriction. Perturbations are assumed to be sufficiently small such that products and cross-products of the perturbations are negligible with respect to the perturbation itself:

$$pv = pw = pq = pr = qu = qw = qr = ru = rv = 0$$

$$u^2 = v^2 = w^2 = p^2 = r^2 = \phi\theta = \psi'\theta = \psi'\phi = \phi\theta' = 0$$

The perturbation force, moment, and kinematic equations are as follows:

$$\dot{f}_x = m(g\theta \cos(\Theta) + W_1 q - V_1 r + u' - R_1 v + Q_1 w)$$

$$\dot{f}_y = m(-g\phi \cos(\Phi_1) \cos(\Theta_1) + g\theta \sin(\Phi_1) \sin(\Theta_1) - W_1 p + U_1 r + R_1 u + v' - P_1 w)$$

$$\dot{f}_z = m(g\phi \cos(\Theta_1) \sin(\Phi_1) + g\theta \cos(\Phi_1) \sin(\Theta_1) + V_1 p - U_1 q - Q_1 u + P_1 v + w')$$

$$l = I_{xx} \dot{p}' - (Q_1 p + P_1 q) I_{xz} + (-I_{yy} + I_{zz})(R_1 q + Q_1 r) - I_{xz} \dot{r}'$$

$$m_a = 2I_{xz} P_1 p + (I_{xx} - I_{zz}) R_1 p + I_{yy} \dot{q}' + (I_{xx} - I_{zz}) P_1 r - 2I_{xz} R_1 r'$$

$$n = (-I_{xx} + I_{yy})(Q_1 p + P_1 q) - I_{xz} \dot{p}' + (R_1 q + Q_1 r) I_{xz} + I_{zz} \dot{r}'$$

$$p = -\theta \dot{\Psi}_1 \cos(\Theta_1) - \dot{\psi}' \sin(\Theta_1) + \dot{\phi}'$$

$$q = \dot{\theta}' \cos(\Phi_1) + \dot{\psi}' \cos(\Theta_1) \sin(\Phi_1) - \dot{\theta}' \dot{\Psi}_1 \sin(\Phi_1) \sin(\Theta_1) + \dot{\Psi}_1' \cos(\Phi_1) \cos(\Theta_1) - \dot{\Theta}_1' \sin(\Phi_1) \dot{\phi}$$

$$r = -(\dot{\Theta}_1' \cos(\Phi_1) + \dot{\Psi}_1' \cos(\Theta_1) \sin(\Phi_1)) \dot{\phi} + \dot{\psi}' \cos(\Phi_1) \cos(\Theta_1) - \dot{\theta}' \sin(\Phi_1) - \dot{\theta}' \dot{\Psi}_1' \cos(\Phi_1) \sin(\Theta_1)$$

1. Longitudinal Equations of Motion

The longitudinal forces in the stability axis system are defined as:

$$F_{x1} = -D \quad F_{z1} = -L \quad D_1 = C_{D1} q_{dyn} S \quad L_1 = C_{L1} q_{dyn} S \quad M_1 = C_{m1} q_{dyn} S c$$

The non-dimensional stability and control derivatives in the stability axis are defined as:

$$\begin{aligned}
C_{D_u} &= \frac{\partial}{\partial \frac{u}{U_1}} C_D & C_{D_\alpha} &= \frac{\partial}{\partial \alpha} C_D & C_{D_q} &= \frac{\partial}{\partial \frac{qc}{2U_1}} C_D & C_{D_{\delta_e}} &= \frac{\partial}{\partial \delta_e} C_D \\
C_{L_u} &= \frac{\partial}{\partial \frac{u}{U_1}} C_L & C_{L_\alpha} &= \frac{\partial}{\partial \alpha} C_L & C_{L_q} &= \frac{\partial}{\partial \frac{qc}{2U_1}} C_L & C_{L_{\delta_e}} &= \frac{\partial}{\partial \delta_e} C_L \\
C_{m_u} &= \frac{\partial}{\partial \frac{u}{U_1}} C_m & C_{m_\alpha} &= \frac{\partial}{\partial \alpha} C_m & C_{m_q} &= \frac{\partial}{\partial \frac{qc}{2U_1}} C_m & C_{m_{\delta_e}} &= \frac{\partial}{\partial \delta_e} C_m
\end{aligned}$$

The longitudinal dimensional stability axis derivatives are defined as:

Axial force:

$$\begin{aligned}
X_u &= \frac{-q_{\dot{\phi}} S (C_{D_u} + 2C_{D_1})}{mU_1} \frac{1}{\text{sec}} & X_\alpha &= \frac{-q_{\dot{\phi}} S (C_{D_\alpha} + 2C_{D_1})}{m} \frac{ft}{\text{rad sec}^2} & X_w &= \frac{X_\alpha}{U_1} \frac{1}{\text{sec}} \\
X_q &= \frac{-q_{\dot{\phi}} S c C_{D_q}}{2mU_1} \frac{ft}{\text{rad sec}} & X_{\delta_e} &= \frac{-q_{\dot{\phi}} S C_{D_{\delta_e}}}{m} \frac{ft}{\text{rad sec}^2}
\end{aligned}$$

Normal force:

$$\begin{aligned}
Z_u &= \frac{-q_{\dot{\phi}} S (C_{L_u} + 2C_{L_1})}{mU_1} \frac{1}{\text{sec}} & Z_\alpha &= \frac{-q_{\dot{\phi}} S (C_{L_\alpha} + 2C_{L_1})}{m} \frac{ft}{\text{rad sec}^2} & Z_w &= \frac{Z_\alpha}{U_1} \frac{1}{\text{sec}} \\
Z_q &= \frac{-q_{\dot{\phi}} S c C_{L_q}}{2mU_1} \frac{ft}{\text{rad sec}} & Z_{\delta_e} &= \frac{-q_{\dot{\phi}} S C_{L_{\delta_e}}}{m} \frac{ft}{\text{rad sec}^2}
\end{aligned}$$

Pitching moment:

$$\begin{aligned}
M_u &= \frac{q_{\dot{\phi}} S c (C_{m_u} + 2C_{m_1})}{I_{yy} U_1} \frac{\text{rad}}{\text{ft sec}} & M_\alpha &= \frac{q_{\dot{\phi}} S c C_{m_\alpha}}{I_{yy}} \frac{1}{\text{sec}^2} & M_w &= \frac{M_\alpha}{U_1} \frac{\text{rad}}{\text{ft sec}} \\
M_q &= \frac{q_{\dot{\phi}} S c^2 C_{m_q}}{2I_{yy} U_1} \frac{1}{\text{sec}} & M_{\delta_e} &= \frac{q_{\dot{\phi}} S c C_{m_{\delta_e}}}{I_{yy}} \frac{1}{\text{sec}^2}
\end{aligned}$$

Recall that motion in the Z direction is constrained due to the runway. Therefore, the downward velocity $W=0$ and the associate forces and moments X_w , Z_w , and M_w are zero and not included in the state space equation.

The pitch moment of inertia changes slightly when the Orbiter touches down. The center of rotation shifts from the center of mass to the axis formed by the line between the points where

the main gear tires meet the runway. The parallel axis theorem [Ref. 11] allows a simple shift of the moment of inertia with the following equation: $I_{y_{mg}} = I_{yy} + mh^2$ where $I_{y_{mg}}$ is the moment of inertia about the main gear, m is the mass of the Orbiter, and h is the distance between the center of mass and the new rotation point. All pitch moment dimensional stability derivative equations will be adjusted accordingly by multiplying by $I_{yy}/I_{y_{mg}}$.

The following are the perturbed longitudinal equations of motion:

$$\begin{aligned} u' &= X_u u + X_\alpha \alpha + X_q q - g \cos(\Theta_1) \theta + X_{\delta_e} \delta_e \\ \alpha' &= \frac{Z_u u}{U_1} + \frac{Z_\alpha \alpha}{U_1} + \frac{(U_1 + Z_q) q}{U_1} - \frac{g \sin(\Theta_1) \theta}{U_1} + \frac{Z_{\delta_e} \delta_e}{U_1} \\ q' &= M_u u + M_\alpha \alpha + M_q q + M_{\delta_e} \delta_e \\ \theta &= q \end{aligned}$$

In state space form, $X' = AX + BU$:

$$\begin{bmatrix} u' \\ \alpha' \\ q' \\ \theta \end{bmatrix} = \begin{bmatrix} X_u & X_\alpha & X_q & -g \cos(\Theta_1) \\ \frac{Z_u}{U_1} & \frac{Z_\alpha}{U_1} & \frac{Z_q}{U_1} + 1 & -\frac{g \sin(\Theta_1)}{U_1} \\ M_u & M_q & M_q & 0 \\ 0 & 0 & 1 & 0 \end{bmatrix} \begin{bmatrix} u \\ \alpha \\ q \\ \theta \end{bmatrix} + \begin{bmatrix} X_{\delta_e} \\ \frac{Z_{\delta_e}}{U_1} \\ M_{\delta_e} \\ 0 \end{bmatrix} \begin{bmatrix} \delta_e \end{bmatrix}$$

2. Lateral-Directional Equations of Motion

The lateral-directional forces are defined as:

$$F_{y1} = C_y q_{dyn} S \quad L_1 = c_{l1} q_{dyn} S b \quad N_1 = C_n q_{dyn} S b$$

The non-dimensional stability and control derivatives are defined as:

$$\begin{aligned} C_{y_\beta} &= \frac{\partial}{\partial \beta} C_y & C_{y_p} &= \frac{\partial}{\partial \frac{pb}{2U_1}} C_y & C_{y_r} &= \frac{\partial}{\partial \frac{rb}{2U_1}} C_y & C_{y_{\delta_a}} &= \frac{\partial}{\partial \delta_a} C_y & C_{y_{\delta_r}} &= \frac{\partial}{\partial \delta_r} C_y \\ C_{l_\beta} &= \frac{\partial}{\partial \beta} C_l & C_{l_p} &= \frac{\partial}{\partial \frac{pb}{2U_1}} C_l & C_{l_r} &= \frac{\partial}{\partial \frac{rb}{2U_1}} C_l & C_{l_{\delta_a}} &= \frac{\partial}{\partial \delta_a} C_l & C_{l_{\delta_r}} &= \frac{\partial}{\partial \delta_r} C_l \end{aligned}$$

$$C_{n_\beta} = \frac{\partial}{\partial \beta} C_n \quad C_{n_p} = \frac{\partial}{\partial \frac{pb}{2U_1}} C_n \quad C_{n_r} = \frac{\partial}{\partial \frac{rb}{2U_1}} C_n \quad C_{n_{\delta_a}} = \frac{\partial}{\partial \delta_a} C_n \quad C_{n_{\delta_r}} = \frac{\partial}{\partial \delta_r} C_n$$

The lateral-directional dimensional stability and control derivatives are defined as:

Side force:

$$Y_\beta = \frac{q_{\text{dyn}} S C_{y_\beta}}{m} \frac{ft}{\text{rad sec}^2} \quad Y_p = \frac{q_{\text{dyn}} S b C_{y_p}}{2mU_1} \frac{ft}{\text{rad sec}} \quad Y_r = \frac{q_{\text{dyn}} S b C_{y_r}}{2mU_1} \frac{ft}{\text{rad sec}}$$

$$Y_{\delta_a} = \frac{q_{\text{dyn}} S C_{y_{\delta_a}}}{m} \frac{ft}{\text{rad sec}^2} \quad Y_{\delta_r} = \frac{q_{\text{dyn}} S C_{y_{\delta_r}}}{m} \frac{ft}{\text{rad sec}^2}$$

Rolling moment:

$$L_\beta = \frac{q_{\text{dyn}} S b C_{l_\beta}}{I_{xx}} \frac{1}{\text{sec}^2} \quad L_p = \frac{q_{\text{dyn}} S b^2 C_{l_p}}{2I_{xx} U_1} \frac{1}{\text{sec}} \quad L_r = \frac{q_{\text{dyn}} S b^2 C_{l_r}}{2I_{xx} U_1} \frac{1}{\text{sec}}$$

$$L_{\delta_a} = \frac{q_{\text{dyn}} S b C_{l_{\delta_a}}}{I_{xx}} \frac{1}{\text{sec}^2} \quad L_{\delta_r} = \frac{q_{\text{dyn}} S b C_{l_{\delta_r}}}{I_{xx}} \frac{1}{\text{sec}^2}$$

Yawing moment:

$$N_\beta = \frac{q_{\text{dyn}} S b C_{n_\beta}}{I_{zz}} \frac{1}{\text{sec}^2} \quad N_p = \frac{q_{\text{dyn}} S b^2 C_{n_p}}{2I_{zz} U_1} \frac{1}{\text{sec}} \quad N_r = \frac{q_{\text{dyn}} S b^2 C_{n_r}}{2I_{zz} U_1} \frac{1}{\text{sec}}$$

$$N_{\delta_a} = \frac{q_{\text{dyn}} S b C_{n_{\delta_a}}}{I_{zz}} \frac{1}{\text{sec}^2} \quad N_{\delta_r} = \frac{q_{\text{dyn}} S b C_{n_{\delta_r}}}{I_{zz}} \frac{1}{\text{sec}^2}$$

The yaw moment of inertia changes slightly when the Orbiter touches down. The center of rotation shifts from the center of mass to a point between the main gear. It is assumed that this point will be directly between the main gear. The parallel axis theorem [Ref. 11] allows a simple shift of the moment of inertia with the following equation: $I_{zmg} = I_{zz} + mh^2$ where I_{zmg} is the moment of inertia about the main gear, m is the mass of the Orbiter, and h is the distance between the center of mass and the new rotation point. All yaw moment dimensional stability derivative equations will be adjusted accordingly by multiplying by I_{zz}/I_{zmg} .

The roll moment of inertia is assumed to remain referenced to the center of mass as the main gear struts are free to compress and extend which permits the Orbiter to roll about a point near the center of mass. I_{xx} will not be adjusted.

The following are the perturbed lateral-directional equations of motion:

$$\beta' = Y_\beta \frac{\beta}{U_1} + Y_p \frac{p}{U_1} + \left(Y_r \frac{1}{U_1} - 1 \right) r + \frac{g \cos(\Theta_1) \varphi}{U_1} + Y_{\delta_a} \frac{\delta_a}{U_1} + Y_{\delta_r} \frac{\delta_r}{U_1}$$

$$p' = L_\beta \beta + L_p p + L_r r + \frac{I_{xz} r'}{I_{xx}} + L_{\delta_a} \delta_a + L_{\delta_r} \delta_r$$

$$r' = N_\beta \beta + N_p p + N_r r + \frac{I_{xz} p'}{I_{zz}} + N_{\delta_a} \delta_a + N_{\delta_r} \delta_r$$

$$\varphi' = p + \tan(\Theta_1) r$$

For small Θ 's and small I_{xz} , inertial coupling is negligible; therefore' the $I_{xz} r'/I_{xx}$ and $I_{xz} p'/I_{zz}$ terms are disregarded.

In state space form, $X' = AX + BU$:

$$\begin{bmatrix} \beta' \\ p' \\ r' \\ \varphi' \end{bmatrix} = \begin{bmatrix} \frac{Y_\beta}{U_1} & \frac{Y_p}{U_1} & \frac{Y_r}{U_1} - 1 & \frac{g \cos(\Theta_1)}{U_1} \\ L_\beta & L_p & L_r & 0 \\ N_\beta & N_p & N_r & 0 \\ 0 & 1 & \tan(\Theta_1) & 0 \end{bmatrix} \begin{bmatrix} \beta \\ p \\ r \\ \varphi \end{bmatrix} + \begin{bmatrix} \frac{Y_{\delta_a}}{U_1} & \frac{Y_{\delta_r}}{U_1} \\ L_{\delta_a} & L_{\delta_r} \\ N_{\delta_a} & N_{\delta_r} \\ 0 & 0 \end{bmatrix} \begin{bmatrix} \delta_a \\ \delta_r \end{bmatrix}$$

3. Longitudinal and Lateral-Directional EOM in State Space Form

The full 8x8 state space equation is shown below: $X' = AX + BU$. The longitudinal and lateral-directional EOM are decoupled in this analysis. The longitudinal EOM need not be solved to analyze this problem. The longitudinal EOM are included for completeness.

$$\begin{bmatrix} u' \\ \alpha' \\ q' \\ \theta' \\ \beta' \\ p' \\ r' \\ \varphi' \end{bmatrix} = \begin{bmatrix} X_u & X_\alpha & X_q & -g \cos(\Theta_1) & 0 & 0 & 0 & 0 \\ Z_u & Z_\alpha & Z_q & \frac{g \sin(\Theta_1)}{U_1} & 0 & 0 & 0 & 0 \\ \frac{U_1}{U_1} & \frac{U_1}{U_1} & \frac{U_1}{U_1} + 1 & -\frac{g \sin(\Theta_1)}{U_1} & 0 & 0 & 0 & 0 \\ M_u & M_\alpha & M_q & 0 & 0 & 0 & 0 & 0 \\ 0 & 0 & 1 & 0 & 0 & 0 & 0 & 0 \\ 0 & 0 & 0 & 0 & \frac{Y_\beta}{U_1} & \frac{Y_p}{U_1} & \frac{Y_r}{U_1} - 1 & \frac{g \cos(\Theta_1)}{U_1} \\ 0 & 0 & 0 & 0 & L_\beta & L_p & L_r & 0 \\ 0 & 0 & 0 & 0 & N_\beta & N_p & N_r & 0 \\ 0 & 0 & 0 & 0 & 0 & 1 & \tan(\Theta_1) & 0 \end{bmatrix} \begin{bmatrix} u \\ \alpha \\ q \\ \theta \\ \beta \\ p \\ r \\ \varphi \end{bmatrix} + \begin{bmatrix} X_{\delta_e} & 0 & 0 \\ \frac{Z_{\delta_e}}{U_1} & 0 & 0 \\ M_{\delta_e} & 0 & 0 \\ 0 & 0 & 0 \\ 0 & \frac{Y_{\delta_a}}{U_1} & \frac{Y_{\delta_r}}{U_1} \\ 0 & L_{\delta_a} & L_{\delta_r} \\ 0 & N_{\delta_a} & N_{\delta_r} \\ 0 & 0 & 0 \end{bmatrix} \begin{bmatrix} \delta_e \\ \delta_a \\ \delta_r \end{bmatrix}$$

4. Determination of the Non-Dimensional Stability Derivatives

The non-dimensional force and moment coefficients were determined in wind tunnel testing and updated based on actual flight data. The equations and coefficients are found in the Operational Aerodynamic Data Book Volumes I and III [Ref. 12].

a. Longitudinal Stability Derivatives

The Taylor series first order expansion of aerodynamic coefficients is given by:

$$C_{D1} = C_{D0} + C_{D\alpha}a1 + C_{D\delta}(\delta_e)_1$$

$$C_{L1} = C_{L0} + C_{L\alpha}a1 + C_{L\delta}(\delta_e)_1$$

$$C_{m1} = C_{m0} + C_{m\alpha}a1 + C_{m\delta}(\delta_e)_1$$

The elevons are at trail (0°) at touchdown [Ref. 2]. Postlanding, the elevon is deflecting as required to balance the longitudinal moment equation and maintain a constant pitch attitude. However, elevon deflection is minimal until the start of derotation. At this time, the elevons ramp quickly downward as theta decreases at a rate of 1-2 deg/sec. Therefore, $(\delta_e)_1$ is negligible in the two point stance and set to 0 in these three equations.

The coefficients [Ref. 12] are defined as:

$$C_{()1} = C_{()BASIC} + \Delta C_{()high\ alt} + \Delta C_{()real\ gas} + \Delta C_{()viscous\ interaction} + \Delta C_{()BF} + \Delta C_{()elevator/aileron} + \Delta C_{()plunging} + \Delta C_{()pitch\ rate} + \Delta C_{()LG} + \Delta C_{()GE} + \Delta C_{()silt\ pod} + \Delta C_{()vehicle}$$

where the subscript () denotes lift force (L), drag force (D), or pitching moment (m) and:

$C_{()BASIC}$ = Basic, full-scale, freestream, rigid body force or moment coefficient.

$\Delta C_{()high\ alt}$ = Change in force or moment coefficient due to high alt. effects ($h > 285,000$ ft).

$\Delta C_{()real\ gas}$ = Change in force or moment coefficient due to real gas effects.

$\Delta C_{()viscous\ interaction}$ = Change in force or moment coefficient due to viscous interaction (V_∞ effects).

$\Delta C_{()BF}$ = Change in force or moment coefficient due to body flap deflection.

$\Delta C_{()elevator/aileron}$ = Change in force or moment coefficient due to elevator and aileron deflection.

$\Delta C_{()plunging}$ = Change in force or moment coefficient due to rate of change of alpha.

$\Delta C_{()pitch\ rate}$ = Change in force or moment coefficient due to pitch rate.

$\Delta C_{()LG}$ = Change in force or moment coefficient due to fully extended landing gear.

$\Delta C_{()GE}$ = Change in force or moment coefficient due to proximity of the ground.

$\Delta C_{()silt\ pod}$ = Change in force or moment coefficient due to addition of silt pods.

$\Delta C_{()vehicle}$ = Change in force or moment coefficient due to geometry differences between vehicles.

$\Delta C_{()high\ alt}$ and $\Delta C_{()real\ gas}$ are not applicable below an altitude of 265,000 ft. and $M < 6.0$, respectively. $\Delta C_{()viscous\ interaction}$ is not a factor since V_∞' is zero. $\Delta C_{()elevator/aileron}$ is assumed to be zero since elevator/aileron deflection is considered negligible. $\Delta C_{()plunging}$ and $\Delta C_{()pitch\ rate}$ are not a factor with the Orbiter on the ground in the two point stance since the pitch rate and angle of attack are essential constant until the initiation of derotation. This analysis will assume Orbiter Vehicle (OV) 103 which does not have a silts pod; therefore' $\Delta C_{()silts\ pod}$ is not applicable. The above equation can be reduced to:

$$C_{()l} = C_{()BASIC} + \Delta C_{()BF} + \Delta C_{()LG} + \Delta C_{()GE} + \Delta C_{()vehicle}$$

Each of the terms in the above equation was obtained by linear interpolation of data extracted from a table at $\alpha = 10^\circ$, $M=0.4$ and $\alpha = 10^\circ$, $M=0.25$ to obtain data applicable for $M=0.325$ (353 fps) for both the lift and drag coefficients. $C_{L\alpha}$ was determined by breaking each of $C_{()BASIC}$, $\Delta C_{()BF}$, $\Delta C_{()LG}$, $\Delta C_{()GE}$, and $\Delta C_{()vehicle}$ terms into C_{L0} and $C_{L\alpha}$ components and summing the $C_{L\alpha}$ contributions. $C_{D\alpha}$ was determined in the same manner.

Since U is considered constant in this analysis, C_{D_u} and C_{L_u} are zero. C_{D_q} and C_{L_q} are zero since the pitch rate is zero. The lift and drag coefficients pertinent to this analysis are summarize in Table 3.

Table 3. Lift and Drag Coefficients

Lift and Drag Coefficients	Value (per °)
C_{L1}	0.54055
$C_{L\alpha}$	0.05948
C_{D1}	0.16712
$C_{D\alpha}$	0.00992

b. *Lateral-Directional Stability Derivatives*

The Taylor series first order expansion of the lateral-directional aerodynamic coefficients are provided for completeness. The Taylor series first order expansion of aerodynamic coefficients is given by:

$$C_{y1} = C_{y0} + C_{y\beta}\beta_1 + C_{y\delta\alpha}(\delta\alpha)_1 + C_{y\delta}(\delta r)_1$$

$$C_{l1} = C_{l0} + C_{l\beta}\beta_1 + C_{l\delta\alpha}(\delta\alpha)_1 + C_{l\delta}(\delta)_1$$

$$C_{m1} = C_{m0} + C_{m\beta}\beta_1 + C_{m\delta\alpha}(\delta\alpha)_1 + C_{m\delta}(\delta)_1$$

The lateral-directional bias coefficients are assumed to be zero for a symmetrical airframe: $C_{y0} = C_{l0} = C_{n0} = 0$. At touchdown, a software flag denoted 'flat turn' is set [Ref. 13]. When this flag is set, lateral motion is accomplished without elevon motion, using rudder only. Therefore, aileron deflection is negligible in the two point stance and $(\delta\alpha)_1$ are set to zero in the above three equations. The coefficients [Ref. 12] are defined as:

$$C_{(l)} = C_{(l)\text{sideslip}} + \Delta C_{(l)\text{aileron}} + \Delta C_{(l)\text{rudder}} + \Delta C_{(l)\text{roll rate}} + \Delta C_{(l)\text{yaw rate}} + \Delta C_{(l)\text{silt pod}} + \Delta C_{(l)\text{vehicle}}$$

where the subscript () denotes side force (y), yawing moment (n), or rolling moment (l), and:

$C_{(l)\text{sideslip}}$ = Basic, full-scale, freestream force or moment coefficient due to sideslip angle.

$\Delta C_{(l)\text{aileron}}$ = Change in force or moment coefficient due to aileron deflection.

$\Delta C_{(l)\text{rudder}}$ = Change in force or moment coefficient due to rudder deflection.

$\Delta C_{(l)\text{roll rate}}$ = Change in force or moment coefficient due to roll rate.

$\Delta C_{(l)\text{yaw rate}}$ = Change in force or moment coefficient due to yaw rate.

$\Delta C_{(l)\text{silt pod}}$ = Change in force or moment coefficient due to addition of silt pods.

$\Delta C_{(l)\text{vehicle}}$ = Change in force or moment coefficient due to geometry differences between vehicles.

$\Delta C_{(l)\text{aileron}}$ may be dropped from this equation since aileron deflection is negligible.

Each of the lateral-directional stability and control derivatives was obtained by linear interpolation of data extracted from a table at $\alpha = 10^\circ$, $M=0.4$ and $\alpha = 10^\circ$, $M=0.25$ to obtain data applicable for $M=0.325$ (353 fps). The side force, rolling moment, and yawing moment coefficients pertinent to this analysis are summarize in Table 4.

Table 4. Side Force, Rolling Moment, and Yawing Moment Coefficients

Side Force, Rolling Moment, and Yawing Moment Coefficients	Value (per °)
$C_{y\beta}$	-0.01705
C_{y_p}	0
C_{y_r}	0
$C_{y_{\delta_r}}$	0.00138
$C_{l\beta}$	-0.00205
C_{l_p}	-0.3189
C_{l_r}	0.1890
$C_{l_{\delta_r}}$	0.0032
$C_{n\beta}$	0.0010
C_{n_p}	0.0280
C_{n_r}	-0.2925
$C_{n_{\delta_r}}$	-0.00054

V. PROPOSED FCS MODIFICATIONS TO IMPROVE DIRECTIONAL CONTROL IN THE TWO POINT STANCE

The rudder FCS susceptibility to PIO results from the slow surface rate, slow response time from rudder pedal input to rudder deflection, the power of the rudder, and the placement of the rudder with respect to the gear. Increasing the surface rate requires hardware modification. Analysis of hardware modifications are beyond the scope of this thesis. Transport delay might be decreased by shortening time delays in the FCS, linearizing the rudder pedal command shaper, and/or disabling Ny feedback. The power of the rudder might be reduced by decreasing the rudder pedal gain.

Options to improve directional control may be categorized into expensive and inexpensive changes. Inexpensive options include those changes which require only software I-load or K-load change or a new piloting technique. Software I-loads and K-loads are constants which are not coded in the software and can be easily changed with no actual software code change. Expensive options include hardware changes, software changes which require a code change, and changes which require FCS recertification.

Table 5 summarizes the problems with the current FCS, potential changes to the FCS to reduce susceptibility to PIO, the relative cost of the change, and whether the change is evaluated in this thesis.

Table 5. Potential Changes to the FCS

Problem	Potential Fixes	Relative Cost	Evaluated
Slow rudder rate	Hardware modification	Very expensive	No
Slow rudder response	Decrease time delays	Inexpensive	Yes
	Linearize rudder command shaper	Inexpensive	Yes
	Disable Ny feedback	Expensive	Yes
Powerful rudder	Decrease pedal gain	Inexpensive	Yes
Position of rudder	Redesign Orbiter	Very expensive	No

A. LINEARIZE THE RUDDER PEDAL COMMAND SHAPER

The rudder command shaper was described in Section III.A.1.b. Recall that the shaping schedule is parabolic and conforms to the following function:

$$DRMS = (0.042)DRMAN^2 + (0.131)DRMAN .$$

The shaper can be linearized by changing 0.042 to 0 and 0.131. to 1.0. The above equation becomes: $DRMS = DRMAN$. This change provides a one-to-one response up to the limits of $\pm 22.5^\circ$ which may result in a more predictable rudder response.

B. REDUCE THE RUDDER PEDAL GAIN

The rudder pedal gain was described in Section III.A.1.c. Reducing the gain will reduce the g-command authority on the rudder and may reduce over-controlling of the Orbiter. The current gain value is 0.08574 for a touchdown speed of 207 KEAS. The proposal is to limit the gain, GNYDRM to 0.04 at 683 fps TAS and below. This change will reduce the gain by 47% which may reduce the over-controlling tendency.

C. DECREASE TIME LAGS

The time lag between rudder pedal input and rudder deflection can be reduced by changing the Ny feedback time constant, described in Section III.A.1.f, from $\tau = 0.8$ s to $\tau = 0.2$ s. This change should result in quicker rudder response from the FCS which should reduce the susceptibility to PIO.

D. DISABLE LATERAL ACCELERATION FEEDBACK

Another option is to disable Ny feedback in combination with changing the Ny feedback time constant from $\tau=0.8$ s to $\tau=0.2$ s. This change would result in a more direct rudder FCS by allowing the rudder command to pass directly through the system with minimal delay. This change would require software code change and is relatively expensive.

VI. YAW FCS SIMULATION

Directional control was evaluated by incorporating Orbiter lateral-directional control laws and longitudinal and lateral-directional EOM in MATLAB 5.0 and Simulink. The script program, 'eom.m', defines the initial conditions, mass properties, stability and control derivatives, and longitudinal and lateral-directional EOM in state space form. The code for 'eom.m' is contained in Appendix A. The code for the Simulink simulation is contained in Appendix B. The plotting program, 'FCSplot.m', is contained in Appendix C.

A. SIMULATION INITIAL CONDITIONS

The case investigated is comparable to the STS-62 touchdown flight conditions. The commander input approximately $+15^\circ$ (right) rudder pedal deflection followed by -15° (left) rudder pedal deflection in the two point stance in an attempt to capture runway centerline. Landing speed was approximately 207 KEAS with minimal crosswind (< 2 knots). Table 6 contains the initial conditions used in the simulation.

Table 6. Initial Conditions

Parameter	Initial Value
Vehicle Weight	228237 lbs
Xcg	1084.15 inches
Ycg	0
Zcg	370.65 inches
Ixx	$8.58677e+05$ slugs*ft ²
Iyy	$6.8699075e+06$ slugs*ft ²
Izz	$7.1334485e+06$ slugs*ft ²
Wing Surface Area	2690 ft ²
Chord Length	39.56 ft
U1	207 KEAS (353 fps)
Runway rolling μ	0.03
Sea Level Density	0.002377 slugs/ft ³
Θ_1	9°
α	10°

B. FCS CONFIGURATIONS EVALUATED

Simulations were run to compare six FCS configurations as defined in Table 7.

Table 7. FCS Configurations Evaluated

Case Number	FCS Configuration (Simulation Name)
0	Current configuration (baseline)
1	Disable Ny feedback (nony)
2	Decrease time lag τ to 0.2 (tau)
3	Linearize rudder shaper (linrud)
4	Reduce rudder pedal gain (rudgain)
5	Cases 3,4,5 combined (done)

C. SIMULATION

The simulations were run in the time domain for 30 seconds using Dormand-Prince integrator. The simulated rudder pedal deflection included a rudder doublet of $+15^\circ$ rudder at 2 seconds followed by -15° as depicted in Figure 19. The master Simulink block diagram is shown in Figures 20.

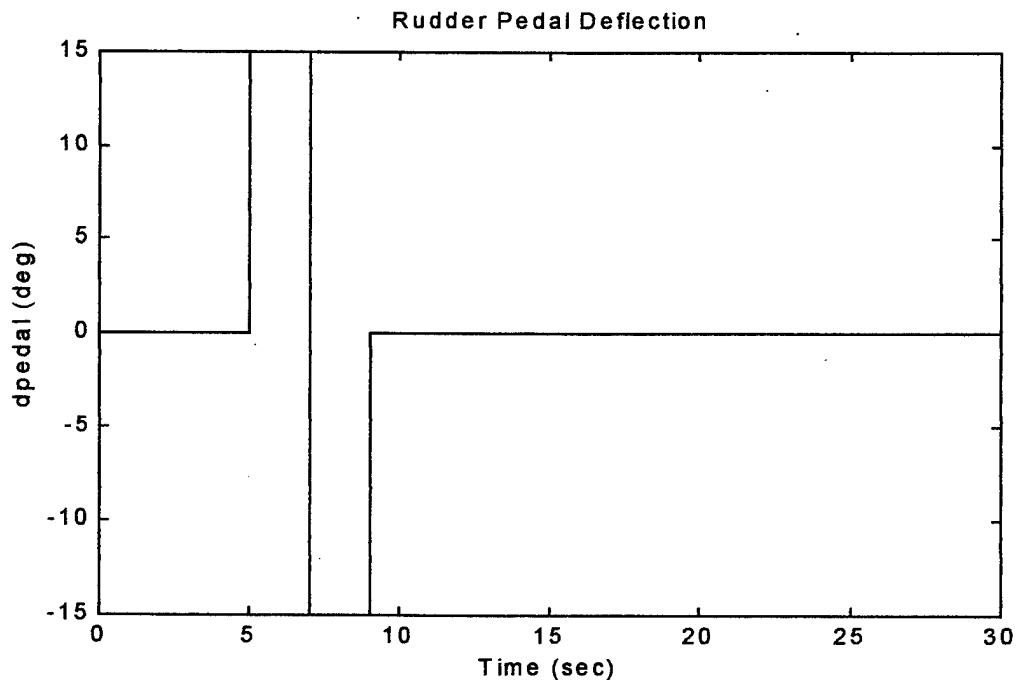


Figure 19. Rudder Pedal Deflection

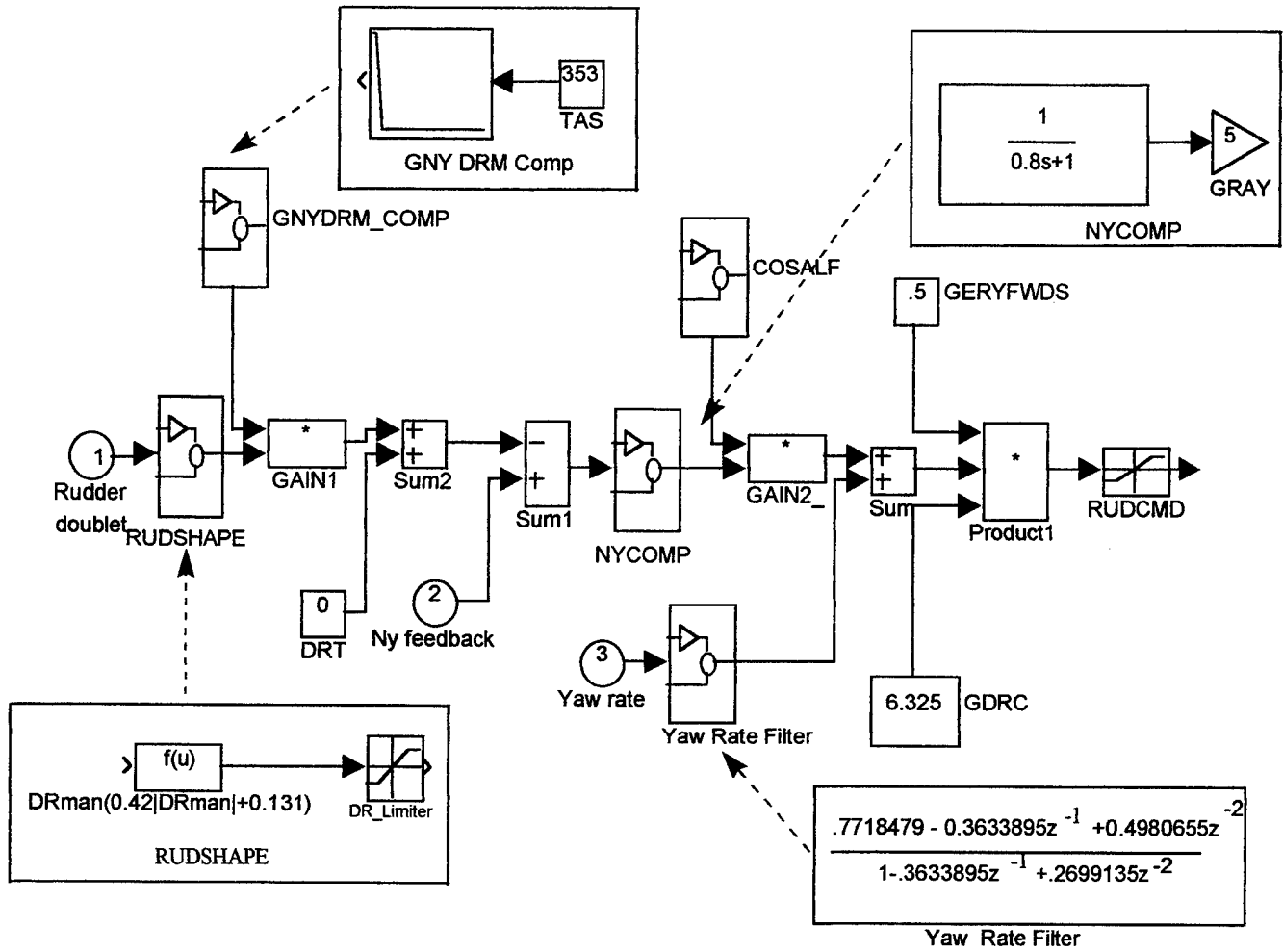


Figure 21. YAW FCS Block Diagram

VII. RESULTS

Traces of δ_{pedal} , δ_r , N_y , β , r , p , ψ and ϕ versus time are shown in Figures 22-28. All six configurations are shown on each plot for comparison of the proposed changes. All Simulink traces shown in Figures 22-28 are in response to the 15° doublet. The Simulink model was validated by comparing the results with actual Shuttle flight data and Shuttle Entry Simulator (SES) simulation results.

A. MODEL VALIDATION

To establish validity of the Simulink model, actual STS-62 flight data and SES simulation results were compared to the Simulink results. The STS-62 flight data and SES results are contained in Appendix D. The STS-62 data is compared to the Simulink 'Baseline' traces, since the onboard FCS is in the same configuration. The STS-62 CDR input a comparable 15° rudder pedal doublet in the two point stance. An SES evaluation, using the same initial conditions as this simulation and the STS-62 flight data, was run for comparison. Two SES runs were made. The SES 'Old FCS' traces contain the same FCS configuration as the Simulink 'Baseline' run. The SES 'CF FCS' (Combined Fix) traces contain the same FCS changes as the Simulink 'Optimum fix'.

Rudder deflection traces for all three data sets (Simulink, STS-62 flight data, and SES) show similar magnitude of nearly 15° deflection, similar response time, and deflection rate. N_y traces exhibit non-minimal phase response as indicated by the initial low magnitude acceleration in the negative direction. Lag times are similar and the magnitude of the N_y traces are comparable. A comparison of the sideslip angle traces indicate the same initial order-of-magnitude β resulting from the doublet. However, the Simulink trace shows an apparent long term directional instability which may be the reason why there is no β response in the opposite direction. The long term directional instability is reported to exist in the actual Orbiter in the two point stance. This instability is most likely not as strong as indicated in the Simulink model.

Simulink yaw rate and roll rate traces also indicate the same magnitude and lag time as SES results and actual flight data. The SES 'Old FCS' roll rate data is 'noisy' due to the gear model.

This comparison of flight data and SES results with these Simulink traces results in a high level of confidence that this model is sufficient to analyze and compare the proposed FCS configurations for short term Orbiter directional response.

B. RUDDER DEFLECTION

The rudder deflection plot in Figure 22 indicates that decreasing the time constant results in the quickest rudder response. Simply reducing τ to 0, as in the 'No Ny feedback' option, yields a rudder response very similar to the pedal command. This option appears the best with respect to rudder surface control, yet the absence of Ny feedback generates other long term anomalies in yaw rate and sideslip stability.

Reducing τ to 0.2 with Ny feedback, as in the 'Shorter time constant' trace, yields an acceptable rudder surface response with the benefits of Ny feedback. This trace shows approximately one half second of time delay by the end of the four second doublet. This time delay could also be considered as $\sim 45^\circ$ of phase lag. While 45° of phase lag is not desired, this option appears to be much better than some of the other options. The baseline configuration shows nearly two seconds of time delay before the rudder returns through the zero deflection position. This delay equates to nearly 180° of phase lag by the end of the maneuver. This response is obviously an unacceptable control response to a low frequency command.

Linearizing the rudder pedal shaper, with no additional changes, would result in an increase in rudder deflection of 25% over the baseline. This larger rudder deflection for the relatively small rudder pedal command would aggravate the already difficult fine directional control. Linearizing the rudder with no other changes is not recommended.

Reducing the rudder pedal gain, with no additional changes, is effective in decreasing the magnitude of the rudder surface response. However, the rise time in the deflection is too slow. The slow rise time distorts the predictability of the rudder response. This change does not effect the excessive phase lag.

The 'optimum fix', which includes the $\tau=0.2$ time constant, linearized rudder shaper, and reduced rudder gain, result in the best shaped rudder response while retaining the Ny feedback. The deflection is shaped more like the rudder pedal input than all other Ny feedback cases.

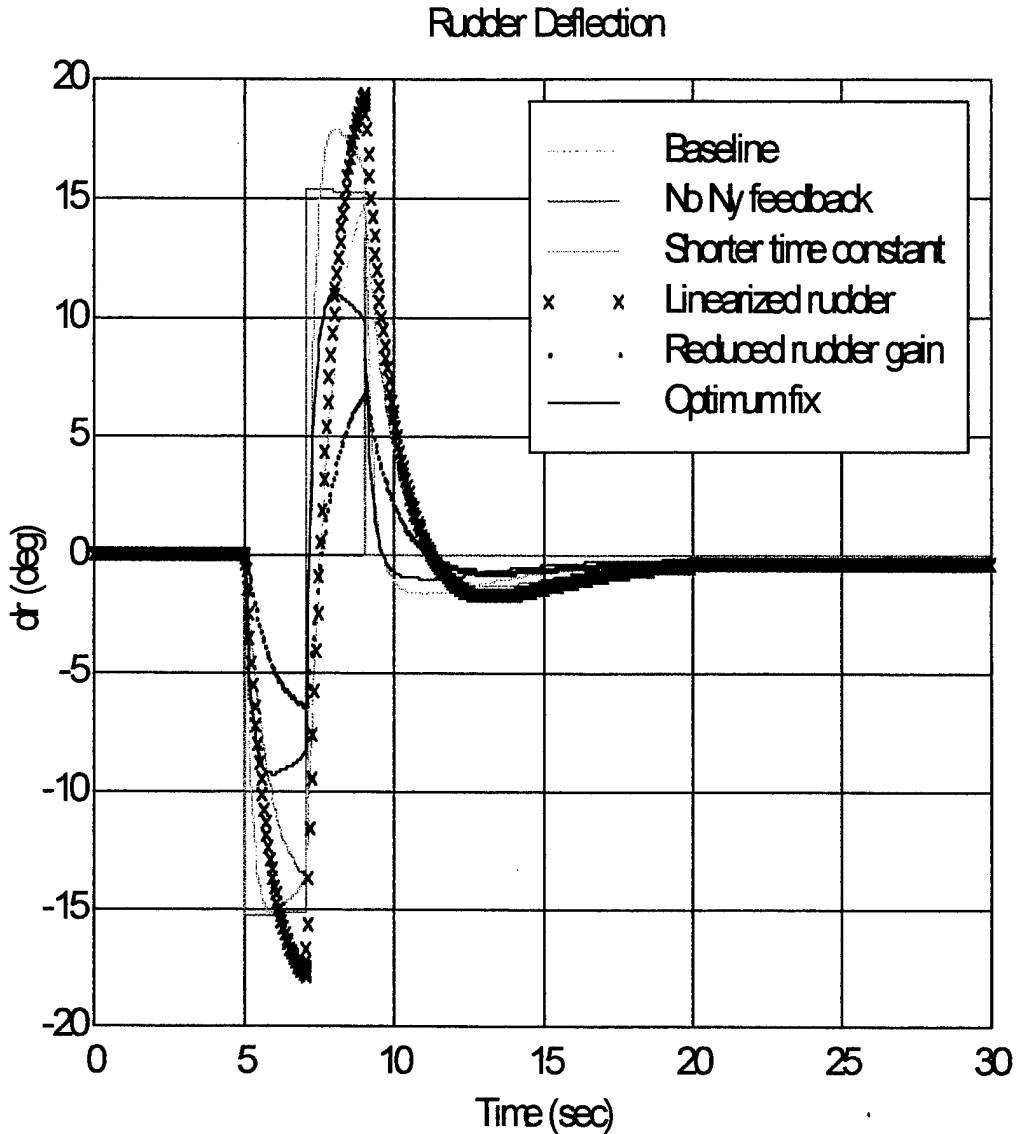


Figure 22. Rudder Surface Deflection

C. LATERAL ACCELERATION AT THE COMMANDER'S STATION

The lateral acceleration plot shown in Figure 23 shows that eliminating Ny feedback results in greater Ny gain and more time required to return to a zero Ny condition. This option displays the worst long term directional stability characteristics.

Both the 'Shorter time constant' and 'Linearized rudder' fixes also result in an increase in g by 25% over the baseline FCS. This increase in lateral acceleration control power could lead to

directional oversensitivity. The 'Shorter time constant' fix results in the least phase lag, while 'Linearized rudder' yields the longest time delay of the Ny feedback options. 'Reduced rudder gain' results in an appropriate decrease in Ny gain. However, this change alone results in excessive time delay.

The 'Optimum fix' has the least time lag and acceptable Ny gain characteristics.

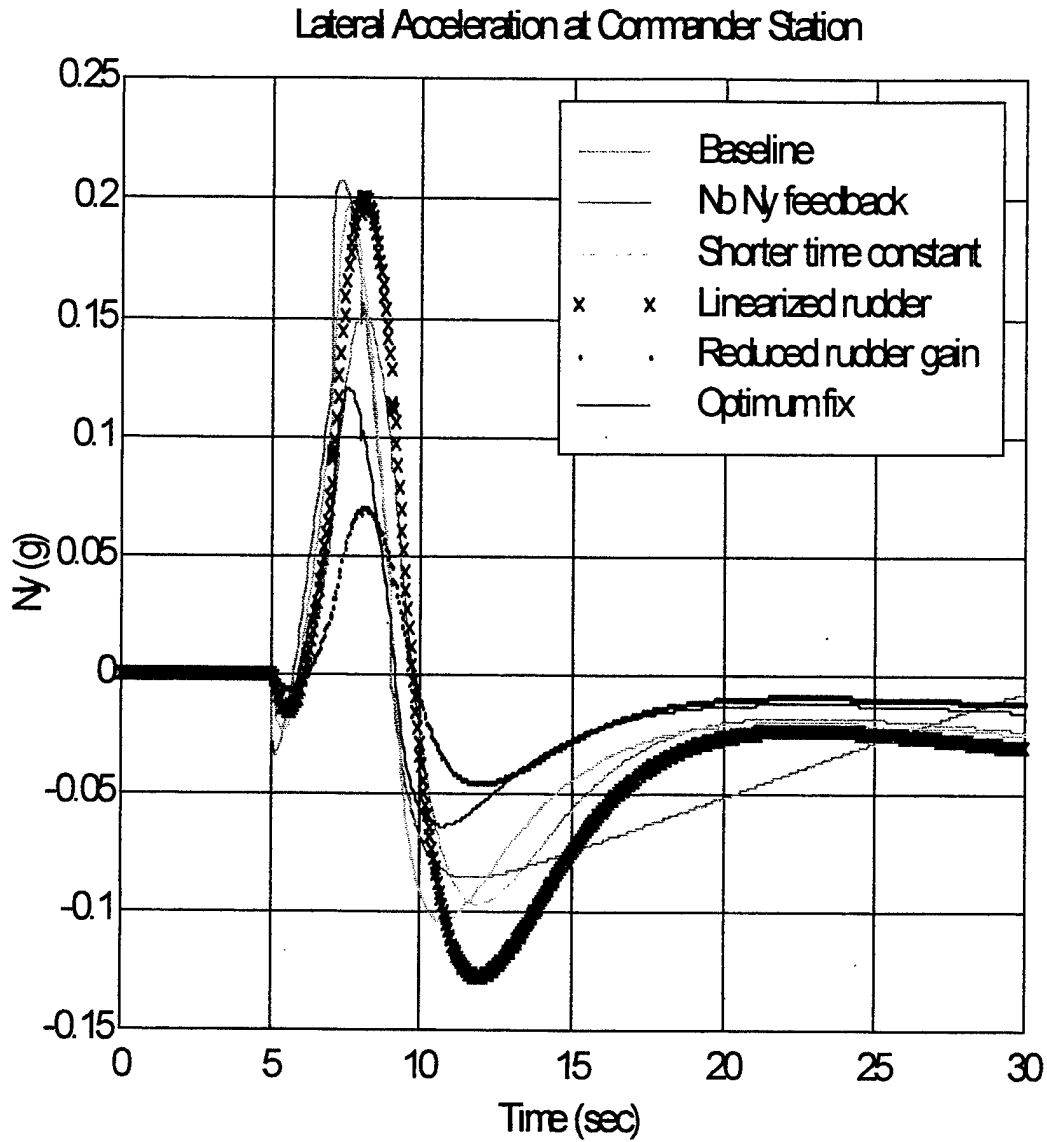


Figure 23. Lateral Acceleration at the Commander's Station

D. SIDESLIP

The sideslip plot shown in Figure 24 shows the total rudder control power in the classic sense of degrees of sideslip per degree of rudder pedal. Most modern aircraft exhibit rudder control power on the order of 1:4, or one degree of sideslip for four degrees of rudder pedal. The 'Baseline' Orbiter trace depicts rudder control power of 1:2.3. This apparent oversensitivity can lead to difficulty in precisely controlling sideslip.

The 'No Ny feedback' option exhibits excessive rudder control power with an additional long term instability. This long term response is unacceptable. The change that optimizes the classic 1:4 rudder control power ratio is the 'Optimum fix'.

The sideslip plot also reveals the inherent long term directional instability of the Orbiter in the two point stance. This instability is due to the change in the center of rotation from the CG to the main wheels as discussed earlier.

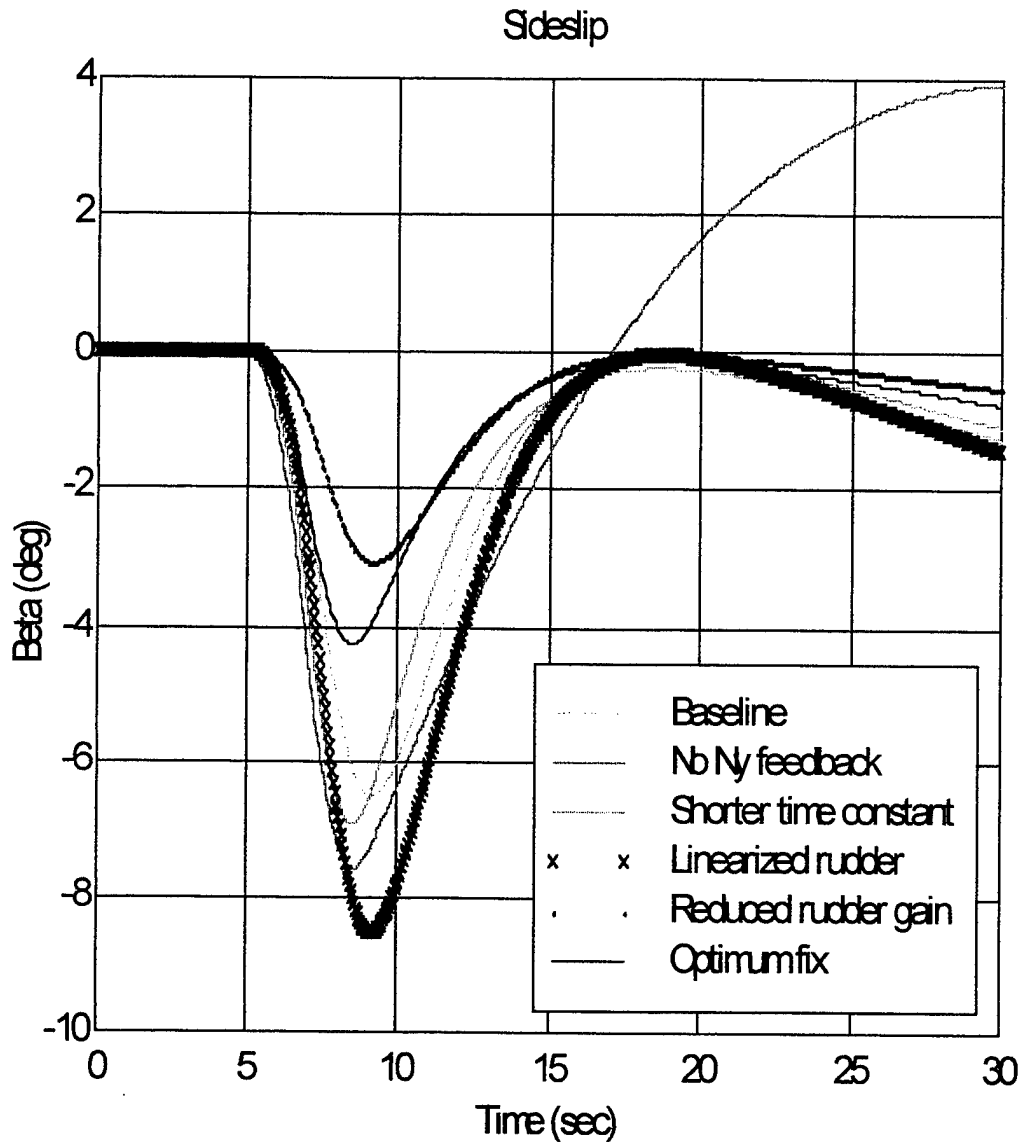


Figure 24. Sideslip Angle

E. YAW RATE AND HEADING

Yaw rate and heading traces are shown in Figures 25 and 26. Heading was derived by integrating yaw rate. Long term directional instability is evident in both yaw rate and heading traces. The 'Shorter time constant' and 'Optimum fix' options indicate the least phase lag of all options with Ny feedback.

YawRate

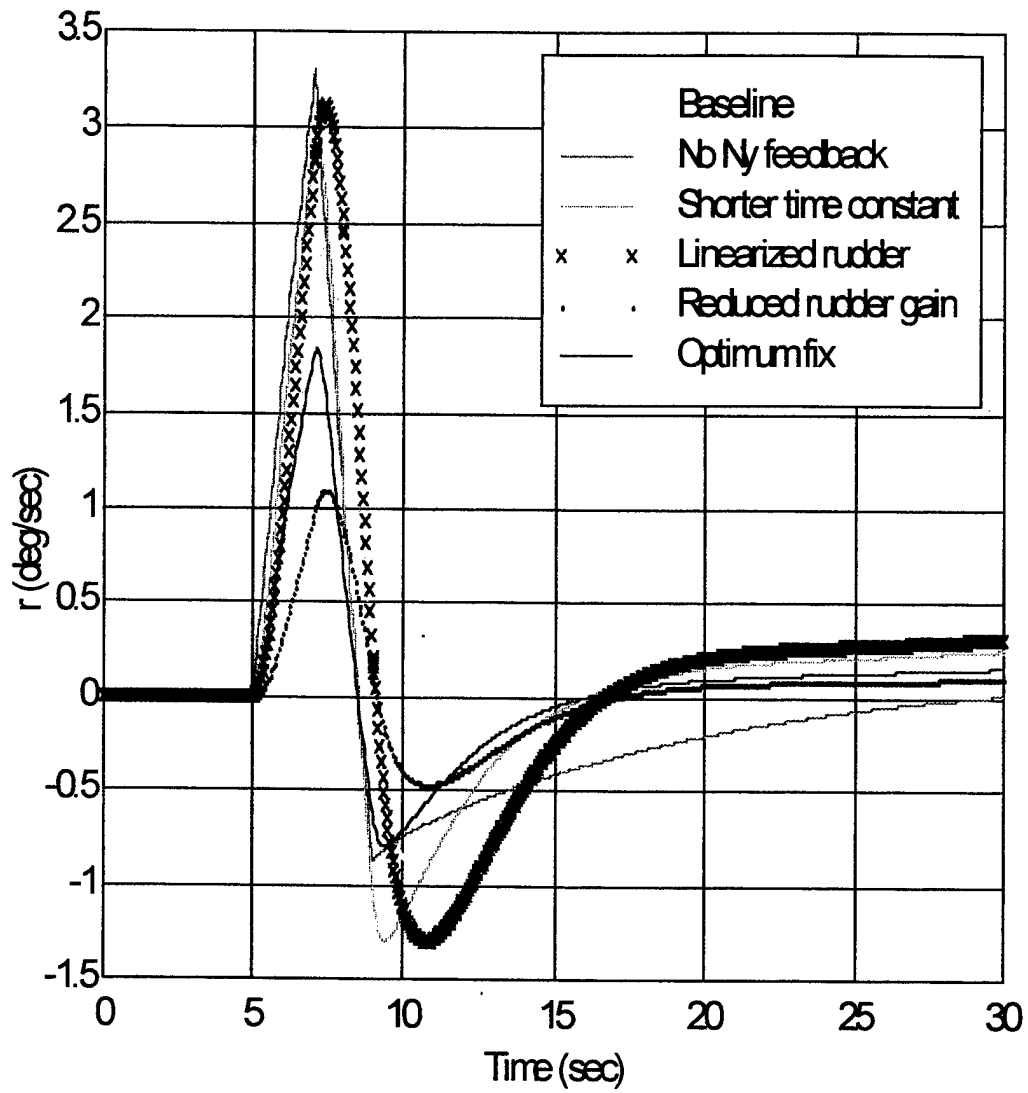


Figure 25. Yaw Rate

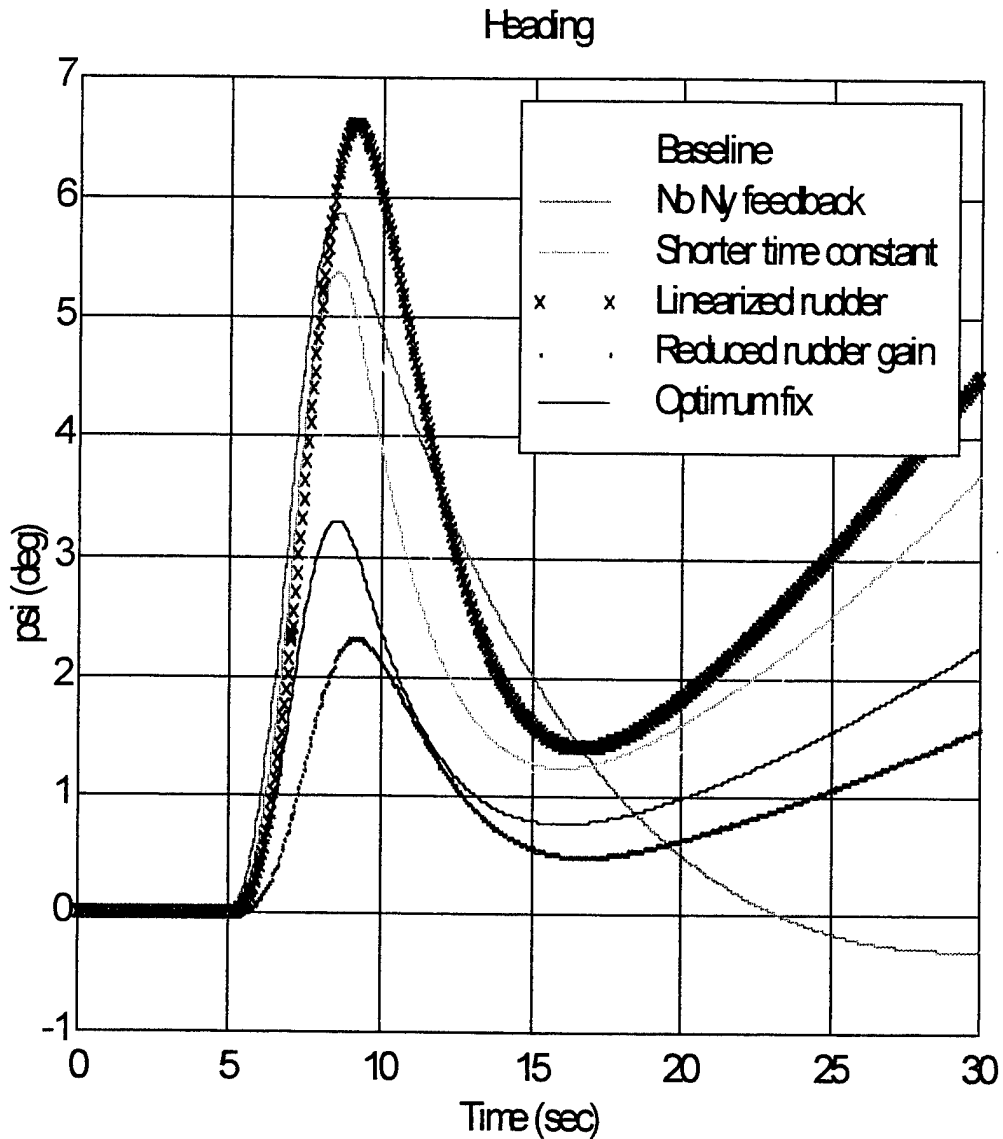


Figure 26. Heading Angle

F. ROLL RATE AND ANGLE OF BANK

Adverse roll is evident as shown in Figures 27 and 28. This response is undesirable because adverse roll contributes to the apparent reduced directional control. The 'Reduced rudder gain' results in the least adverse roll. However, this option results in significant phase lag. The 'Optimum fix' offers reduce adverse roll and the least phase lag. The long term positive dihedral

is evident in the long term positive roll rate. This roll rate is in response to the long term negative sideslip.

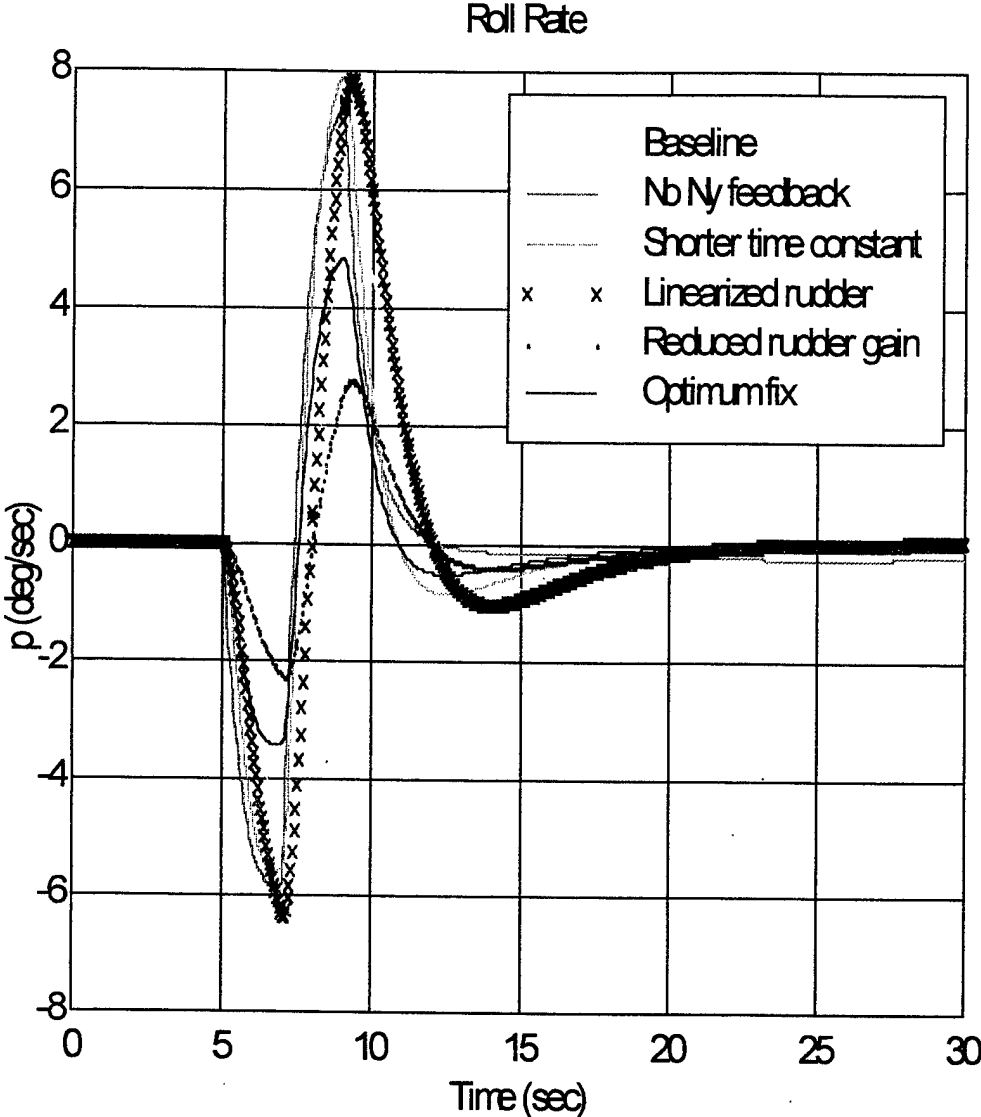


Figure 27. Roll Rate

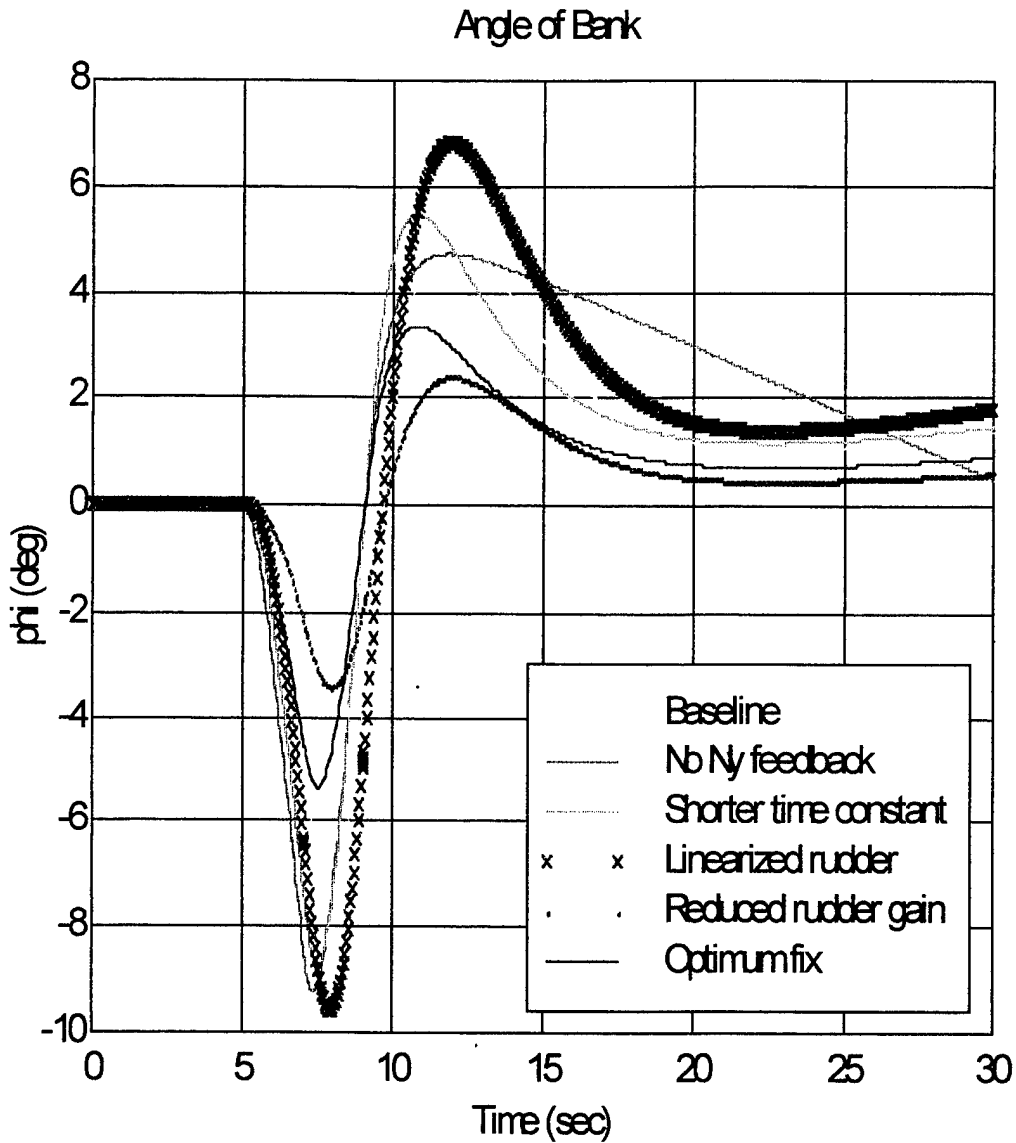


Figure 28. Angle of Bank

G. NATURAL FREQUENCY AND DAMPING RATIO

The so called 'directional natural frequency', ω_D , and damping ratio, ζ_D , were estimated from the plots after completion of the doublet. The damping ratio was estimated using the following equation:

$$\zeta_D = \sin \left[\tan^{-1} \left(\frac{\ln \frac{D_1}{D_2}}{\pi} \right) \right]$$

Estimations from the plots indicate that $\omega_D = 0.6$ rad/sec and $\zeta_D = 0.45$. As expected, the natural frequency and damping ratio are low. This low natural frequency and low damping ratio can result in the tendency of the FCS to be susceptible to PIO.

VIII. CONCLUSIONS

Orbiter landings indicate both long term directional instability and the potential for pilot induced oscillations during landing and rollout before nosewheel touchdown with the baseline (current) FCS. The Orbiter's FCS requires improvements to increase directional control in the two point stance. This thesis described the control deficiency, potential improvements to the FCS, and evaluated six FCS configurations to determine their effect on directional control. The evaluation was performed by modeling the Orbiter's postlanding lateral-directional control laws using MATLAB 5.0 and Simulink. The longitudinal equations of motion were included so that this model can more readily be adapted to evaluate longitudinal control problems.

A. RECOMMENDATIONS

Of the six FCS configurations evaluated, the option which provides the most improvement over the baseline configuration is the 'Optimum fix'. This fix includes reducing the time lag τ from 0.8 sec to 0.2 sec, linearizing the rudder pedal shaper, and reducing the rudder gain. This change minimizes the apparent phase lag, minimizes the adverse roll, reduces directional oversensitivity, and provides the most traditional rudder control power. This option is relatively inexpensive since only software K-load and I-load changes are required. Software code and hardware modifications are not required. The data indicates that PIO tendencies would be reduced over the baseline system if this option were implemented.

This simulation was limited to analyzing the response of the FCS to a rudder doublet since the initial Orbiter directional difficulties were in response to a CDR doublet. The doublet input, in essence, is a frequency domain input. Therefore, frequency domain analysis would be appropriate. However, the validity of the Simulink model can more accurately be determined by comparing the time domain response traces of the individual states to actual flight data. Although this method was used as a diagnostic tool to study a frequency-concerned phenomenon, phase lag can be estimated from the traces. In addition, these changes can be compared and evaluated with a pilot in the loop in time-based simulators such as the SES and Ames VMS.

This author recommends further investigation of the 'Optimum fix' in the SES and Ames VMS. Frequency domain analysis would also be appropriate. In addition, the MATLAB/Simulink program used for this evaluation should be upgraded to include a gear model,

drag chute model, and wind model. The roll and pitch channels should be incorporated for completeness.

B. USE OF COTS SOFTWARE FOR ENGINEERING EVALUATION

This author concludes that commercially available engineering software packages such as MATLAB may be used to analysis proposed FCS changes prior to full up simulation in more expensive simulators. Future programs, such as X38, as well as Orbiter upgrade projects can benefit from the use of PC-based simulation.

APPENDIX A. MATLAB CODE FOR SCRIPT PROGRAM

This appendix contains the Matlab code for the script program, "eom.m". EOM.M defines the initial conditions, mass properties, stability and control derivatives, and longitudinal and lateral/directional EOM in state space form.

```
%Initial conditions and EOM
clear
S = 2690;    %surface area of the wing in ft^2
C = 39.56;   %chord length in ft
B = 78.057;  %wing span in feet
W = 228237;  %weight in lbs
g = 32.174;  %gravitational constant
M = W/g;     %mass in slugs
Ixx = 858677;
Iyy = 6869907.5;
Izz = 7133448.5;

%Shift the moments of inertia from the cg to center of rotation
%(between the main gear)
Izmg = Izz + M * ((1172.6 - 1084.15) / 12)^2

%b/h = 0.05 at alpha = 10

Mu = 0.03;    %runway rolling Mu
U1 = 353;     %initial velocity in the x direction ft/sec
rho = 0.002377; %sea level pressure
theta = 9 * pi / 180 %Pitch angle in radians
alpha = 10 * pi / 180 %Angle of attack in radians
q = 0.5 * rho * U1^2 %Dynamic pressure at sea level

%Non-Dimensional Stability and Control Derivatives
CLa = 0.05948;
CDa = 0.009924;
CL1 = 0.54055;
CD1 = 0.16712;
CLu = 0;
CDu = 0;

Cyb = -0.01705;
Cyp = 0;
Cyr = 0;
Cydelstar = 0.00138;
Clb = -0.00205;
Clp = -0.3189;
Clr = 0.1890;
Cldelstar = 0.00032;
Cnb = 0.0010;
Cnp = 0.028;
Cnr = -0.2925;
Cndelstar = -0.00054;

%Longitudinal Dimensional Stability and Control Derivatives
Xu = -q * S * (CDu + 2 * CD1) / (M * U1)
Xa = -q * S * (CDa + 2 * CL1) / M
```

```

Xq=0;
Xdeltae=0;
Zu=-q*S*(CLu+2*CL1)/(M*U1)
Za=-q*S*(CLa+2*CD1)/M
Zq=0;
Zdeltae=0;
Mu=0;
Ma=0;
Mq=0;
Mdeltae=0;

%Lateral-directional Dimensional Stability and Control Derivatives
Yb=q*S*Cyb/M
Yp=q*S*B*Cyp/(2*M*U1) %is zero
Yr=q*S*B*Cyr/(2*M*U1) %is zero
Ydeltaa=0;
Ydeltar=q*S*Cydeltar/M

Lb=q*S*B*Clb/Ixx
Lp=q*S*B^2*Clp/(2*Ixx*U1)
Lr=q*S*B^2*Clr/(2*Ixx*U1)
Ldeltaa=0;
Ldeltar=q*S*B*Cldeltar/Ixx

Nb=q*S*B*Cnb/Izmg
Np=q*S*B^2*Cnp/(2*Izmg*U1)
Nr=q*S*B^2*Cnr/(2*Izmg*U1)
Ndeltaa=0;
Ndeltar=q*S*B*Cndeltar/Izmg

%Definition of dx/dt= Ax+Bu

%xdot=[udot alphadot qdot thetadot betadot pdot rdot phidot]
%x=[u alpha q theta beta p r phi]
%U=[DELTAE DELTAA DELTAR]

A = [Xu Xa Xq -g*cos(theta) 0 0 0 0;
Zu/U1 Za/U1 Zq/U1+1 -g*sin(theta)/U1 0 0 0 0;
Mu Ma Mq 0 0 0 0 0;
0 0 1 0 0 0 0 0;
0 0 0 0 Yb/U1 Yp/U1 Yr/U1-1 g*cos(theta)/U1;
0 0 0 0 Lb Lp Lr 0;
0 0 0 0 Nb Np Nr 0;
0 0 0 0 0 1 tan(theta) 0]

B=[Xdeltae 0 0;
Zdeltae/U1 0 0;
Mdeltae 0 0;
0 0 0;
0 Ydeltaa/U1 Ydeltar/U1;
0 Ldeltaa Ldeltar;
0 Ndeltaa Ndeltar;
0 0 0]

% dy/dt = Cx+Du; C= identity matrix D=0 so that the output
%of the state space is X
C=[eye(8)]

```

```
D=zeros(8,3)

B=[Xdeltae 0 0;
Zdeltae/U1 0 0;
Mdeltae 0 0;
0 0 0;
0 Ydeltaa/U1 Ydeltar/U1;
0 Ldeltaa Ldeltar;
0 Ndeltaa Ndeltar;
0 0 0]
```


APPENDIX B. MATLAB CODE FOR SIMULATION

The code for the actual simulation, "baseline.m" is contained in this Appendix. The code is for the baseline system.

```
Model {
  Name          "baseline"
  Version       2.00
  SimParamPage  Solver
  SampleTimeColors  off
  WideVectorLines  off
  PaperOrientation  landscape
  StartTime     "0.0"
  StopTime     "30"
  Solver        ode45
  RelTol        ".01"
  AbsTol        "1e-6"
  Refine        "1"
  MaxStep       ".05"
  InitialStep   "auto"
  FixedStep     "auto"
  MaxOrder      5
  OutputOption  RefineOutputTimes
  OutputTimes   "[]"
  LoadExternalInput  off
  ExternalInput "[t, u]"
  SaveTime      off
  TimeSaveName  "tout"
  SaveState     off
  StateSaveName "xout"
  SaveOutput    off
  OutputSaveName "yout"
  LoadInitialState  off
  InitialState  "xInitial"
  SaveFinalState  off
  FinalStateName "xFinal"
  LimitMaxRows  off
  MaxRows       "1000"
  Decimation    "1"
  AlgebraicLoopMsg  warning
  MinStepSizeMsg  warning
  UnconnectedInputMsg  warning
  UnconnectedOutputMsg  warning
  UnconnectedLineMsg  warning
  ConsistencyChecking  off
  ZeroCross     on
  BlockDefaults {
    Orientation  right
    ForegroundColor  black
  }
}
```

```

BackgroundColor      white
DropShadow          off
NamePlacement       normal
FontName            "Helvetica"
FontSize            10
FontWeight          normal
FontAngle           normal
ShowName            on
}
AnnotationDefaults {
  HorizontalAlignment center
  VerticalAlignment  middle
  ForegroundColor   black
  BackgroundColor   white
  DropShadow        off
  FontName          "Helvetica"
  FontSize          10
  FontWeight        normal
  FontAngle         normal
}
System {
  Name      "baseline"
  Location  [0, 3, 644, 447]
  Open      on
  ScreenColor white
  Block {
    BlockType  Derivative
    Name       "BETADOT"
    Position   [385, 320, 415, 340]
    Orientation left
  }
  Block {
    BlockType  Clock
    Name       "Clock"
    Position   [30, 330, 50, 350]
    DeleteFcn  "simclock BlockIsBeingDestroyed"
    PostSaveFcn "simclock Save"
    Location   [12, 31, 119, 76]
  }
  Block {
    BlockType  Demux
    Name       "Demux"
    Position   [370, 154, 405, 236]
    Outputs    "8"
  }
  Block {
    BlockType  Mux
    Name       "Mux"
    Position   [310, 253, 335, 347]
    Orientation left
    Inputs     "3"
  }
}

```

```

}
Block {
  BlockType      Mux
  Name           "Mux1"
  Position       [235, 178, 270, 212]
  Inputs        "3"
}
Block {
  BlockType      Scope
  Name          "Ny"
  Position       [215, 395, 245, 425]
  Orientation    down
  NamePlacement alternate
  Floating       off
  Location       [188, 235, 512, 474]
  Open          off
  Grid          on
  TickLabels    on
  ZoomMode      on
  TimeRange     "auto"
  YMin         "-5"
  YMax         "5"
  SaveToWorkspace off
  SaveName      "ScopeData"
  LimitMaxRows on
  MaxRows       "5000"
  Decimation    "1"
  SampleInput  off
  SampleTime    "0"
}
Block {
  BlockType      Fcn
  Name          "Ny_"
  Position       [240, 277, 275, 323]
  Orientation    left
  Expr          "-(353*u[3]+353*u[2]+u[1]*60)/g"
}
Block {
  BlockType      Integrator
  Name          "PSI"
  Position       [505, 380, 525, 400]
  ExternalReset none
  InitialConditionSource internal
  InitialCondition "0"
  LimitOutput    off
  UpperSaturationLimit "inf"
  LowerSaturationLimit "-inf"
  ShowSaturationPort off
  ShowStatePort   off
  AbsoluteTolerance "auto"
}

```

```

Block {
  BlockType      SubSystem
  Name           "Pulse\nGenerator1"
  Position       [25, 35, 55, 65]
  ShowPortLabels on
  MaskType       "Pulse Generator"
  MaskDescription "Pulse Generator"
  MaskHelp       "Pulse generator which ensures pulse transitions "
                "are hit. Provides a vector of pulses when "
                "the height is entered as a vector. Unmask "
                "to see how it works."
  MaskPromptString "Period (secs):|Duty cycle (% of period):|Amplitu"
                "de:|Start time:"
  MaskStyleString "edit,edit,edit,edit"
  MaskVariables   "period=@1;duty=@2;amplitude=@3;start=@4;"
  MaskInitialization "\n"
  MaskDisplay     "plot(0,0,100,100,[95,90,90,75,75,60,60,45,45,30,"
                "30,15,15,5],[25,25,75,75,25,25,75,75,25,25,75,75,"
                ",25,25]); \n"
                " "
                " \n "
                " "
                " "
  MaskIconFrame  on
  MaskIconOpaque on
  MaskIconRotate off
  MaskIconUnits  autoscale
  MaskValueString "1000|.2|15|5"
  System {
    Name           "Pulse\nGenerator1"
    Location       [205, 368, 544, 559]
    Open           off
    ScreenColor    white
    Block {
      BlockType    Constant
      Name         "Constant1"
      Position     [40, 135, 60, 155]
      Value        "0"
    }
    Block {
      BlockType    Sin
      Name         "Sine Wave"
      Position     [35, 83, 65, 107]
      Amplitude    "1"
      Frequency    "2*pi./period"
      Phase        "-2*pi*(start./period + duty/200 - 1/4)"
      SampleTime   "-1"
    }
    Block {
      BlockType    Step
      Name         "Step"
    }
  }
}

```

```

    Position          [35, 27, 65, 53]
    Time              "start"
    Before            "0"
    After             "amplitude"
  }
  Block {
    BlockType        Switch
    Name              "Switch"
    Position          [120, 65, 155, 125]
    Threshold         "sin(pi*(0.5 - duty/100))"
  }
  Block {
    BlockType        Outputport
    Name              "out1"
    Position          [250, 88, 280, 102]
    Port              "1"
    OutputWhenDisabled held
    InitialOutput     "0"
  }
  Line {
    SrcBlock          "Sine Wave"
    SrcPort            1
    Points             [5, 0; 20, 0]
    DstBlock          "Switch"
    DstPort            2
  }
  Line {
    SrcBlock          "Switch"
    SrcPort            1
    DstBlock          "out1"
    DstPort            1
  }
  Line {
    SrcBlock          "Constant1"
    SrcPort            1
    Points             [25, 0; 0, -30]
    DstBlock          "Switch"
    DstPort            3
  }
  Line {
    SrcBlock          "Step"
    SrcPort            1
    Points             [20, 0; 0, 35]
    DstBlock          "Switch"
    DstPort            1
  }
}
}
Block {
  BlockType          SubSystem
  Name                "Pulse\nGenerator2"
}

```

```

Position          [25, 95, 55, 125]
ShowPortLabels   on
MaskType         "Pulse Generator"
MaskDescription   "Pulse Generator"
MaskHelp         "Pulse generator which ensures pulse transitions "
                 "are hit. Provides a vector of pulses when "
                 "the height is entered as a vector. Unmask "
                 "to see how it works."
MaskPromptString "Period (secs):|Duty cycle (% of period):|Amplitu"
                 "de:|Start time:"
MaskStyleString  "edit,edit,edit,edit"
MaskVariables    "period=@1;duty=@2;amplitude=@3;start=@4;"
MaskInitialization "\n"
MaskDisplay      "plot(0,0,100,100,[95,90,90,75,75,60,60,45,45,30,"
                 "30,15,15,5],[25,25,75,75,25,25,75,75,25,25,75,75,"
                 ",25,25]); \n          "
                 "          \n          "
                 "          "
                 "          "
MaskIconFrame    on
MaskIconOpaque   on
MaskIconRotate   off
MaskIconUnits    autoscale
MaskValueString  "1000|.2|-15|7"
System {
    Name          "Pulse\nGenerator2"
    Location      [205, 368, 544, 559]
    Open          off
    ScreenColor   white
    Block {
        BlockType Constant
        Name      "Constant 1"
        Position  [40, 135, 60, 155]
        Value     "0"
    }
    Block {
        BlockType Sin
        Name      "Sine Wave"
        Position  [35, 83, 65, 107]
        Amplitude "1"
        Frequency "2*pi./period"
        Phase     "-2*pi*(start./period + duty/200 - 1/4)"
        SampleTime "-1"
    }
    Block {
        BlockType Step
        Name      "Step"
        Position  [35, 27, 65, 53]
        Time      "start"
        Before    "0"
    }
}

```

```

    After          "amplitude"
  }
  Block {
    BlockType      Switch
    Name           "Switch"
    Position       [120, 65, 155, 125]
    Threshold      "sin(pi*(0.5 - duty/100))"
  }
  Block {
    BlockType      Outputport
    Name           "out1"
    Position       [250, 88, 280, 102]
    Port           "1"
    OutputWhenDisabled held
    InitialOutput  "0"
  }
  Line {
    SrcBlock       "Step"
    SrcPort        1
    Points         [20, 0; 0, 35]
    DstBlock       "Switch"
    DstPort        1
  }
  Line {
    SrcBlock       "Constant1"
    SrcPort        1
    Points         [25, 0; 0, -30]
    DstBlock       "Switch"
    DstPort        3
  }
  Line {
    SrcBlock       "Switch"
    SrcPort        1
    DstBlock       "out1"
    DstPort        1
  }
  Line {
    SrcBlock       "Sine Wave"
    SrcPort        1
    Points         [5, 0; 20, 0]
    DstBlock       "Switch"
    DstPort        2
  }
}
}
Block {
  BlockType      Derivative
  Name           "RDOT"
  Position       [385, 260, 415, 280]
  Orientation    left
}

```

```

Block {
  BlockType      Scope
  Name           "Scope"
  Position       [395, 435, 425, 465]
  Floating       off
  Location       [115, 431, 439, 670]
  Open           off
  Grid           on
  TickLabels     on
  ZoomMode       on
  TimeRange      "auto"
  YMin           "-5"
  YMax           "5"
  SaveToWorkspace off
  SaveName       "ScopeData"
  LimitMaxRows   on
  MaxRows        "5000"
  Decimation     "1"
  SampleInput    off
  SampleTime     "0"
}
Block {
  BlockType      Scope
  Name           "Scope1"
  Position       [390, 380, 420, 410]
  Floating       off
  Location       [100, 161, 424, 400]
  Open           off
  Grid           on
  TickLabels     on
  ZoomMode       on
  TimeRange      "auto"
  YMin           "-5"
  YMax           "5"
  SaveToWorkspace off
  SaveName       "ScopeData"
  LimitMaxRows   on
  MaxRows        "5000"
  Decimation     "1"
  SampleInput    off
  SampleTime     "0"
}
Block {
  BlockType      StateSpace
  Name           "State-space"
  Position       [295, 180, 355, 210]
  A              "A"
  B              "B"
  C              "C"
  D              "D"
  X0             "[0;0;0;0;0;0;0;0]"
}

```

```

}
Block {
  BlockType      Sum
  Name           "Sum"
  Position       [100, 77, 130, 108]
  Inputs        "++"
}
Block {
  BlockType      ToWorkspace
  Name           "To Workspace"
  Position       [95, 145, 155, 175]
  VariableName   "doublet"
  Buffer         "inf"
  Decimation     "1"
  SampleTime     "-1"
}
Block {
  BlockType      ToWorkspace
  Name           "To Workspace1"
  Position       [175, 250, 235, 280]
  VariableName   "dr"
  Buffer         "inf"
  Decimation     "1"
  SampleTime     "-1"
}
Block {
  BlockType      ToWorkspace
  Name           "To Workspace2"
  Position       [95, 365, 155, 395]
  Orientation    left
  VariableName   "Ny"
  Buffer         "inf"
  Decimation     "1"
  SampleTime     "-1"
}
Block {
  BlockType      ToWorkspace
  Name           "To Workspace3"
  Position       [540, 110, 600, 140]
  VariableName   "beta"
  Buffer         "inf"
  Decimation     "1"
  SampleTime     "-1"
}
Block {
  BlockType      ToWorkspace
  Name           "To Workspace4"
  Position       [570, 150, 630, 180]
  VariableName   "p"
  Buffer         "inf"
  Decimation     "1"
}

```

```

    SampleTime    "-1"
}
Block {
    BlockType    ToWorkspace
    Name         "To Workspace5"
    Position     [585, 220, 645, 250]
    VariableName "r"
    Buffer        "inf"
    Decimation   "1"
    SampleTime   "-1"
}
Block {
    BlockType    ToWorkspace
    Name         "To Workspace6"
    Position     [585, 335, 645, 365]
    VariableName "psi"
    Buffer        "inf"
    Decimation   "1"
    SampleTime   "-1"
}
Block {
    BlockType    ToWorkspace
    Name         "To Workspace7"
    Position     [70, 320, 130, 350]
    VariableName "time"
    Buffer        "inf"
    Decimation   "1"
    SampleTime   "-1"
}
Block {
    BlockType    ToWorkspace
    Name         "To Workspace8"
    Position     [585, 280, 645, 310]
    VariableName "aob"
    Buffer        "inf"
    Decimation   "1"
    SampleTime   "-1"
}
Block {
    BlockType    SubSystem
    Name         "YAW FCS"
    Position     [175, 179, 205, 231]
    ShowPortLabels off
    System {
        Name         "YAW FCS"
        Location     [4, 44, 648, 440]
        Open         off
        ScreenColor  white
        Block {
            BlockType Inport
            Name       "in_1"
        }
    }
}

```

```

Position          [35, 180, 50, 200]
Port              "1"
PortWidth        "-1"
SampleTime       "-1"
}
Block {
  BlockType      Inport
  Name           "in_2"
  Position       [100, 290, 120, 310]
  Port           "2"
  PortWidth     "-1"
  SampleTime    "-1"
}
Block {
  BlockType      Inport
  Name           "in_3"
  Position       [290, 270, 310, 290]
  Port           "3"
  PortWidth     "-1"
  SampleTime    "-1"
}
Block {
  BlockType      SubSystem
  Name           "COSALF"
  Position       [320, 70, 350, 120]
  Orientation    down
  ShowPortLabels off
  System {
    Name         "COSALF"
    Location     [318, 77, 607, 247]
    Open         off
    ScreenColor  white
    Block {
      BlockType  MATLABFcn
      Name       "Cos(Alpha)"
      Position   [57, 95, 133, 125]
      Orientation down
      MATLABFcn "cos"
      OutputWidth "-1"
    }
    Block {
      BlockType  Constant
      Name       "alpha"
      Position   [58, 50, 132, 65]
      Orientation down
      Value      "10*pi/180"
    }
  }
  Block {
    BlockType  Outport
    Name       "out_1"
    Position   [85, 150, 105, 170]
  }
}

```

```

Orientation    down
Port           "1"
OutputWhenDisabled held
InitialOutput  "0"
}
Line {
SrcBlock       "Cos(Alpha)"
SrcPort        1
DstBlock       "out_1"
DstPort        1
}
Line {
SrcBlock       "alpha"
SrcPort        1
DstBlock       "Cos(Alpha)"
DstPort        1
}
}
}
}
Block {
BlockType      Constant
Name           "Constant"
Position       [60, 125, 80, 145]
Value         ".04"
}
Block {
BlockType      SubSystem
Name           "DRERR"
Position       [335, 255, 365, 305]
ShowPortLabels off
System {
Name           "DRERR"
Location       [180, 294, 476, 476]
Open           off
ScreenColor    white
Block {
BlockType      Inport
Name           "in_1"
Position       [15, 75, 35, 95]
Port           "1"
PortWidth      "-1"
SampleTime     "-1"
}
Block {
BlockType      DiscreteFilter
Name           "YAW_RATE_BBF"
Position       [60, 56, 245, 114]
Numerator      "[.7718479 -.3633895 .4980655]"
Denominator    "[1 -.3633895 .2699135]"
SampleTime     "1"
}
}
}
}

```

```

Block {
  BlockType      Outputport
  Name           "out_1"
  Position       [265, 75, 285, 95]
  Port           "1"
  OutputWhenDisabled held
  InitialOutput  "0"
}
Line {
  SrcBlock       "YAW_RATE_BBF"
  SrcPort        1
  DstBlock       "out_1"
  DstPort        1
}
Line {
  SrcBlock       "in_1"
  SrcPort        1
  DstBlock       "YAW_RATE_BBF"
  DstPort        1
}
}
}
Block {
  BlockType      Constant
  Name           "DRT"
  Position       [135, 245, 150, 265]
  Value          "0"
}
Block {
  BlockType      Product
  Name           "GAIN"
  Position       [135, 175, 160, 195]
  Inputs         "2"
}
Block {
  BlockType      Product
  Name           "GAIN_"
  Position       [355, 185, 380, 205]
  Inputs         "2"
}
Block {
  BlockType      Constant
  Name           "GDRC"
  Position       [475, 300, 515, 330]
  Orientation    up
  Value          "6.325"
}
Block {
  BlockType      Constant
  Name           "GERYFWDS"
  Position       [485, 105, 505, 125]
}

```

```

Orientation      down
Value            ".5"
}
Block {
  BlockType      SubSystem
  Name            "GNYDRM_COMP"
  Position        [105, 65, 135, 115]
  Orientation      down
  ShowPortLabels off
  System {
    Name          "GNYDRM_COMP"
    Location        [355, 132, 620, 292]
    Open            off
    ScreenColor     white
    Block {
      BlockType      Lookup
      Name            "GNY DRM Comp"
      Position        [75, 43, 150, 107]
      Orientation      left
      InputValues     "[0 250 900 10000]"
      OutputValues    "[0.1 0.1 0.01 0.01]"
    }
  }
  Block {
    BlockType      Constant
    Name            "TAS"
    Position        [170, 75, 190, 95]
    Orientation      left
    Value            "353"
  }
  Block {
    BlockType      Outputport
    Name            "GNYDRM"
    Position        [15, 70, 35, 90]
    Orientation      left
    Port            "1"
    OutputWhenDisabled held
    InitialOutput    "0"
  }
  Line {
    SrcBlock        "GNY DRM Comp"
    SrcPort          1
    DstBlock        "GNYDRM"
    DstPort          1
  }
  Line {
    SrcBlock        "TAS"
    SrcPort          1
    DstBlock        "GNY DRM Comp"
    DstPort          1
  }
}
}

```

```

}
Block {
  BlockType      SubSystem
  Name           "NYCOMP"
  Position       [295, 170, 325, 220]
  ShowPortLabels off
  System {
    Name         "NYCOMP"
    Location     [227, 109, 594, 284]
    Open        off
    ScreenColor  white
    Block {
      BlockType  Inport
      Name       "in_1"
      Position   [15, 80, 35, 100]
      Port       "1"
      PortWidth  "-1"
      SampleTime "-1"
    }
    Block {
      BlockType  Gain
      Name       "GRAY"
      Position   [215, 77, 240, 103]
      Gain       "5"
    }
    Block {
      BlockType  TransferFcn
      Name       "Transfer Fcn"
      Position   [80, 65, 175, 115]
      Numerator  "[1]"
      Denominator "[0.8 1]"
    }
    Block {
      BlockType  Output
      Name       "out_1"
      Position   [260, 80, 280, 100]
      Port       "1"
      OutputWhenDisabled held
      InitialOutput "0"
    }
    Line {
      SrcBlock   "in_1"
      SrcPort    1
      DstBlock   "Transfer Fcn"
      DstPort    1
    }
    Line {
      SrcBlock   "GRAY"
      SrcPort    1
      DstBlock   "out_1"
      DstPort    1
    }
  }
}

```

```

    }
    Line {
        SrcBlock          "Transfer Fcn"
        SrcPort           1
        DstBlock          "GRAY"
        DstPort           1
    }
}
}
Block {
    BlockType           Product
    Name                "Product1"
    Position             [510, 177, 535, 213]
    Inputs              "3"
}
Block {
    BlockType           Saturate
    Name                "RUDCMD"
    Position             [555, 190, 580, 210]
    UpperLimit          "27.1"
    LowerLimit          "-27.1"
}
Block {
    BlockType           SubSystem
    Name                "RUDSHAPE"
    Position             [80, 165, 110, 215]
    ShowPortLabels      off
    System {
        Name            "RUDSHAPE"
        Location        [75, 132, 474, 272]
        Open            off
        ScreenColor     white
        Block {
            BlockType   Inport
            Name         "in_1"
            Position     [15, 70, 35, 90]
            Port         "1"
            PortWidth    "-1"
            SampleTime   "-1"
        }
        Block {
            BlockType   Saturate
            Name         "DR_Limiter"
            Position     [210, 66, 235, 94]
            FontSize     8
            UpperLimit   "+22.5"
            LowerLimit   "-22.5"
        }
        Block {
            BlockType   Fcn
            Name         "DRman(0.42|DRman|+0.131)"
        }
    }
}

```

```

    Position          [105, 70, 145, 90]
    Expr              "(abs(u)*0.042+.131)*u"
  }
  Block {
    BlockType        Outport
    Name              "out_1"
    Position          [265, 70, 285, 90]
    Port              "1"
    OutputWhenDisabled held
    InitialOutput     "0"
  }
  Line {
    SrcBlock          "DR_Limiter"
    SrcPort            1
    DstBlock           "out_1"
    DstPort            1
  }
  Line {
    SrcBlock          "in_1"
    SrcPort            1
    DstBlock           "DRman(0.42|DRman|+0.131)"
    DstPort            1
  }
  Line {
    SrcBlock          "DRman(0.42|DRman|+0.131)"
    SrcPort            1
    DstBlock           "DR_Limiter"
    DstPort            1
  }
}
}
}
Block {
  BlockType          Scope
  Name                "Scope"
  Position            [400, 130, 430, 160]
  Floating            off
  Location             [188, 365, 512, 604]
  Open                off
  Grid                on
  TickLabels          on
  ZoomMode            yonly
  TimeRange           "auto"
  YMin                "-5"
  YMax                "5"
  SaveToWorkspace     off
  SaveName            "ScopeData"
  LimitMaxRows        on
  MaxRows             "5000"
  Decimation          "1"
  SampleInput         off
  SampleTime          "0"
}

```

```

}
Block {
  BlockType      Scope
  Name           "Scope1"
  Position       [275, 110, 305, 140]
  Floating       off
  Location       [188, 365, 512, 604]
  Open           off
  Grid           on
  TickLabels     on
  ZoomMode       on
  TimeRange      "auto"
  YMin           "-5"
  YMax           "5"
  SaveToWorkspace off
  SaveName       "ScopeData"
  LimitMaxRows  on
  MaxRows        "5000"
  Decimation     "1"
  SampleInput    off
  SampleTime     "0"
}
Block {
  BlockType      Scope
  Name           "Scope2"
  Position       [425, 300, 455, 330]
  Floating       off
  Location       [188, 365, 512, 604]
  Open           off
  Grid           on
  TickLabels     on
  ZoomMode       on
  TimeRange      "auto"
  YMin           "-5"
  YMax           "5"
  SaveToWorkspace off
  SaveName       "ScopeData"
  LimitMaxRows  on
  MaxRows        "5000"
  Decimation     "1"
  SampleInput    off
  SampleTime     "0"
}
Block {
  BlockType      Scope
  Name           "Scope3"
  Position       [215, 115, 245, 145]
  Floating       off
  Location       [188, 365, 512, 604]
  Open           off
  Grid           on

```

```

TickLabels          on
ZoomMode            on
TimeRange           "auto"
YMin                "-5"
YMax                "5"
SaveToWorkspace     off
SaveName            "ScopeData"
LimitMaxRows        on
MaxRows             "5000"
Decimation           "1"
SampleInput         off
SampleTime          "0"
}
Block {
  BlockType          Scope
  Name               "Scope4"
  Position            [240, 250, 270, 280]
  Floating            off
  Location            [188, 365, 512, 604]
  Open               off
  Grid                on
  TickLabels          on
  ZoomMode            on
  TimeRange           "auto"
  YMin                "-5"
  YMax                "5"
  SaveToWorkspace     off
  SaveName            "ScopeData"
  LimitMaxRows        on
  MaxRows             "5000"
  Decimation           "1"
  SampleInput         off
  SampleTime          "0"
}
Block {
  BlockType          Sum
  Name               "Sum"
  Position            [420, 190, 440, 210]
  Inputs              "++"
}
Block {
  BlockType          Sum
  Name               "Sum1"
  Position            [235, 177, 255, 208]
  Inputs              "-+"
}
Block {
  BlockType          Sum
  Name               "Sum2"
  Position            [180, 175, 200, 195]
  Inputs              "++"
}

```

```

}
Block {
  BlockType      SubSystem
  Name           "YBB_FILTER"
  Position       [445, 15, 475, 65]
  ShowPortLabels off
  System {
    Name         "YBB_FILTER"
    Location     [55, 69, 652, 308]
    Open        off
    ScreenColor  white
    Block {
      BlockType  Inport
      Name       "in_1"
      Position   [15, 90, 35, 110]
      Port       "1"
      PortWidth  "-1"
      SampleTime "-1"
    }
    Block {
      BlockType  DiscreteFilter
      Name       "Filter1"
      Position   [60, 76, 265, 124]
      Numerator  "[.699558 -.82766 +.5599439]"
      Denominator "[1 -1.08273 +.554071]"
      SampleTime "1"
    }
    Block {
      BlockType  DiscreteFilter
      Name       "Filter2"
      Position   [325, 79, 525, 121]
      Numerator  "[.940726 -1.04423 .801291]"
      Denominator "[1 -.96303 .66162]"
      SampleTime "1"
    }
    Block {
      BlockType  Outputport
      Name       "out_1"
      Position   [550, 90, 570, 110]
      Port       "1"
      OutputWhenDisabled held
      InitialOutput "0"
    }
  }
  Line {
    SrcBlock     "Filter2"
    SrcPort      1
    DstBlock     "out_1"
    DstPort      1
  }
  Line {
    SrcBlock     "in_1"

```

```

    SrcPort          1
    DstBlock         "Filter1"
    DstPort          1
  }
  Line {
    SrcBlock         "Filter1"
    SrcPort          1
    DstBlock         "Filter2"
    DstPort          1
  }
}
}
Block {
  BlockType         Output
  Name              "out_1"
  Position          [605, 190, 625, 210]
  Port              "1"
  OutputWhenDisabled held
  InitialOutput     "0"
}
Line {
  SrcBlock          "Sum"
  SrcPort           1
  Points            [50, 0]
  DstBlock          "Product1"
  DstPort           2
}
Line {
  SrcBlock          "in_2"
  SrcPort           1
  Points            [95, 0]
  DstBlock          "Sum1"
  DstPort           2
}
Line {
  SrcBlock          "in_1"
  SrcPort           1
  DstBlock          "RUDSHAPE"
  DstPort           1
}
Line {
  SrcBlock          "DRT"
  SrcPort           1
  Points            [10, 0]
  DstBlock          "Sum2"
  DstPort           2
}
Line {
  SrcBlock          "RUDSHAPE"
  SrcPort           1
  DstBlock          "GAIN"
}

```

```

    DstPort          2
  }
  Line {
    SrcBlock         "GAIN"
    SrcPort          1
    DstBlock         "Sum2"
    DstPort          1
  }
  Line {
    SrcBlock         "NYCOMP"
    SrcPort          1
    Points           [5, 0; 0, 5]
    DstBlock         "GAIN_"
    DstPort          2
  }
  Line {
    SrcBlock         "COSALF"
    SrcPort          1
    Points           [0, 65]
    DstBlock         "GAIN_"
    DstPort          1
  }
  Line {
    SrcBlock         "Product1"
    SrcPort          1
    DstBlock         "RUDCMD"
    DstPort          1
  }
  Line {
    SrcBlock         "GERYFWDS"
    SrcPort          1
    DstBlock         "Product1"
    DstPort          1
  }
  Line {
    SrcBlock         "GDRC"
    SrcPort          1
    DstBlock         "Product1"
    DstPort          3
  }
  Line {
    SrcBlock         "RUDCMD"
    SrcPort          1
    DstBlock         "out_1"
    DstPort          1
  }
  Line {
    SrcBlock         "GAIN_"
    SrcPort          1
    Points           [0, 0]
    Branch {

```

```

    DstBlock      "Sum"
    DstPort      1
  }
  Branch {
    DstBlock      "Scope"
    DstPort      1
  }
}
Line {
  SrcBlock      "Sum1"
  SrcPort      1
  Points      [0, 0]
  Branch {
    DstBlock      "NYCOMP"
    DstPort      1
  }
  Branch {
    DstBlock      "Scope1"
    DstPort      1
  }
}
Line {
  SrcBlock      "in_3"
  SrcPort      1
  DstBlock      "DRERR"
  DstPort      1
}
Line {
  SrcBlock      "DRERR"
  SrcPort      1
  Points      [20, 0]
  Branch {
    Points      [15, 0]
    DstBlock      "Sum"
    DstPort      2
  }
  Branch {
    Points      [0, 35]
    DstBlock      "Scope2"
    DstPort      1
  }
}
Line {
  SrcBlock      "Sum2"
  SrcPort      1
  Points      [0, 0]
  Branch {
    DstBlock      "Sum1"
    DstPort      1
  }
  Branch {

```

```

        Points          [0, -55]
        DstBlock        "Scope3"
        DstPort         1
    }
}
Line {
    SrcBlock           "GNYDRM_COMP"
    SrcPort            1
    DstBlock           "GAIN"
    DstPort            1
}
}
}
Block {
    BlockType          Scope
    Name               "alfa"
    Position           [415, 25, 445, 55]
    Orientation        up
    NamePlacement      alternate
    Floating           off
    Location           [188, 365, 512, 604]
    Open              off
    Grid               on
    TickLabels         on
    ZoomMode           yonly
    TimeRange          "auto"
    YMin               "0.15"
    YMax               "0.25"
    SaveToWorkspace    off
    SaveName           "ScopeData"
    LimitMaxRows       on
    MaxRows            "5000"
    Decimation         "1"
    SampleInput        off
    SampleTime         "0"
}
Block {
    BlockType          Scope
    Name               "aob"
    Position           [550, 300, 580, 330]
    Floating           off
    Location           [188, 235, 512, 474]
    Open              off
    Grid               on
    TickLabels         on
    ZoomMode           on
    TimeRange          "auto"
    YMin               "-0.1"
    YMax               "0.02"
    SaveToWorkspace    off
    SaveName           "ScopeData"
}

```

```

LimitMaxRows      on
MaxRows           "5000"
Decimation        "1"
SampleInput       off
SampleTime        "0"
}
Block {
BlockType         Scope
Name              "beta"
Position          [505, 155, 535, 185]
Floating          off
Location          [188, 235, 512, 474]
Open              off
Grid              on
TickLabels        on
ZoomMode          on
TimeRange         "auto"
YMin              "-0.4"
YMax              "0"
SaveToWorkspace  off
SaveName          "ScopeData"
LimitMaxRows      on
MaxRows           "5000"
Decimation        "1"
SampleInput       off
SampleTime        "0"
}
Block {
BlockType         Constant
Name              "deltaa"
Position          [190, 135, 210, 155]
Value             "0"
}
Block {
BlockType         Constant
Name              "deltae"
Position          [190, 95, 210, 115]
Value             "0"
}
Block {
BlockType         Scope
Name              "doublet"
Position          [145, 30, 175, 60]
Orientation        up
NamePlacement     alternate
Floating          off
Location          [188, 365, 512, 604]
Open              off
Grid              on
TickLabels        on
ZoomMode          on
}

```

```

TimeRange      "auto"
YMin           "-5"
YMax           "5"
SaveToWorkspace off
SaveName       "ScopeData"
LimitMaxRows   on
MaxRows        "5000"
Decimation     "1"
SampleInput    off
SampleTime     "0"
}
Block {
BlockType      Scope
Name           "dr"
Position       [240, 230, 270, 260]
Floating       off
Location       [188, 365, 512, 604]
Open           off
Grid           on
TickLabels     on
ZoomMode       yonly
TimeRange      "auto"
YMin           "-5"
YMax           "5"
SaveToWorkspace off
SaveName       "ScopeData"
LimitMaxRows   on
MaxRows        "5000"
Decimation     "1"
SampleInput    off
SampleTime     "0"
}
Block {
BlockType      Scope
Name           "psi"
Position       [565, 375, 595, 405]
Floating       off
Location       [188, 235, 512, 474]
Open           off
Grid           on
TickLabels     on
ZoomMode       on
TimeRange      "auto"
YMin           "-0.05"
YMax           "0.15"
SaveToWorkspace off
SaveName       "ScopeData"
LimitMaxRows   on
MaxRows        "5000"
Decimation     "1"
SampleInput    off

```

```

    SampleTime    "0"
  }
  Block {
    BlockType     Scope
    Name          "q"
    Position      [455, 55, 485, 85]
    Floating      off
    Location      [188, 365, 512, 604]
    Open         off
    Grid         on
    TickLabels    on
    ZoomMode      yonly
    TimeRange     "auto"
    YMin         "-5"
    YMax         "5"
    SaveToWorkspace off
    SaveName      "ScopeData"
    LimitMaxRows on
    MaxRows      "5000"
    Decimation    "1"
    SampleInput   off
    SampleTime    "0"
  }
  Block {
    BlockType     Scope
    Name          "rollrate"
    Position      [545, 195, 575, 225]
    Floating      off
    Location      [188, 235, 609, 474]
    Open         off
    Grid         on
    TickLabels    on
    ZoomMode      on
    TimeRange     "auto"
    YMin         "-0.05"
    YMax         "0.01"
    SaveToWorkspace off
    SaveName      "ScopeData"
    LimitMaxRows on
    MaxRows      "5000"
    Decimation    "1"
    SampleInput   off
    SampleTime    "0"
  }
  Block {
    BlockType     Scope
    Name          "theta"
    Position      [475, 100, 505, 130]
    Floating      off
    Location      [188, 365, 512, 604]
    Open         off

```

```

Grid          on
TickLabels    on
ZoomMode      yonly
TimeRange     "auto"
YMin          "-1"
YMax          "1.5"
SaveToWorkspace off
SaveName      "ScopeData"
LimitMaxRows  on
MaxRows       "5000"
Decimation    "1"
SampleInput   off
SampleTime    "0"
}
Block {
BlockType     Scope
Name          "u"
Position      [375, 65, 405, 95]
Orientation   left
Floating      off
Location      [188, 365, 512, 604]
Open          off
Grid          on
TickLabels    on
ZoomMode      on
TimeRange     "auto"
YMin          "-100"
YMax          "0"
SaveToWorkspace off
SaveName      "ScopeData"
LimitMaxRows  on
MaxRows       "5000"
Decimation    "1"
SampleInput   off
SampleTime    "0"
}
Block {
BlockType     Scope
Name          "yawrate"
Position      [555, 245, 585, 275]
Floating      off
Location      [188, 235, 512, 474]
Open          off
Grid          on
TickLabels    on
ZoomMode      on
TimeRange     "auto"
YMin          "0"
YMax          "0.05"
SaveToWorkspace off
SaveName      "ScopeData"

```

```

LimitMaxRows      on
MaxRows           "5000"
Decimation        "1"
SampleInput       off
SampleTime        "0"
}
Line {
  SrcBlock         "Demux"
  SrcPort          8
  Points           [95, 0; 0, 85; 30, 0]
  Branch {
    Points         [0, -20]
    DstBlock       "To Workspace8"
    DstPort        1
  }
  Branch {
    DstBlock       "aob"
    DstPort        1
  }
}
Line {
  SrcBlock         "Demux"
  SrcPort          5
  Points           [50, 0]
  Branch {
    Points         [35, 0; 0, 130]
    DstBlock       "BETADOT"
    DstPort        1
  }
  Branch {
    Points         [0, -30; 25, 0]
    Branch {
      Points       [0, -25; 40, 0]
      DstBlock     "To Workspace3"
      DstPort      1
    }
    Branch {
      DstBlock     "beta"
      DstPort      1
    }
  }
}
Line {
  SrcBlock         "Demux"
  SrcPort          4
  Points           [40, 0; 0, -75]
  DstBlock         "theta"
  DstPort          1
}
Line {
  SrcBlock         "Demux"

```

```

SrcPort          3
Points          [0, -5; 30, 0]
DstBlock        "q"
DstPort         1
}
Line {
SrcBlock        "Demux"
SrcPort         2
Points          [20, 0]
DstBlock        "alfa"
DstPort         1
}
Line {
SrcBlock        "Demux"
SrcPort         1
Points          [10, 0]
DstBlock        "u"
DstPort         1
}
Line {
SrcBlock        "YAW FCS"
SrcPort         1
Points          [5, 0]
Branch {
DstBlock        "Mux1"
DstPort         3
}
Branch {
Points          [0, 40]
Branch {
DstBlock        "dr"
DstPort         1
}
Branch {
Points          [-50, 0; 0, 20]
DstBlock        "To Workspace1"
DstPort         1
}
}
}
Line {
SrcBlock        "Mux"
SrcPort         1
DstBlock        "Ny_"
DstPort         1
}
Line {
SrcBlock        "Mux1"
SrcPort         1
DstBlock        "State-space"
DstPort         1
}

```

```

}
Line {
  SrcBlock      "deltae"
  SrcPort       1
  Points        [5, 0]
  DstBlock      "Mux1"
  DstPort       1
}
Line {
  SrcBlock      "deltaa"
  SrcPort       1
  Points        [0, 50]
  DstBlock      "Mux1"
  DstPort       2
}
Line {
  SrcBlock      "Demux"
  SrcPort       7
  Points        [25, 0]
  Branch {
    Points      [55, 0]
    Branch {
      Points    [-5, 0; 0, 170]
      DstBlock  "PSI"
      DstPort   1
    }
    Branch {
      Points    [30, 0; 0, 40; 20, 0]
      Branch {
        DstBlock "yawrate"
        DstPort  1
      }
      Branch {
        Points   [30, 0]
        DstBlock "To Workspace5"
        DstPort  1
      }
    }
  }
}
Branch {
  Points      [15, 0; 0, 155; -290, 0]
  DstBlock    "YAW FCS"
  DstPort     3
}
Branch {
  Points      [0, 50]
  DstBlock    "RDOT"
  DstPort     1
}
Branch {
  Points      [40, 0; 0, 80]
}

```

```

        DstBlock      "Mux"
        DstPort      2
    }
}
Line {
    SrcBlock      "State-space"
    SrcPort      1
    DstBlock      "Demux"
    DstPort      1
}
Line {
    SrcBlock      "RDOT"
    SrcPort      1
    Points      [-5, 0]
    Branch {
        DstBlock      "Mux"
        DstPort      1
    }
    Branch {
        DstBlock      "Scope1"
        DstPort      1
    }
}
Line {
    SrcBlock      "BETADOT"
    SrcPort      1
    Points      [-10, 0]
    Branch {
        DstBlock      "Mux"
        DstPort      3
    }
    Branch {
        Points      [0, 120]
        DstBlock      "Scope"
        DstPort      1
    }
}
Line {
    SrcBlock      "Pulse\nGenerator1"
    SrcPort      1
    Points      [25, 0]
    DstBlock      "Sum"
    DstPort      1
}
Line {
    SrcBlock      "Pulse\nGenerator2"
    SrcPort      1
    Points      [25, 0]
    DstBlock      "Sum"
    DstPort      2
}

```

```

Line {
  SrcBlock      "Ny_"
  SrcPort       1
  Points        [-5, 0]
  Branch {
    Points      [-110, 0; 0, -95]
    DstBlock    "YAW FCS"
    DstPort     2
  }
  Branch {
    Points      [0, 80]
    Branch {
      DstBlock  "Ny"
      DstPort   1
    }
    Branch {
      DstBlock  "To Workspace2"
      DstPort   1
    }
  }
}
}
}
Line {
  SrcBlock      "Sum"
  SrcPort       1
  Points        [10, 0]
  Branch {
    Points      [0, 40; -65, 0]
    DstBlock    "To Workspace"
    DstPort     1
  }
  Branch {
    Points      [10, 0]
    Branch {
      Points    [5, 0]
      DstBlock  "doublet"
      DstPort   1
    }
    Branch {
      Points    [0, 95]
      DstBlock  "YAW FCS"
      DstPort   1
    }
  }
}
}
}
Line {
  SrcBlock      "Demux"
  SrcPort       6
  Points        [120, 0]
  Branch {
    DstBlock    "rollrate"
    DstPort     1
  }
}

```

```

    }
    Branch {
        Points          [0, -20; 25, 0; 0, -20]
        DstBlock        "To Workspace4"
        DstPort         1
    }
}
}
Line {
    SrcBlock           "PSI"
    SrcPort            1
    Points             [15, 0]
    Branch {
        DstBlock        "psi"
        DstPort         1
    }
    Branch {
        Points          [0, -40]
        DstBlock        "To Workspace6"
        DstPort         1
    }
}
}
Line {
    SrcBlock           "Clock"
    SrcPort            1
    DstBlock           "To Workspace7"
    DstPort            1
}
}
}
}

```

APPENDIX C. MATLAB CODE FOR PLOT PROGRAM

```
plot(time,doublet,'b')
title('Rudder Pedal Deflection')
xlabel('Time (sec)')
ylabel('dpedal (deg)')
figure
```

```
plot(time,dr,'-',time,dr1,'--',time,dr2,':',time,dr3,'x',time,dr4,'.',time,dr5,'-.')
grid
title('Rudder Deflection')
xlabel('Time (sec)')
ylabel('dr (deg)')
legend('Baseline','No Ny feedback','Shorter time constant','Linearized rudder','Reduced rudder gain','Optimum fix',1)
figure
```

```
plot(time,Ny,'-',time,Ny1,'--',time,Ny2,':',time,Ny3,'x',time,Ny4,'.',time,Ny5,'-.')
grid
title('Lateral Acceleration at Commander Station')
xlabel('Time (sec)')
ylabel('Ny (g)')
legend('Baseline','No Ny feedback','Shorter time constant','Linearized rudder','Reduced rudder gain','Optimum fix',1)
figure
```

```
plot(time,beta*180/pi,'-',time,beta1*180/pi,'--',time,beta2*180/pi,':',time,beta3*180/pi,'x',time,beta4*180/pi,'.',time,beta5*180/pi,'-.')
grid
title('Sideslip')
xlabel('Time (sec)')
ylabel('Beta (deg)')
legend('Baseline','No Ny feedback','Shorter time constant','Linearized rudder','Reduced rudder gain','Optimum fix',4)
figure
```

```
plot(time,r*180/pi,'-',time,r1*180/pi,'--',time,r2*180/pi,':',time,r3*180/pi,'x',time,r4*180/pi,'.',time,r5*180/pi,'-.')
grid
title('Yaw Rate')
xlabel('Time (sec)')
ylabel('r (deg/sec)')
legend('Baseline','No Ny feedback','Shorter time constant','Linearized rudder','Reduced rudder gain','Optimum fix',1)
figure
```

```
plot(time,p*180/pi,'-',time,p1*180/pi,'--',time,p2*180/pi,':',time,p3*180/pi,'x',time,p4*180/pi,'.',time,p5*180/pi,'-.')
grid
title('Roll Rate')
```

```

xlabel('Time (sec)')
ylabel('p (deg/sec)')
legend('Baseline','No Ny feedback','Shorter time constant','Linearized rudder','Reduced rudder gain','Optimum fix',1)
figure

```

```

plot(time,psi*180/pi,'-',time,psi1*180/pi,'--
',time,psi2*180/pi,'.',time,psi3*180/pi,'x',time,psi4*180/pi,'.',time,psi5*180/pi,'-'.)
grid

```

```

title('Heading')
xlabel('Time (sec)')
ylabel('psi (deg)')
legend('Baseline','No Ny feedback','Shorter time constant','Linearized rudder','Reduced rudder gain','Optimum fix',1)
figure

```

```

plot(time,aob*180/pi,'-',time,aob1*180/pi,'--
',time,aob2*180/pi,'.',time,aob3*180/pi,'x',time,aob4*180/pi,'.',time,aob5*180/pi,'-'.)
grid
title('Angle of Bank')
xlabel('Time (sec)')
ylabel('phi (deg)')
legend('Baseline','No Ny feedback','Shorter time constant','Linearized rudder','Reduced rudder gain','Optimum fix',4)

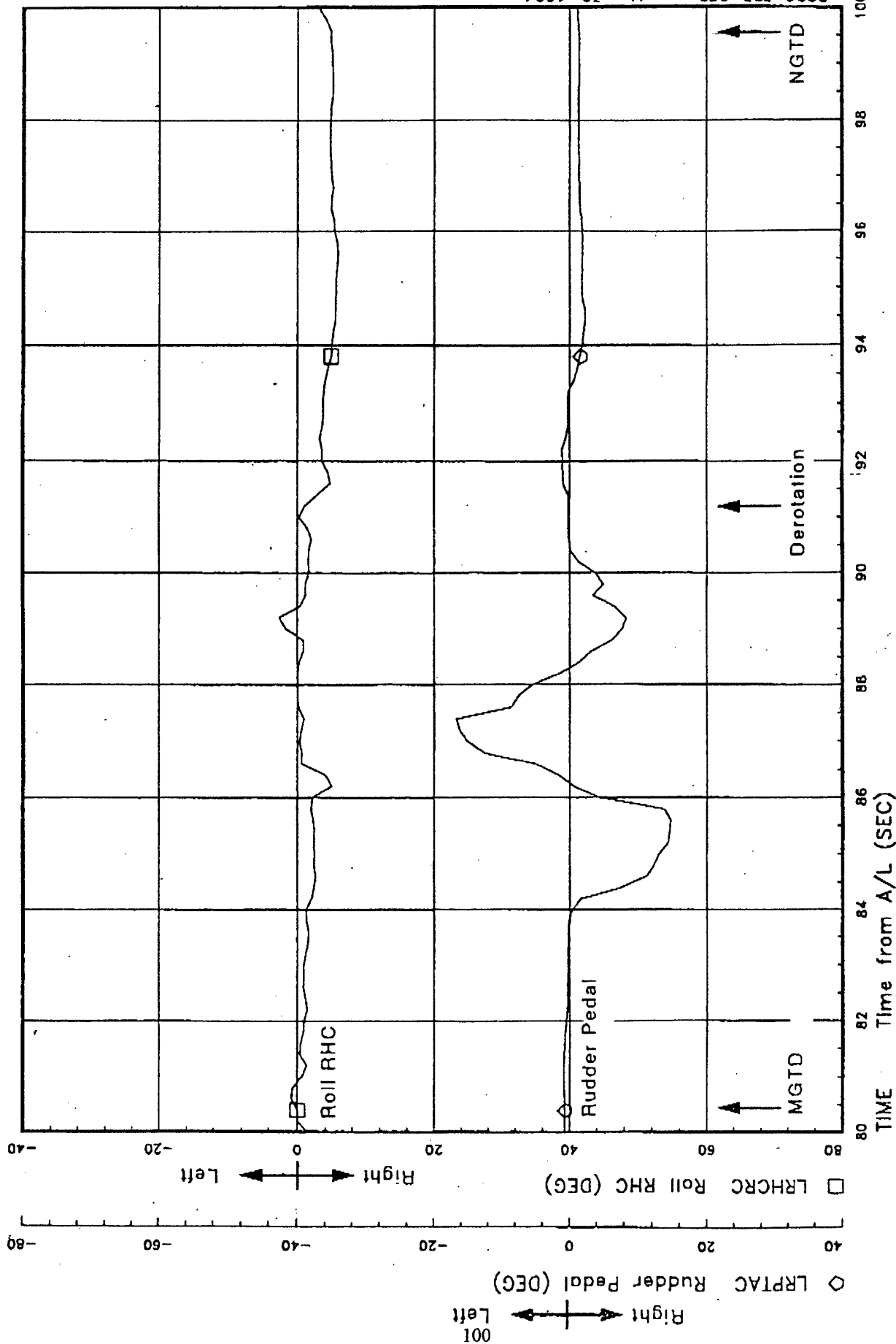
```

APPENDIX D. STS-62 FLIGHT DATA AND SES SIMULATION

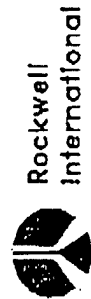
RESULTS

The first four plots contain the STS-62 data. The remaining six plots are the SES results. For all cases, Main Gear Touch Down (MGTD) occurs at 80.3 seconds with derotation at 91 seconds. The X scale reflects time from the Approach and Land (A/L) transition, which normally occurs around 10,000 feet.

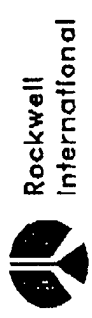
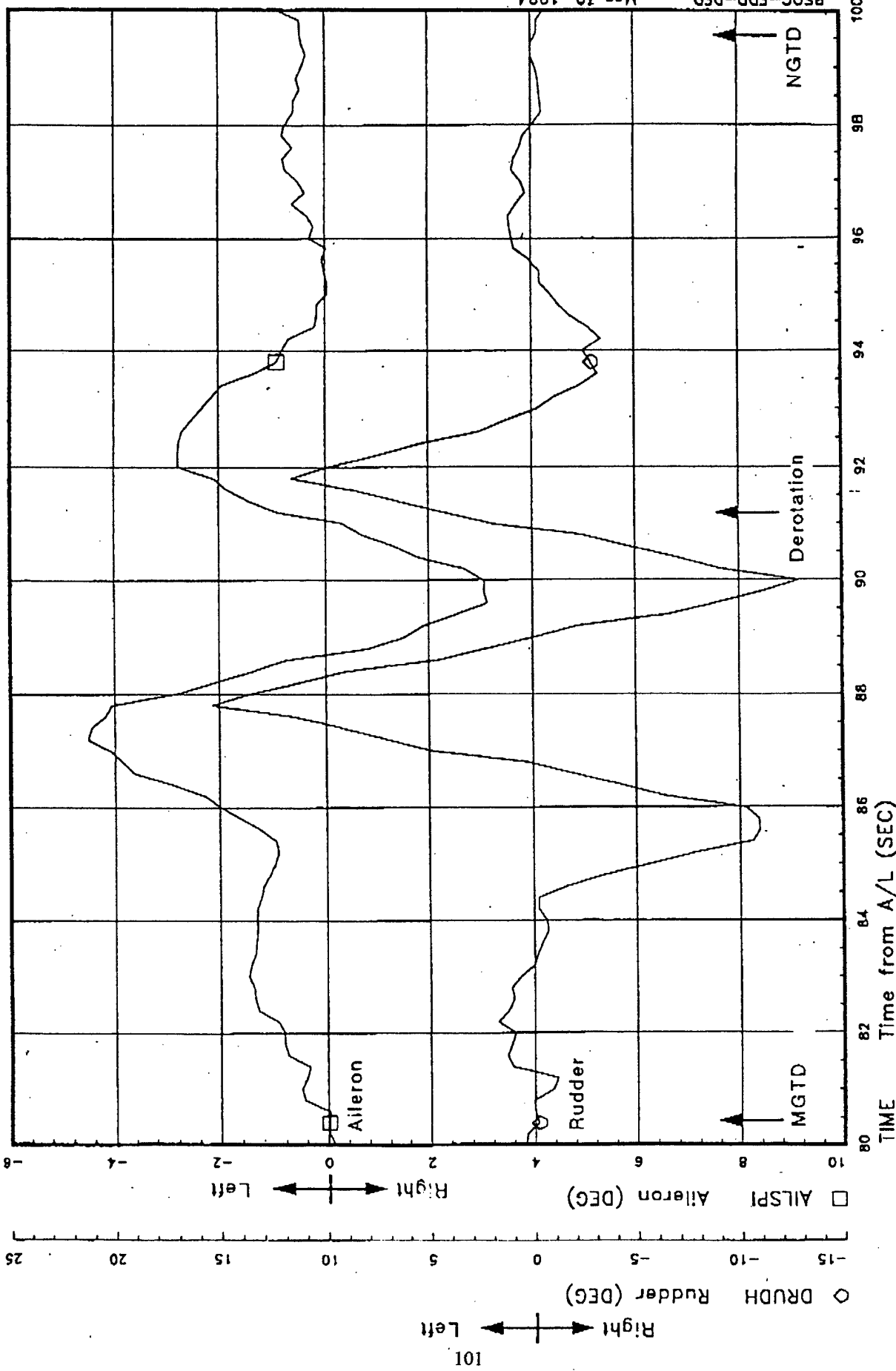
STS-62 Real-Time Data - Plot 1



Rudder Pedal And Roll RHC Inputs



STS-62 Real-Time Data - Plot 2



Rudder and Aileron Deflections

- Post MGTD

1 XEROX #78

RSOC-FDD-DFD - Mar 30, 1994

101 Right ← Left

Right ← Left

□ AII SPI Aileron (DEG)

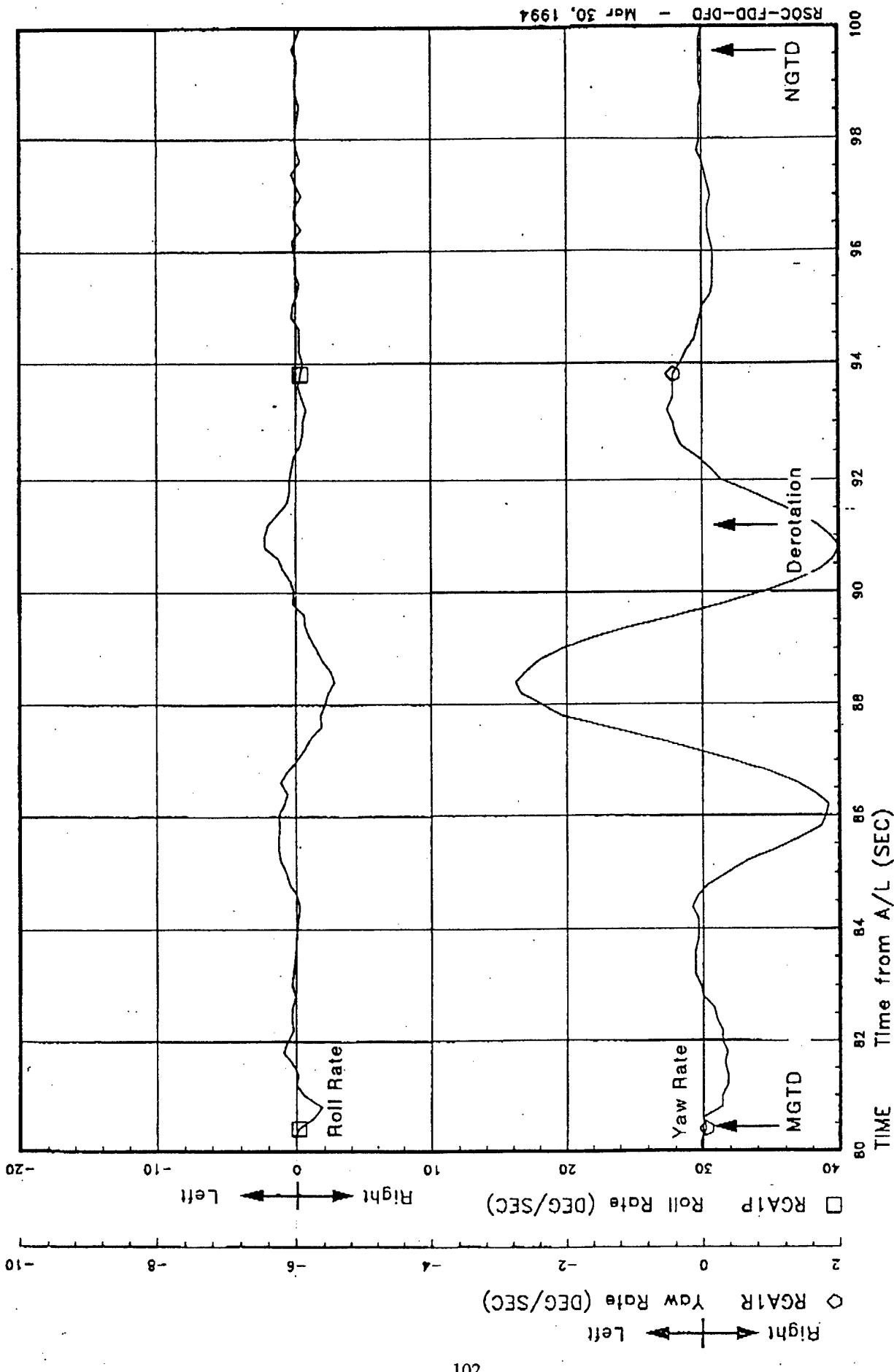
◇ DRUDH Rudder (DEG)

MGTD

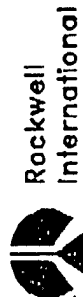
Derotation

NGTD

STS-62 Real-Time Data - Plot 3



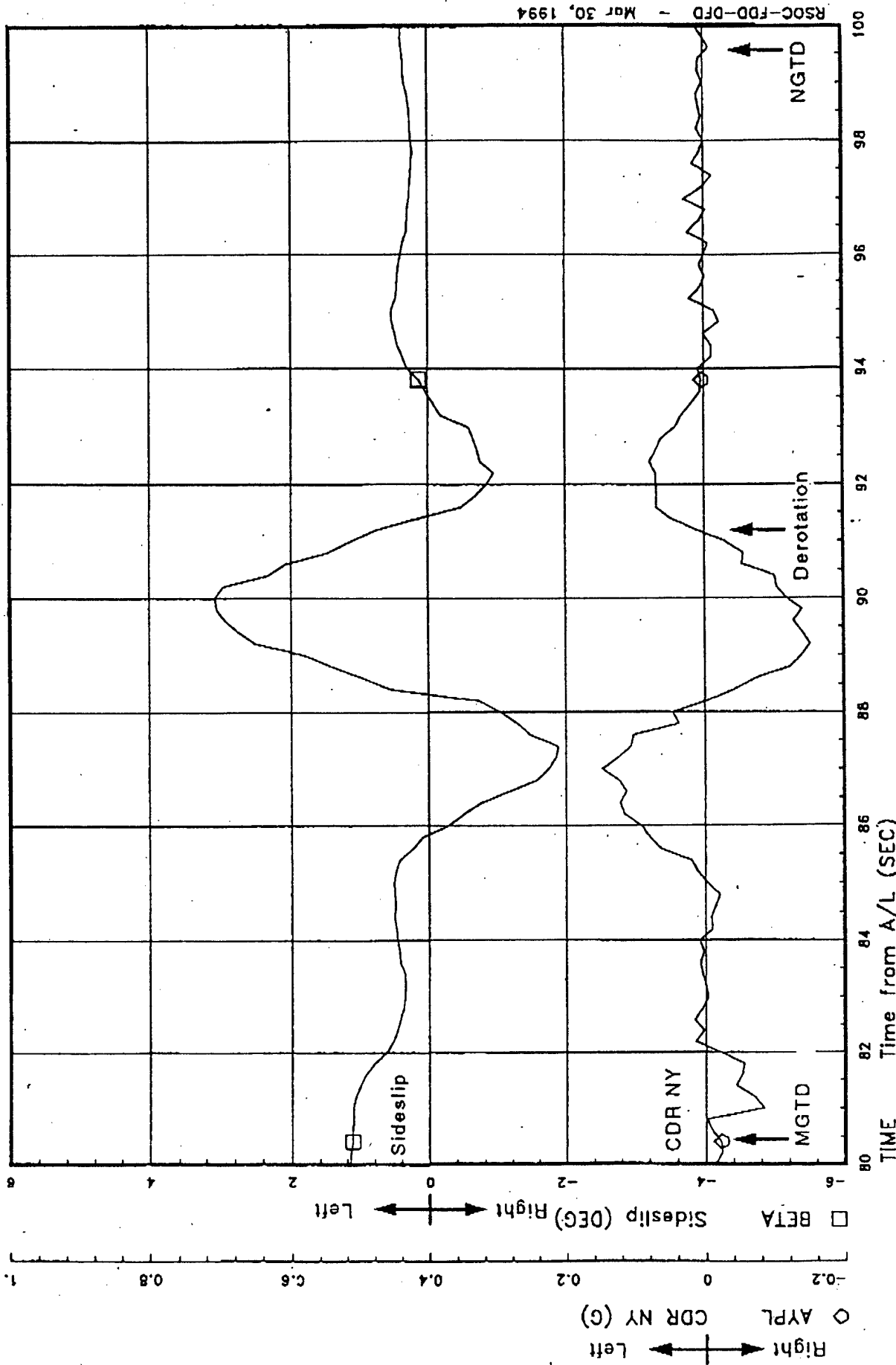
DTO Rates Profile (RCA1)



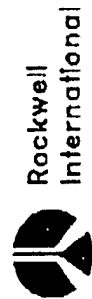
Post MGTD

ROCKWELLCOPIER #78

STS-62 Real-Time Data - Plot 4



RSOC-FDD-DFD - Mar 30, 1994



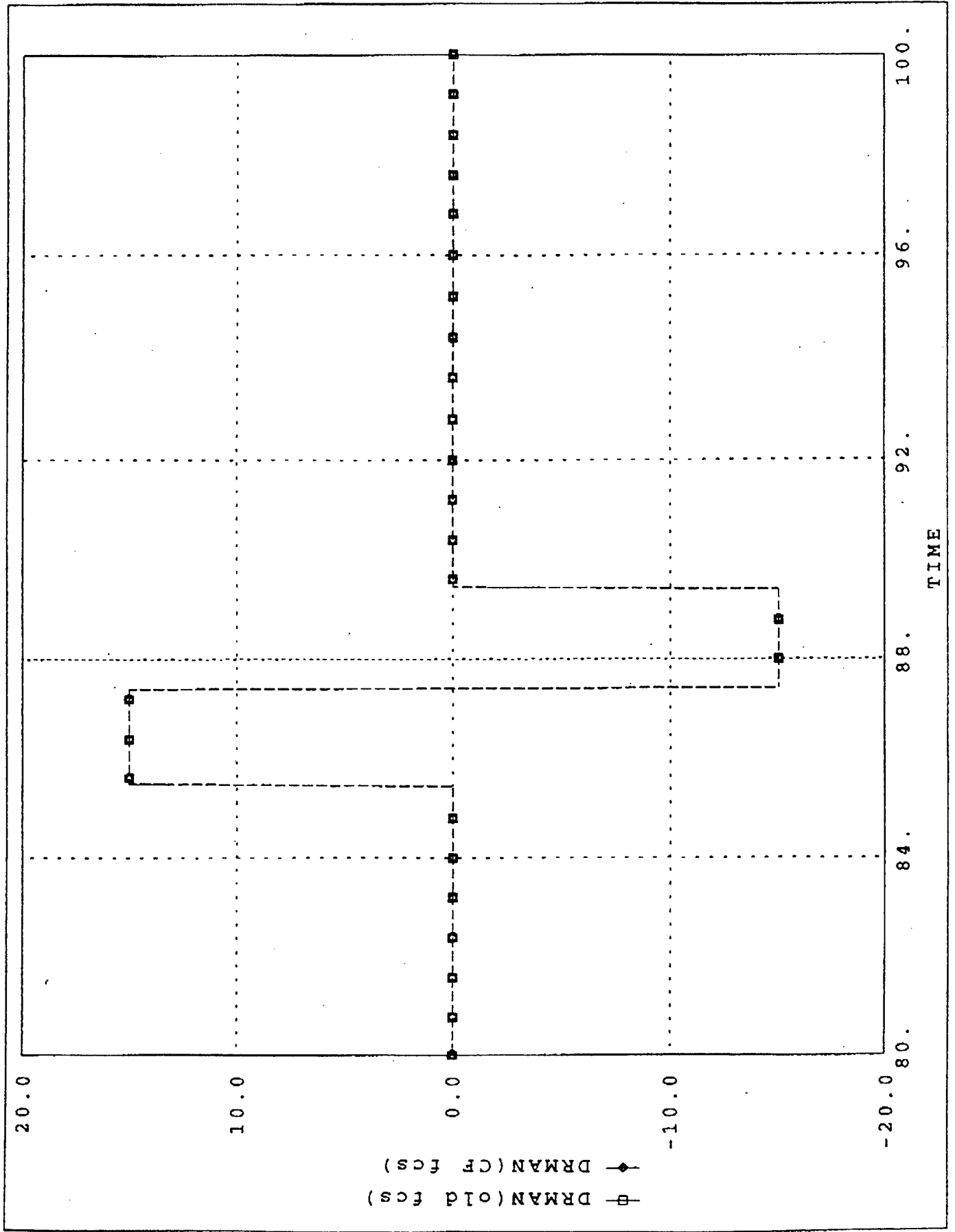
DTO Sideslip - Pilot Station Lateral Forces

- Post MGTD

HELICOPIER #78

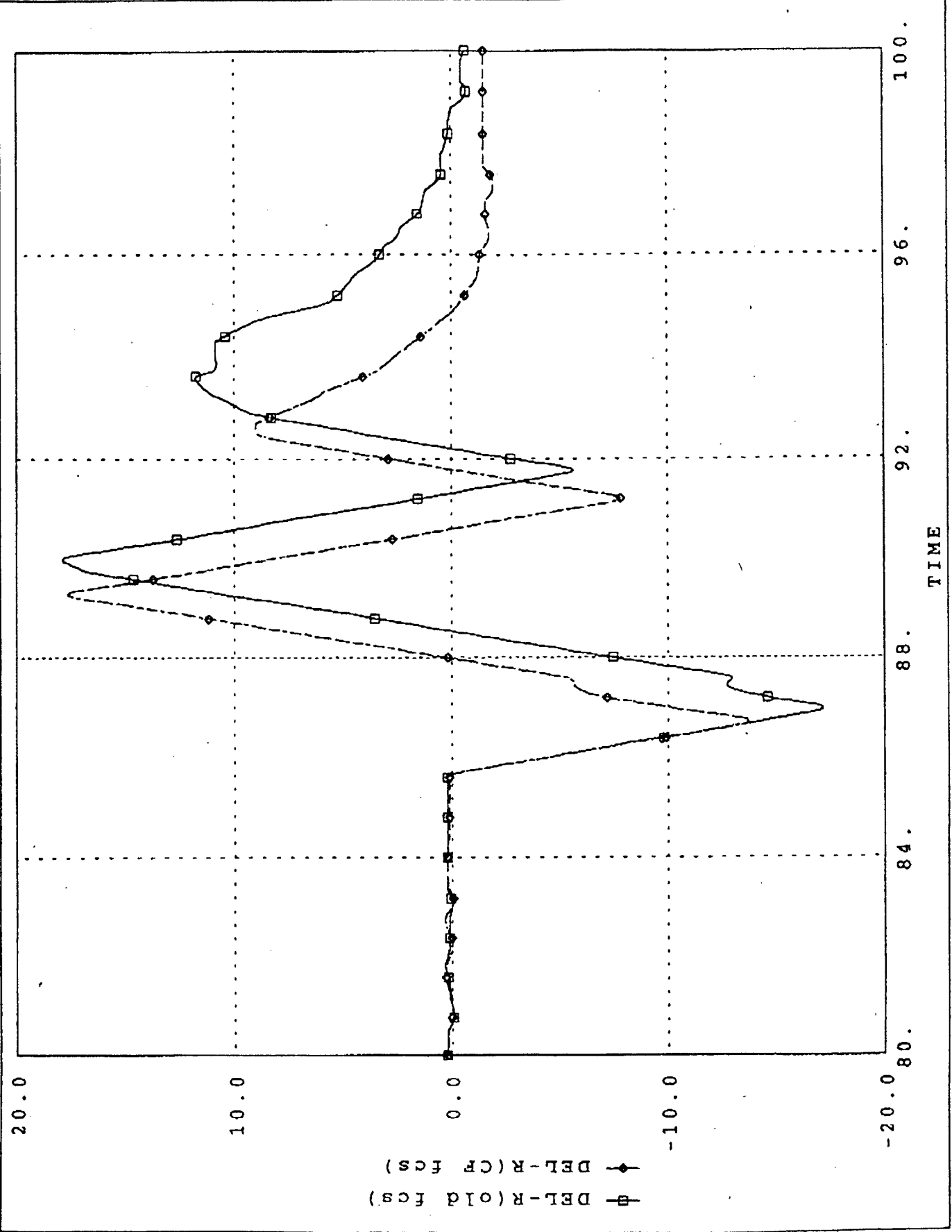
SES:

STS-62 MASS PROPERTIES, RUDDER PULSE, AND FCS TESTS



SES:

STS-62 MASS PROPERTIES, RUDDER PULSE, AND FCS TESTS

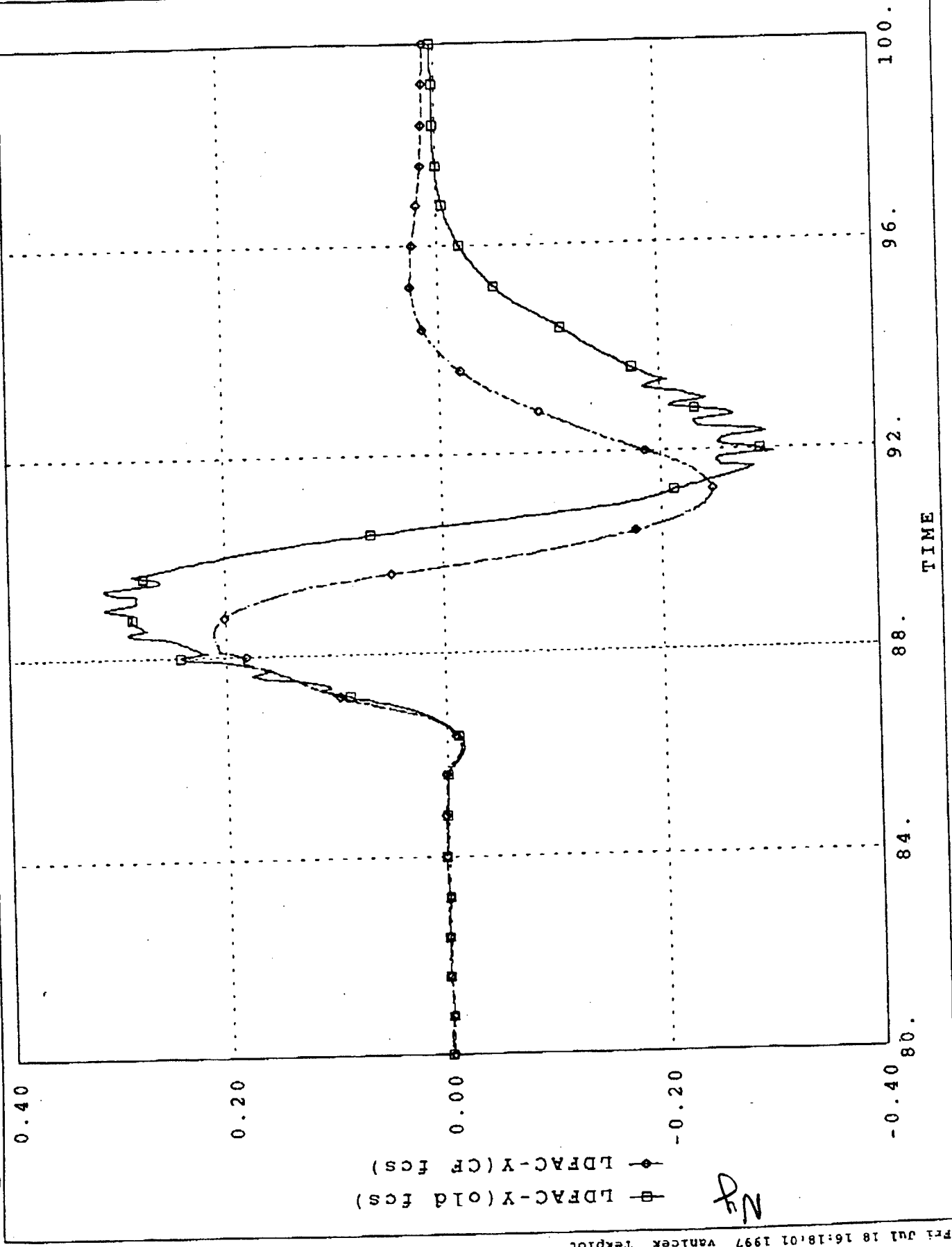


—◆— DEL-R (CF FCS)
 —□— DEL-R (Old FCS)

FRS JUL 18 16:33:13 1997 vanicek Tekplot

STS-62 MASS PROPERTIES, RUDDER PULSE, AND FCS TESTS

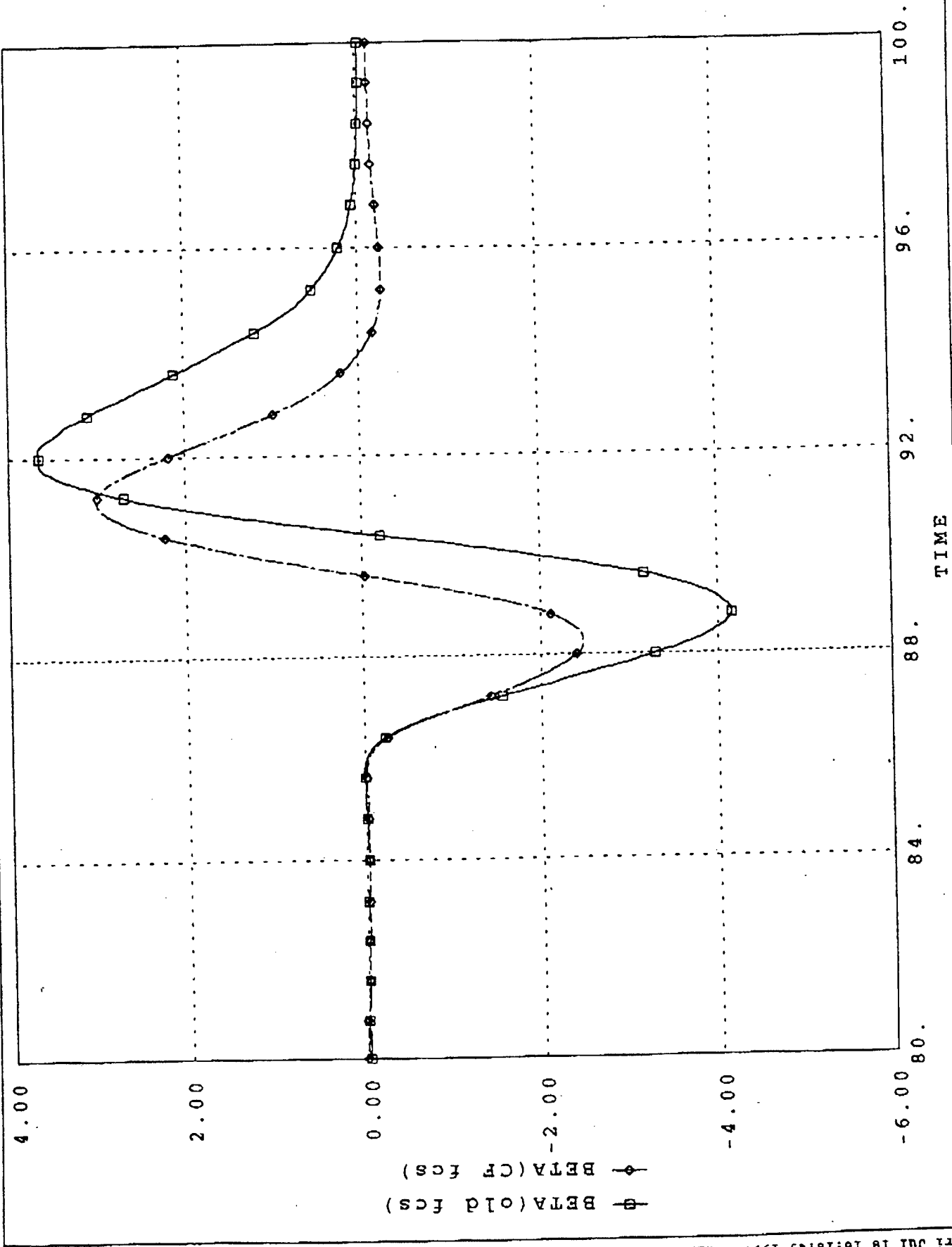
5551



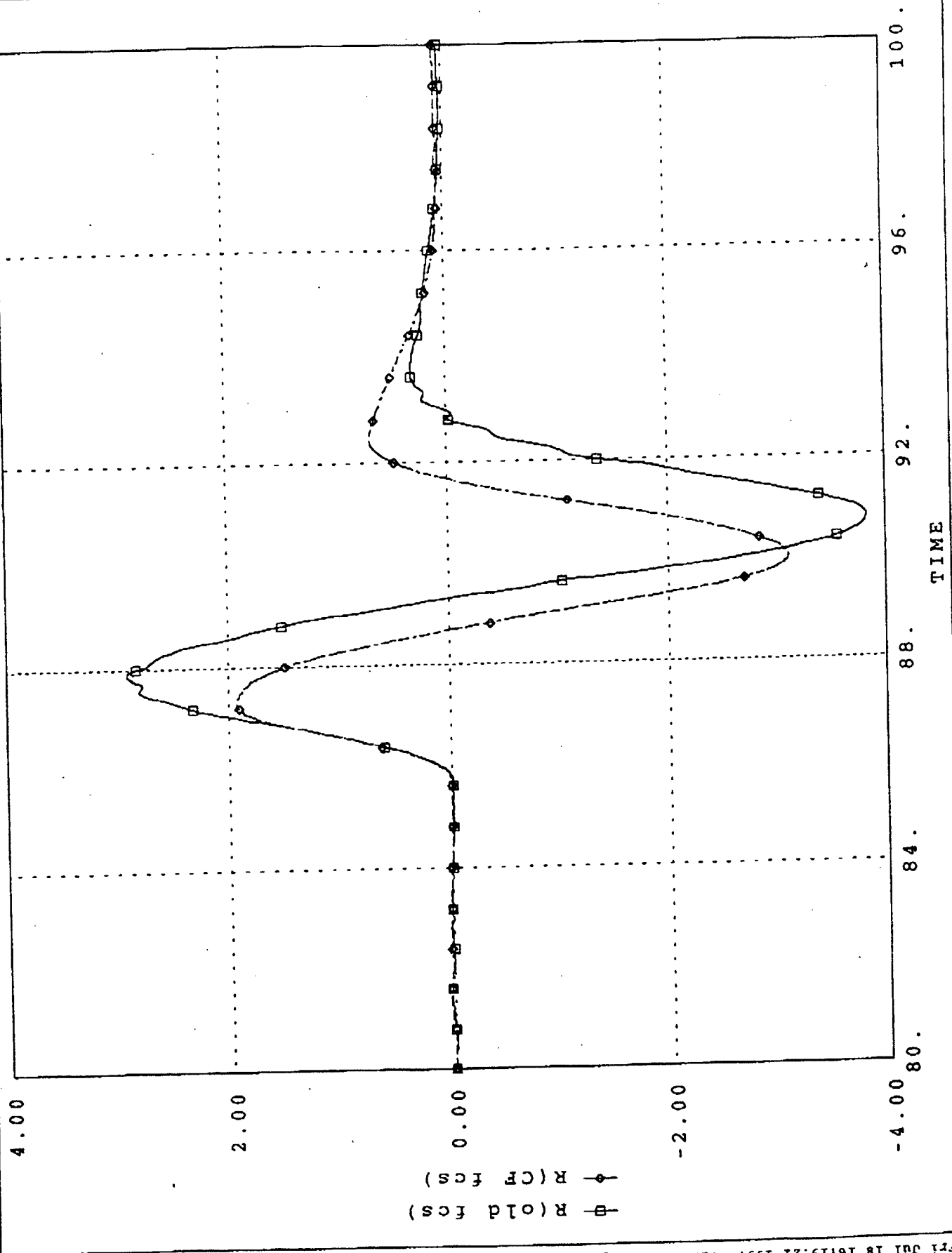
NY

Printed on 18:18:01 1997 vanlec Tekplot

STS-62 MASS PROPERTIES, RUDDER PULSE, AND FCS TESTS

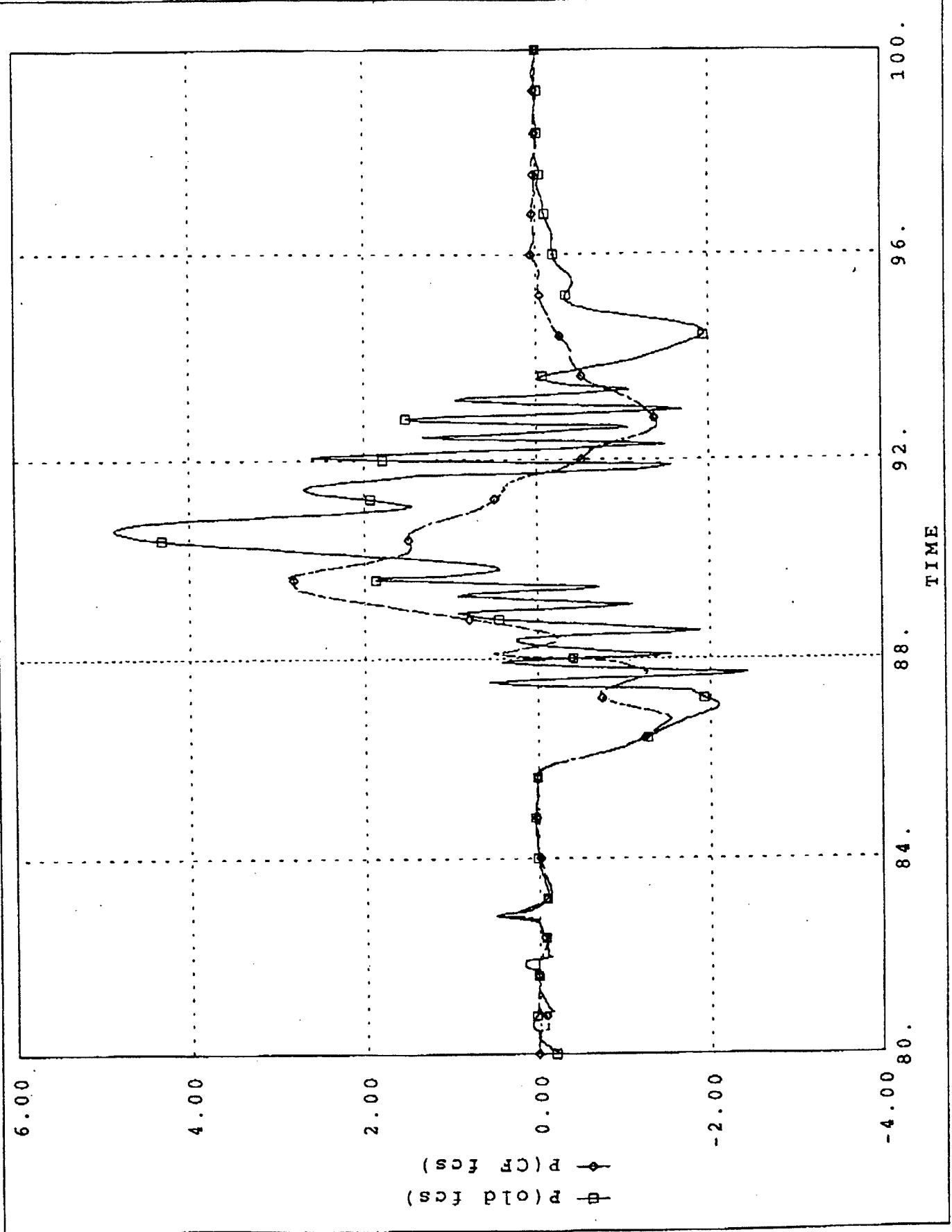


SES
STS-62 MASS PROPERTIES, RUDDER PULSE, AND FCS TESTS



□ R (old fcs)
◇ R (CF fcs)

SES: STS-62 MASS PROPERTIES, RUDDER PULSE, AND FCS TESTS



Fri Jul 18 16:19:43 1997 vanlec Tekplot

LIST OF REFERENCES

1. Ascent/Entry Flight Techniques Panel #123 Minutes, June 1995.
2. Post flight data analysis of the approach and landing flight phase, 1990 - 1997.
3. Space Shuttle Operational Flight Rules, Final, PCN-4, August 1996.
4. Flight Procedures Handbook for Approach, Landing, and Rollout, November 1992.
5. Space Shuttle Systems Handbook (SSSH) Drawings, 1996.
6. Guidance, Navigation, and Control Systems Briefs, 1996.
7. Ames VMS Test Results, 1993-1997.
8. Space Shuttle Orbiter Operational Level C Functional Subsystem Software Requirements (FSSR) Guidance, Navigation, and Control, Part C; Flight Control Entry-GRTLS, April 1993.
9. Lockheed Engineering and Sciences Company, Houston FCS Descent Configuration Drawings, 1997.
10. Roskam, Jan, Airplane Flight Dynamics and Automatic Flight Controls, Part I and II, Roskam Aviation and Engineering Corporation, 1982.
11. Halliday, Resnick, Walker, Fundamentals of Physics Extended, John Wiley & Sons, Inc., 1993.
12. Operational Aerodynamic Data Book, Volumes I, II, and III, September 1985.
13. GNC Entry 2202, GN&C Entry Operations - Flight Control, 1979.

INITIAL DISTRIBUTION LIST

1. Defense Technical Information Center.....2
 8725 John J. Kingman Rd., Ste 0944
 Ft. Belvoir, VA 22060-6218
2. Dudley Knox Library.....2
 Naval Postgraduate School
 411 Dyer Rd.
 Monterey, CA 93943-5101
3. Chairman, Code AA.....1
 Department of Aeronautics and Astronautics
 Naval Postgraduate School
 411 Dyer Rd.
 Monterey, CA 93943-5002
4. Chairman, Code SP.....1
 Space Systems Academic Group
 Naval Postgraduate School
 411 Dyer Rd.
 Monterey, CA 93943-5000
5. Curricular Officer, Code 31.....1
 Aerospace Engineering Curricular Office
 Naval Postgraduate School
 411 Dyer Rd.
 Monterey, CA 93943-5107
6. Curricular Officer, Code 37.....1
 Naval Postgraduate School
 411 Dyer Rd.
 Monterey, CA 93943-5000
7. Dr. Richard M. Howard, Code AA.....1
 Aerospace Engineering Curricular Office
 Naval Postgraduate School
 411 Dyer Rd.
 Monterey, CA 93943-5107
8. Linda J. Ham.....1
 NASA/JSC
 Mail Code DA8
 Houston, TX 77058